OPEN ACCESS

Original research

Faecal microbiota transplantation halts progression of human new-onset type 1 diabetes in a randomised controlled trial

Pieter de Groot,[1] Tanja Nikolic,[2] Silvia Pellegrini,[3] Valeria Sordi,[4] Sultan Imangaliyev,[1] Elena Rampanelli,[1] Nordin Hanssen,[1] Ilias Attaye,[1] Guido Bakker,[1] Gaby Duinkerken,[2] Antoinette Joosten,[2] Andrei Prodan,[1] Evgeni Levin,[1] Han Levels,[1] Bartjan Potter van Loon,[5] Arianne van Bon,[6] Catherina Brouwer,[7] Sytze van Dam,[7] Suat Simsek,[8] Daniel van Raalte,[1] Frank Stam,[8] Victor Gerdes,[1] Roel Hoogma,[9] Martin Diekman,[10] Martin Gerding,[10] Cees Rustemeijer,[11] Bernadette de Bakker,[1] Joost Hoekstra,[1] Aeilko Zwinderman,[12] Jacques Bergman ,[13] Frits Holleman,[1] Lorenzo Piemonti ,[3] Willem De Vos,[14] Bart Roep,[2,15] Max Nieuwdorp [1]

► Additional material is published online only. To view, please visit the journal online (http://dx.doi.org/10.1136/gutjnl-2020-322630).

For numbered affiliations see end of article.

Correspondence to
Professor Max Nieuwdorp, Vascular Medicine, Amsterdam University Medical Centres, Amsterdam, Noord-Holland, Netherlands; m.nieuwdorp@amsterdamumc.nl

Received 29 July 2020
Revised 29 September 2020
Accepted 30 September 2020
Published Online First 26 October 2020

Linked

► http://dx.doi.org/10.1136/gutjnl-2020-323252

Check for updates

To cite: de Groot P, Nikolic T, Pellegrini S, *et al*. *Gut* 2021;**70**:92–105.

ABSTRACT

Objective Type 1 diabetes (T1D) is characterised by islet autoimmunity and beta cell destruction. A gut microbiota–immunological interplay is involved in the pathophysiology of T1D. We studied microbiota-mediated effects on disease progression in patients with type 1 diabetes using faecal microbiota transplantation (FMT).

Design Patients with recent-onset (<6 weeks) T1D (18–30 years of age) were randomised into two groups to receive three autologous or allogenic (healthy donor) FMTs over a period of 4 months. Our primary endpoint was preservation of stimulated C peptide release assessed by mixed-meal tests during 12 months. Secondary outcome parameters were changes in glycaemic control, fasting plasma metabolites, T cell autoimmunity, small intestinal gene expression profile and intestinal microbiota composition.

Results Stimulated C peptide levels were significantly preserved in the autologous FMT group (n=10 subjects) compared with healthy donor FMT group (n=10 subjects) at 12 months. Small intestinal *Prevotella* was inversely related to residual beta cell function (r=−0.55, p=0.02), whereas plasma metabolites 1-arachidonoyl-GPC and 1-myristoyl-2-arachidonoyl-GPC levels linearly correlated with residual beta cell preservation (rho=0.56, p=0.01 and rho=0.46, p=0.042, respectively). Finally, baseline CD4 +CXCR3+T cell counts, levels of small intestinal *Desulfovibrio piger* and CCL22 and CCL5 gene expression in duodenal biopsies predicted preserved beta cell function following FMT irrespective of donor characteristics.

Conclusion FMT halts decline in endogenous insulin production in recently diagnosed patients with T1D in 12 months after disease onset. Several microbiota-derived plasma metabolites and bacterial strains were linked to preserved residual beta cell function. This study provides insight into the role of the intestinal gut microbiome in T1D.

Trial registration number NTR3697.

Significance of this study

What is already known on this subject?
- Gut microbiota are involved in human metabolic and autoimmune disease.
- Changes in faecal microbiota are associated with human type 1 diabetes (T1D).
- Animal studies have suggested that faecal transplantation can alter T1D.

What are the new findings?
- Faecal microbiota transplantation (FMT) stabilises residual beta cell function in subjects with new-onset T1D.
- These differential changes are accompanied by alterations in plasma metabolites, T cell autoimmunity, small intestinal gene expression as well as small intestinal and faecal microbiota composition.
- New correlations between changes in microbiota strains and plasma (targeted) metabolites in relation to small intestinal gene expression and T cell autoimmunity in human T1D were observed.

How might it impact on clinical practice in the foreseeable future?
- This study helps to quantify magnitude of gut microbiota-driven effects in humans with new-onset T1D using FMT.
- This study provides sample sizes for future trials and underscores that gut microbiota play a role in beta cell destruction seen in T1D subjects.

INTRODUCTION

Type 1 diabetes mellitus (T1D) is an autoimmune disease characterised by progressive beta cell destruction. The T cell mediated autoimmune origin of T1D has prompted efforts to prevent disease progression by targeting T lymphocytes

using immunosuppressive drugs including cyclosporine,[1] anti-CD3 antibody treatment,[2] antithymocyte globulin[3] and anti-CD80 and anti-CD86 antibody treatment.[4 5] However, these treatment strategies have (at best) a temporary impact on disease progression with no effect on long-term progression and are accompanied by serious side effects.[6 7] Therefore, additional insights into T1D pathophysiology are urgently needed to find novel therapeutic interventions.

T1D pathophysiology has been linked to altered intestinal microbiota.[8–12] Studies in non-obese diabetic (NOD) mice suggested that interaction of the intestinal microbes with the innate immune system is a critical factor for the development of T1D[13] and can be improved by faecal microbiota transplantation (FMT) and specific microbes.[14] Moreover, a growing number of studies point towards a role for the small intestinal immune system. For instance, in NOD mice segmented filamentous bacterial strains induce autoimmune diabetes by interaction with T-helper type 17 cells in the small intestinal lamina propria.[15] Accordingly, infusion of bacterial strains into the pancreatic ductal system of a rat could induce T1D with pancreatic histological findings that mimic those observed in patients with T1D.[16] Also, a recent study showed marked differences in small intestinal microbiota and duodenal gene expression between (long-standing) human T1D and healthy control subjects.[17] T1D is thus believed to develop due to an altered intestinal epithelial barrier function induced by an impaired intestinal short-chain fatty acid (SCFA) production.[18] This barrier is presumably necessary to prevent priming of the immune system to beta cell epitopes that are mimicked by harmful bacteria[19] to which tolerance may be lost.[20] Indeed, intestinal SCFAs butyrate and acetate administration were shown to improve beta cell function in NOD mice.[21] However, we recently conducted a human intervention study in which butyrate administration had little immunological or metabolic effects in in T1D subjects.[22] Finally, FMT is shown to be safe, can significantly alter the recipient gut microbiota composition (increasing butyrate producing bacterial strains) and can affect glycaemic control in metabolic syndrome subjects based on baseline microbiota.[23–25] Therefore, this exploratory randomised controlled FMT trial in recent onset T1D subjects aimed to study the effects of sequential treatments of either healthy donor (allogenic) FMT or own (autologous) FMT on residual beta cell function (mixed meal test (MMT) stimulated C peptide response) during active FMT treatment (0–6 months) as well as long-term effects (0–12 months). Moreover, the relation with changes in duodenal microbiota composition, duodenal gene expression, faecal microbiota phylogenetic and metagenomic composition, whole blood T cell autoimmunity and fasting plasma metabolites was studied in these new-onset adult patients with T1D. A graphical summary of the study design is provided in figure 1A and B.

MATERIALS AND METHODS

Patient recruitment

New-onset patients with T1D were recruited from outpatient clinics in the Amsterdam region. Subjects aged 18–35 years with normal body mass index (BMI) (18.5–25 kg/m^2 and anti-GAD/IA-2 positive) were enrolled when diagnosed with T1D and with a maximum period of 6 weeks before inclusion and when there was still a residual beta cell function (plasma C peptide >0.2 mmol/L and/or >1.2 ng/mL after MMT). Exclusion criteria were a diagnosis or symptoms of another autoimmune disease, compromised immunity, use of any systemic medication (barring insulin) and use of antibiotics or proton-pump inhibitors in the last 3 months.

Faecal donor recruitment, randomisation and FMT procedures

Lean (BMI <25 kg/m^2), omnivorous, healthy male and female Caucasians were recruited to serve as faecal donors. Selection criteria are described in the online supplemental methods. Subjects were allocated in a 1:1 fashion using computerised randomisation to receive three autologous or allogenic faecal transplantations by nasoduodenal tube using freshly produced faeces at 0, 2 and 4 months (figure 1B) from the same sex matched donor as previously described[24] and detailed in the online supplemental methods. All patients and investigators were masked to treatment assignment.

Analysis of primary and secondary endpoints

A detailed description of each study visit can be found in the online supplemental methods. Mixed-meal tests (for residual beta cell function), intestinal microbiota analyses and immunological assays including fluorescent-activated cell sorting, lymphocyte stimulation assays (LST) and human leucocyte antigen multimer analyses to enumerate CD8 T cell autoimmunity to islet autoantigens (CD8 Quantum dot (QDot)) were performed at 0, 2, 6, 9 and 12 months. Targeted plasma metabolites (Metabolon, Morrisville, North Carolina, USA) were measured at 0, 6 and 12 months. Gastroduodenoscopy with duodenal biopsies was performed at 0 and 6 months to assess small intestinal microbiota and perform quantitative reverse transcription PCR to assess duodenal gene expression (see online supplemental table 1). Biometric measurements and glycaemic parameters were performed on all time points (figure 1B). For a detailed description of these analysis techniques, please refer to the online supplemental methods.

Power calculation

A sample size of 17 patients in each group (34 patients in total) was needed to provide 80% power to detect a 50% difference in the Mixed Meal Test (MMT)-stimulated C peptide area under the curve (AUC) (360 mmol/L/min vs 180 mmol/L/min with an SD of 170 mmol/L/min) between treatment groups at 12 months[26 27] with a two-sided test at α=0.05 and assuming a 10% dropout. This cut-off point was chosen because it is an established cut-off point in T1D research commonly employed by other intervention studies in T1D.[27] All analyses were based on the prespecified intention-to-treat cohorts. Complete case analysis was done for the primary endpoint, the immunological parameters that are mentioned in the text and figures and for faecal microbiota and metabolites. Missing values in other (secondary) endpoints were assumed to be missing at random or completely at random. Details on missing values are found in the online supplemental methods (under subheading 'missing values'). The primary endpoint of the trial was the preservation of (MMT stimulated) C peptide release at 6 and 12 months compared with baseline (0 months). This primary endpoint was thus chosen because this study focuses mainly on gut microbiota mediated effects on beta cell function. Although there are better clinical markers to monitor diabetes treatment effect such as A1c, homeostatic model assessment (HOMA) or number of daily insulin units, these are affected by endogenous insulin production and by diet, insulin compliance and insulin resistance; therefore, we did not consider these markers useful as primary endpoint for our study. The study was conducted at the Academic Medical Center (Amsterdam), in accordance with the Declaration of Helsinki (updated version 2013). All participants provided written informed consent. The study was prospectively registered at the Dutch trial registry (https://www.trialregister.nl/

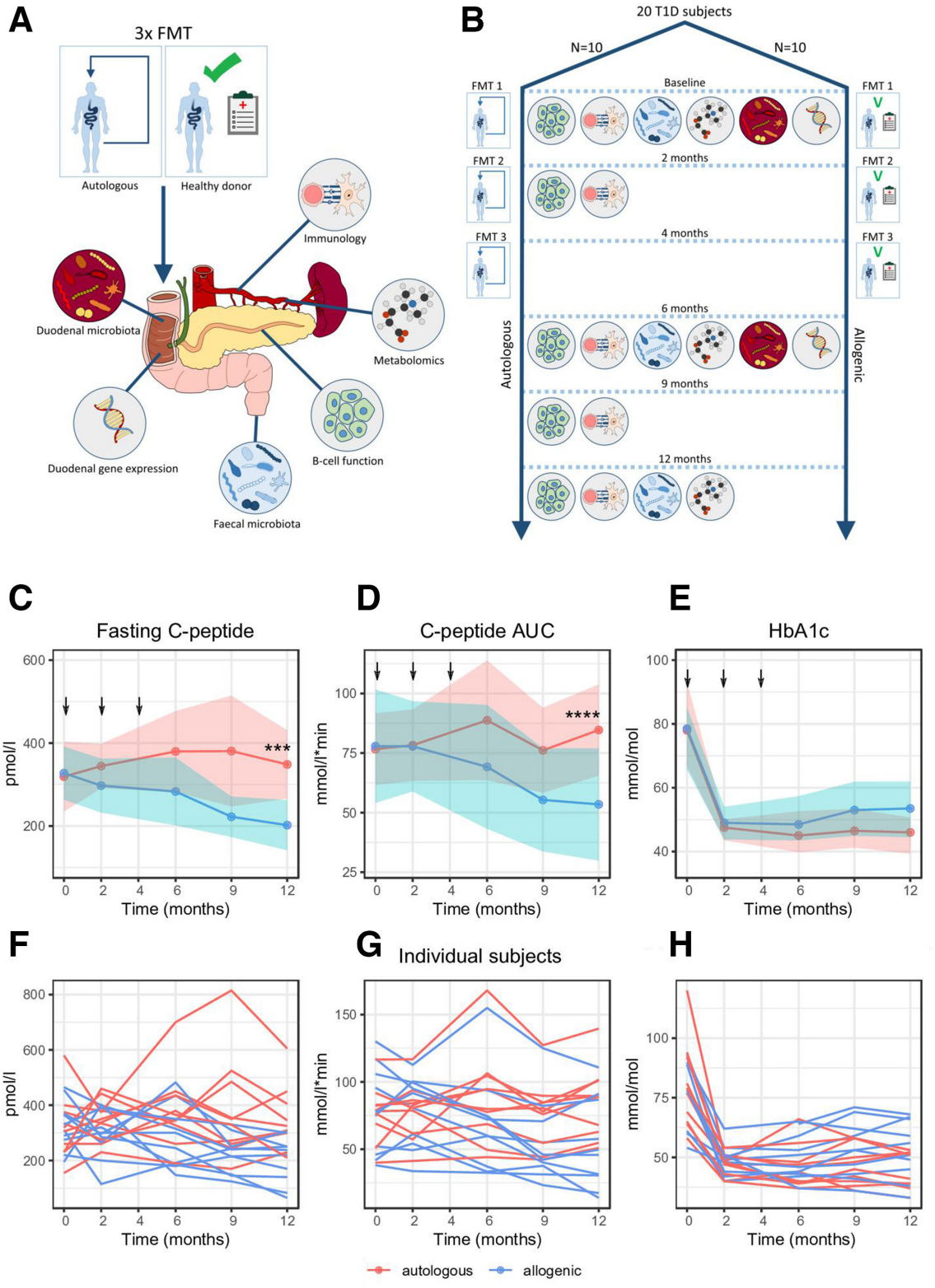

Figure 1 Schematic overview of study. (A) Study schematic showing which analyses were performed. (B) Study timeline showing FMTs were performed at 0, 2 and 4 months and which analyses where performed at each follow-up time point. (C) Change in fasting C peptide over time. Arrows indicate when FMT (allogenic: blue and autologous: pink with width of colour band indicating SD) was performed. Ribbons indicate CIs. Significance was calculated using LMM (see methods), *** p=0.00019. P values calculated using a Student's t-test between groups at each time point were p=0.028 at 9 months and p=0.0049 at 12 months. (D) Change in C peptide AUC over time. Significance was calculated using LMM, **** p=0.000067. P value calculated using a Student's t-test between groups at 12 months was p=0.033. (E) Change in A1c over time. Significance was calculated using LMM, p=0.12. P value calculated using a Mann-Whitney U test between groups at 12 months was p=0.19. SDs are depicted by the coloured width in the respective figures. (F, G and H) Individual trend lines for fasting C peptide, C peptide AUC and A1c respectively. AUC, area under the curve; FMT, faecal microbiota transplantation; LMM, linear mixed model; T1D, type 1 diabetes.

trial/3542). The safety of the patients was guarded by an independent Data Safety Monitoring Board (DSMB). Patients were not involved in the research process.

Statistical analysis, machine learning and follow-up statistical analyses

Details regarding statistical analysis of the primary and secondary endpoints are described in the online supplemental methods. To identify which parameters (either as values at baseline or as relative changes) best predicted treatment groups and responders versus non-responders, we applied the Extreme Gradient Boosting (XGBoost) machine learning classification algorithm,[28] in combination with a stability selection procedure.[29] An overview of these predictive model analyses with area under the receiver-operator curve (AUROC) values and top three predictive features from each model is provided in online supplemental table S2. Details regarding these analyses are described in the online supplemental methods.

Analysis of responders and non-responders irrespective of treatment group

Effects of autologous FMT were not surprising, as it affects homeostasis by introducing faecal microecology into the much less densely populated small intestine.[30] Therefore, post hoc analyses were performed studying responders compared with non-responders to FMT, irrespective of treatment group, of which the most relevant features are shown in online supplemental table 2. Details regarding these analyses are described in the online supplemental methods.

RESULTS

Patients were included between 2013 and 2017. Patients with new-onset T1D (referred by their treating physician) were randomly assigned to donor FMT (n=11 subjects) or autologous FMT (n=10 subjects). One participant retracted consent after the first study visit before FMT intervention was performed. Due to lack of funding, the trial was stopped after 20 subjects were enrolled and completed the study protocol. Baseline characteristics are shown in table 1. Seven healthy lean donors (of whom three were used twice) donated for the allogenic gut microbiota transfer to patients with new-onset T1D, and the same donor was used for the three consecutive FMTs in an individual patient with T1D. There were no differences at baseline between both groups, and gastroenterological interventions were well tolerated in all subjects throughout the follow-up period. Also, there were no serious adverse clinical events nor adverse changes in plasma biochemistry observed.

Autologous FMT preserves (stimulated) C peptide levels compared with allogenic FMT

Mean fasting plasma C peptide at baseline was similar between groups (319 pmol/L±118 (SD) in the autologous group vs 327±89 in the allogenic group; p=0.86, Student's t-test) but preserved in the autologous FMT group compared with

Table 1 Baseline characteristics

Variable	Measure	Autologous group (n=10)	Allogenic group (n=10)	P value
Sex (M:F)	Amount	8:2	8:2	0.92
Age (at diagnosis, years)	Mean	25.0±3.5	24.3±5.4	0.73
Weight (kg)	Mean	75.0±13.0	71.0±10.9	0.46
BMI (kg/m²)	Mean	23.0±2.0	21.8±2.5	0.24
Insulin use per day (IU)	Mean	37±13	30±15	0.26
Daily insulin use (IU/kg/day)	Mean	0.49±0.13	0.43±0.24	0.55
HbA1c (mmol/mol)	Median	78 (66–90)	78.5 (67–90)	0.68
Fasting C peptide (pmol/L)	Mean	319±118	327±89	0.86
Microalbumin/creat ratio (mg/mmol)	Median	0.38 (0.34–0.41)	0.84 (-0.59–2.26)	0.31
C peptide AUC (mmol/L/min)	Mean	77±21	78±33	0.92
Anti-GAD (U/mL)	Median	110 (46–173)	103 (57–149)	0.85
Anti-IA2 (U/mL)	Median	696 (291–1094)	623 (345–901)	0.87
Ketoacidosis (DKA) at diagnosis	Amount	4/10	4/10	0.92
CRP (mg/L)	Median	0.8 (-20–22)	0.7 (-13–15)	0.83
Leukocytes (×10^9/L)	Mean	5.7±2.5	6.0±1.3	0.71
Faecal calprotectin (mg/kg)	Median	42 (21–63)	26 (12–40)	0.15
Total cholesterol (mmol/L)	Mean	4.7±1.0	4.4±0.37	0.39
HDL-c (mmol/L)	Mean	1.41±0.31	1.58±0.43	0.34
LDL-c (mmol/L)	Mean	2.90±0.89	2.46±0.37	0.16
Triglycerides (mmol/L)	Mean	0.86±0.47	0.81±0.41	0.78
Total caloric intake (kcal/day)	Mean	1999±548	2051±512	0.83
Fat intake (g/day)	Mean	78±23	123±74	0.09
Sat. fat intake (g/day)	Mean	45±55	64±70	0.51
Protein intake (g/day)	Mean	124±73	99±35	0.34
Carbohydrate intake (g/day)	Mean	176±92	220±143	0.41
Fibre intake (g/day)	Mean	27±12	27±8	0.97

For normally distributed parameters, the mean is shown ±SD, and p values were calculated using a Student's t-test and for not normally distributed parameters, the median with IQR (P25–P75) is shown, and the p value was calculated using Mann-Whitney U test.
Anti-GAD, antiglutamic acid decarboxylase; anti-IA2, anti-islet antigen 2; AUC, area under the curve; BMI, body mass index; CRP, C-reactive protein; DKA, diabetic ketoacidosis; HbA1c, hemoglobin A1c; HDL, high-density protein cholesterol; LDL, low-density protein cholesterol.

Table 2

Test	Baseline			6 months			12 months		
	Auto (n=10)	Allo (n=10)	P value	Auto (n=10)	Allo (n=10)	P value	Auto (n=10)	Allo (n=10)	P value
C peptide, fasting (pmol/L)	319±118	327±89	0.86	380±136	283±114	0.1	348±115	202±85	0.0045
C peptide, peak (t=90 min)(pmol/L)	766±264	748±369	0.9	855±350	671±371	0.27	805±255	511±342	0.043
C peptide, AUC (mmol/L/min)	77±21	78±33	0.92	89±35	69±36	0.24	85±27	53±33	0.032
Insulin dose (IU/kg/day)	0.49±0.13	0.43±0.24	0.55	0.41±0.10	0.37±0.18	0.57	0.47±0.10	0.45±0.18	0.71
HbA1c (mmol/mol)	78 (66–90)	78.5 (67–90)	0.68	45 (41–49)	48.5 (41–56)	0.41	46 (40–53)	53.5 (44–63)	0.19

The means±SD in the autologous and allogenic group at baseline, 6 and 12 months follow-up are shown. P values were calculated using the Student's t-test. For HbA1c, the median and IQR (P25-P75) is shown, and the p value was calculated using a Mann-Whitney U test as it is not normally distributed. C peptide peak was measured at 90 min after ingestion of a mixed meal test. C peptide AUC designates the AUC of 120 min after the mixed meal with blood sampling at 0, 15, 30, 45, 60, 90 and 120 min.
AUC, area under the curve.

deterioration the allogenic FMT group at 12 months (348 pmol/L±115 vs 202±85, Student's t-test p value=0.0049; linear mixed models (LMMs) p=0.00019, figure 1C and F). A similar effect was seen in residual beta cell function as expressed by stimulated C peptide response AUC, which was equal at baseline (77 mmol/L/min±21 in the autologous group vs 78±33 in the allogenic group; p=0.92, Student's t-test) but significantly more preserved at 12 months after autologous FMT (85 mmol/L/min±27 vs 53±33, Student's t-test p value=p=0.033, LMM p value=0.000067, figure 1D and G). As expected, after exogenous insulin treatment started after T1D diagnosis A1c levels decreased in both the autologous and allogenic FMT groups at 12 months. Similar amounts of daily exogenous insulin (0.47 IU/kg/day vs 0.45 IU/kg/day, p value 0.71, respectively) were provided. No significant improvement of glycaemic control was noticed in the autologous FMT group compared with the allogenic FMT group (A1c 46 vs 53.5 mmol/mol, p=0.19, Mann-Whitney U test (MWU) p=0.19, LMM p value=0.12, figure 1E and H). Glucometabolic parameters at 0, 6 and 12 months are shown in table 2. Finally, weight, faecal calprotectin, microalbuminuria, lipid profiles and dietary intake (separate assessment of total calories, fat, saturated fat, protein, carbohydrates and fibre) were not different at baseline (table 1) nor during the course of the study (online supplemental figure S1A-E shows dietary parameters and S1F shows weight).

T cell immunology changes in a similar fashion in autologous and allogenic FMT-treated group

A wide range of innate and adaptive immune cell phenotypes samples were analysed from whole blood (baseline medians in each group are listed in online supplemental table S3). Individual T cell responses against IA-2, GAD65 and preproinsulin (proliferation assay and LST) or blood frequencies of islet autoreactive CD8+ T cells (Qdot) showed no significant differential change between treatment groups using predictive modelling or MWU at the study time points 6 and 12 months. Similarly, frequencies of islet autoreactive CD8+ T cells did not differ significantly between treatment groups. In addition, FMT did not cause significant changes in the frequency of 35 leucocyte subsets as defined by flow cytometry (online supplemental figure 2). Of note, however, CD4+ CXCR3+ cells did change differentially between groups (p=0.01, MWU). The change between the baseline and 12 months correlated negatively with a change in our primary endpoint C peptide AUC (p=0.046, rho=−0.47) (online supplemental figure 3A-C). CD8+ CXCR3+ cells were different between study groups at baseline (p=0.0076, MWU). Change in CD8+ CXCR3+ cells also differed between treatment groups; however, this did not correlate with changes in C peptide AUC (online supplemental figure 3D-F).

Treatment allocation of FMT is associated with changes in (small) intestinal gut microbiota composition and plasma metabolites

Alpha diversity of the small intestinal microbiota was not significantly different between treatment groups at baseline. At 6 months, there was a borderline significant difference between autologous and allogenic FMT group (p=0.054) concomitant with a significant increase in diversity in the allogenic FMT group (p=0.009; figure 2A). When plotted along ordination axes in a redundancy analysis (RDA-plot), small intestinal microbiota compositions clustered differently at baseline between groups and also changed between treatment groups (figure 2B). FMT treatment group allocation could be predicted reliably by change in specific small intestinal bacterial strains (AUROC 0.89±0.18 (CI)) including two species of *Prevotella* and *Streptococcus oralis* (figure 2C). However, changes on the phylum, family, genus and species level showed no major shifts in small intestinal microbiota composition (online supplemental figure 4). Relative abundances of all these species decreased after autologous faecal transplantation, but increased after allogenic faecal transplantation (figure 2D–F). Of note, the relative abundance of *Prevotella 1* showed a baseline difference between groups (p=0.033). The delta was significantly different between groups for *Prevotella 2* (p=0.048) but not for *Prevotella 1* (p=0.069) or *S. oralis*. Furthermore, a significant inverse correlation was observed between *Prevotella 1* relative abundance and stimulated C peptide AUC (Spearman p=0.015, rho=−0.55, see figure 2G). Of note, change in duodenal gene expression (measured at 0 and 6 months) did not predict treatment group allocation reliably (AUROC of 0.61±0.22).

Faecal microbiota changes upon FMT

Faecal microbiota composition was different between T1D and healthy donors at baseline and also changed differentially between treatment groups (online supplemental figure S5A and B). However, alpha diversity did not differ significantly between FMT treatment groups at baseline, 6 or 12 months

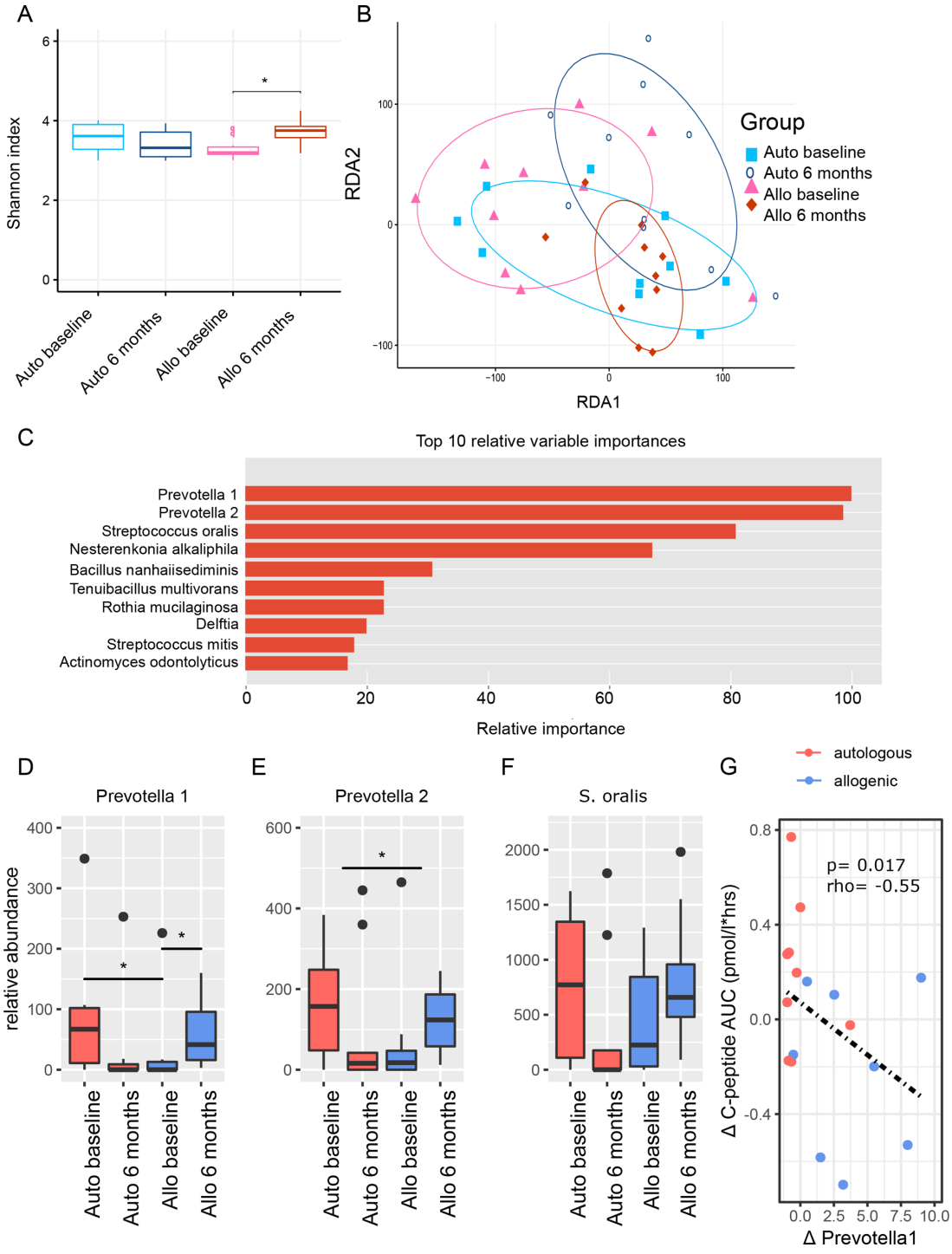

Figure 2 Small intestinal microbiota. (A) Boxplots of Shannon diversity between treatment groups at baseline and 6 months, which is the moment at which follow-up duodenal biopsies were taken. (B) RDA-plot showing clustering of treatment groups at baseline and at 6 months follow-up. (C) Top 10 small intestinal microbiota with relative importance that best predicted treatment group allocation allocation (XGBoost predictive modelling algorithm). Percentages are scaled towards the largest which is set at 100%. The top four microbiota stand out with higher relative importance. (D–F) Boxplots of top three small intestinal microbiota before and 6 months after FMT. P values were calculated using Mann-Whitney U test. The upper p value '(delta)' was calculated by doing Mann-Whitney U test between the relative delta's ((value after – value before)/value before) between treatment groups. Panel D: *Prevotella 1* auto baseline versus allo baseline p value=0.033, *Prevotella 1* allo baseline versus allo 6 months p value=0.049, *Prevotella 2* delta auto versus delta allo p value=0.048, *Streptococcus oralis* auto baseline versus auto 6 months p value=0.012. Figure part G shows the Spearman correlation between our top microbe *Prevotella 1* and our primary endpoint of Mixed Meal Test (MMT) stimulated C peptide release. FMT, faecal microbiota transplantation; RDA, redundancy analysis.

nor between donors and recipients. Some shifts were seen on phylum, family, genus and species level between groups (online supplemental figure 5). Group allocation prediction based on faecal microbiota taxonomic changes between 0 and 12 months showed a moderate AUROC of 0.72±0.24. *Desulfovibrio piger* stood out as the most differentiating bacterial strain between

treatment groups (online supplemental figure 6A). Treatment group prediction based on metabolic pathways showed a relatively poor AUROC of 0.68±0.27. The most differentiating metabolic pathway between both FMT groups was the selenoamino acid biosynthesis pathway (online supplemental figure 6B). Interestingly, abundance of *D. piger* changed differentially between treatment groups at 6 (p=0.024, MWU) and 12 (p=0.023) months follow-up (figure 3A–B). Furthermore, change in *D. piger* correlated positively with change in fasting C peptide (p=0.009, figure 3C) and with plasma 1-arachidonoyl-GPC levels (p=0.004, figure 3D, this metabolite is discussed in the next paragraph). Moreover, a change in relative abundance of *D. piger* was inversely correlated with changes in relative abundance of both *Prevotella 1* (figure 3E) and *Prevotella* 2 (figure 3F).

Plasma metabolite changes upon FMT

Treatment group allocation was predicted reliably by change in fasting plasma metabolites between 0 and 12 months (AUROC 0.79±0.23). The relative importance of the 10 most predictive metabolites are shown in figure 3G. From the top three metabolites, *1-myristoyl-2-arachidonoyl-GPC (MA-GPC)* (p=0.02, MWU) and *1-arachidonoyl-GPC* (A-GPC) (p=0.02), but not *1-(1-enyl-palmitoyl)−2-linoleoyl-GPE* (EPL-GPE), were different between groups at 12 months (figure 3H–J). Also, changes in plasma MA-GPC levels correlated significantly with changes in fasting C peptide (p=0.012, MWU, figure 3K) as well as overall plasma metabolites changes over time between FMT groups and donors (figure 3L).

Baseline faecal microbiota composition, baseline faecal metabolic pathways and baseline duodenal gene expression predict FMT response

We next performed post hoc analyses to study if baseline faecal microbiota composition predicted clinical response on FMT (figure 4A–B), which indeed was the case (AUROC 0.93±0.14). In this regard, intestinal levels of *Bacteroides caccae* and *Coprococcus catus* stood out as most differentiating microbes (online supplemental figure 7), both of which were significantly more abundant at baseline in responders than in non-responders (figure 4C–D). Other differentiating intestinal bacterial strains, *Paraprevotella* spp, *Collinsella aerofaciens*, *Bacteroides eggerthii* and *Ruminococcus callidus* were also significantly different at baseline between responders and non-responders (online supplemental figure 8A-E). A borderline significant negative correlation was observed between change in *C. catus* abundance and stimulated C peptide AUC (p=0.053, r=−0.44, figure 4E).

In contrast, response to treatment was predicted less accurately by change in faecal microbiota composition (AUROC 0.76±0.23) than by baseline composition. Nevertheless, the species of which change best differentiated response were *Bacteroidales bacterium ph8, Actinomyces viscosus, Bacteroides thetaoitaomicron, Streptococcus salivarius, Ruminococcus bromii* and *Clostridium leptum* (online supplemental figure 9A), of which *B. bacterium ph8* (p=0.015, MWU) and *R. bromii* (p=0.013) became less abundant in responders versus non-responders, *S. salivarius* (p=0.045) became more abundant in responders versus non-responders and *B. thetaiotaomicron* was significantly different at baseline and showed a downwards trend in responders (online supplemental figure 9B-I).

Similarly, clinical response was more accurately predicted by baseline faecal microbial metabolic pathways (AUROC 0.85±0.22) than by change in faecal microbial metabolic pathways (AUROC 0.69±0.27). Metabolic pathways of which baseline abundance best predicted response included fatty acid and beta oxidation I, pyruvate fermentation to acetone and colanic acid building blocks biosynthesis (online supplemental figure 10), which were significantly higher in responders versus non-responders at baseline (p=0.014, p=0.0015 and p=0.015 respectively, MWU, figure 4F–H). However, there was no significant differential change in these pathways between responders versus non-responders. Also, neither baseline abundance of these pathways nor change in these pathways correlated with the primary endpoint (MMT stimulated C peptide response).

In line, baseline duodenal gene expression predicted clinical response more accurately (AUROC 0.83±0.21) than change in duodenal gene expression (AUROC 0.73 ± 0.24). At baseline, the most differentiating genes were CCL22, CLDN12, CCL4, CD86, CCL13, CCL19, CXCL12, CLDN14, CX3CL1 and CXCL1 (figure 5A), while CCR5 and CCL18 (figure 5B) were the genes with the most notable differential change. Expression of several of these genes was significantly different between responders and non-responders at baseline: CCL22 (p=0.0039, MWU), CCL19 (p=0.011), CXCL12 (p=0.0039), CXCL1 (p=0.021) and CCR5 (p=0.015) (figure 5C–G). Moreover, baseline values of these genes correlated well with change in stimulated C peptide AUC (figure 5H–L). Interestingly, all these genes decreased after FMT treatment, but only the decrease in CCL19 (p=0.049) was statistically significant. Finally, gene expression of tight junction protein CLDN12 was high in non-responders at baseline (online supplemental figure S11A), while gene expression of CCL4 and CD86 were higher in responders (online supplemental figure S11B and C).

Integration of multiomics analyses

Correlations between parameters found to be significantly affected by FMT were explored. Since responders were found in both treatment groups, correlations were first explored in our pooled dataset (n=20) (figure 6A) and then within treatment groups separately (figure 6B and C) and in clinical responders to FMT (online supplemental figure S12). In the pooled dataset (figure 6A), an intertwined cluster of notable parameters was found which positively and negatively associated with markers of glucose regulation (ie, C peptide AUC, fasting C peptide and A1c; figure 6A). On one hand, the highly correlated plasma metabolites MA-GPC and A-GPC accurately predicting preservation of insulin secretion, correlate positively to *D. piger*, which correlates positively to fasting C peptide. On the other hand, *Prevotella 1*, *Prevotella 2* and *S. oralis* correlate negatively to glucose regulation and to the metabolites MC-GPC and A-GPC. In addition, residual beta cell function correlates negatively to CCL22 activity and CD4+ CXCR3+ T cells, which in turn correlate negatively to *D. piger*. Analysing treatment groups separately, preserved beta cell function (high C peptide) in the autologous group was characterised at baseline by high *C. catus*, high induction of the colanic acid biosynthesis, fatty acid and beta oxidation pathways and high CCL22 and CXCL12 expression, as well as a subsequent decrease in *R. bromii*, which correlates negatively with these two pathways and CCL22 at baseline (figure 6B). In the allogenic group, preserved beta cell function was characterised by a decrease in faecal *Roseburia intestinalis* and a decrease in the UMP biosynthesis pathway (which incidentally correlates positively with *Prevotella 1* and *2*) and a decrease in CD86 and CCL18 expression, which were both higher in responders at baseline and subsequently decreased. Both CD86 and CCL18 genes in turn correlate with *R. intestinalis*, while CCL18 in addition correlates positively with the UMP

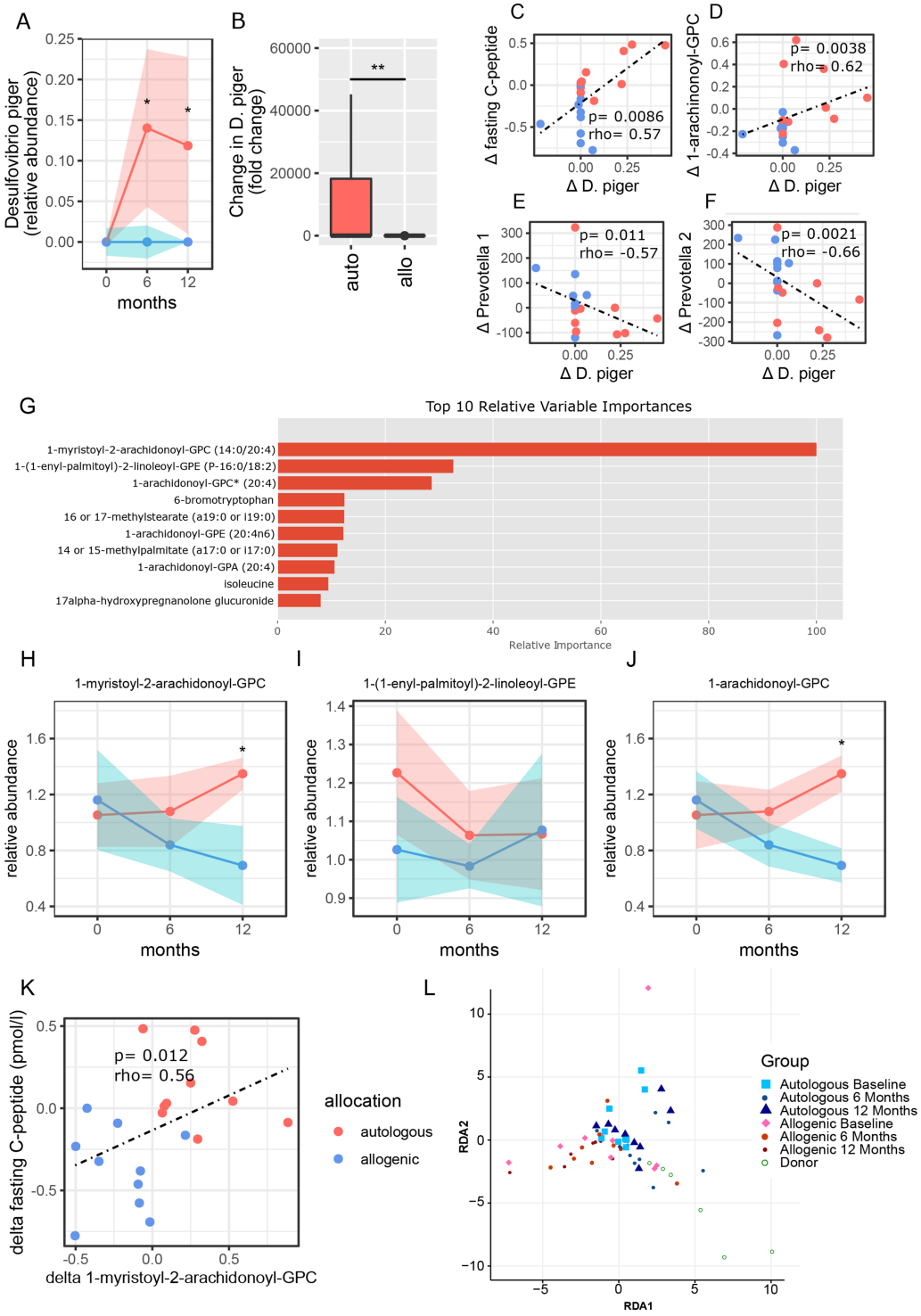

Figure 3 Correlations of clinical outcomes with plasma metabolites and *Desulfovibrio piger*. (A) Abundance of faecal *D. piger* over time (allogenic: blue, and autologous: pink with width of colour band indicating SD). P values were calculated using Mann-Whitney U test. At 6 months p value=0.024, at 12 months p value=0.023. (B) Fold change in *D. piger* between the groups (allogenic: blue and autologous: pink). The delta p value was calculated by doing Mann-Whitney U test on the delta's between 0 and 12 months of each group, p value=0.006. (C) Spearman correlation plot of delta (0–12 months) faecal *D. piger* and delta (0–12 months) of fasting C peptide. (D) Correlation plot of faecal *D. piger* and 1-arachidonoyl-GPC. (E) Correlation plot of faecal *D. piger* and small intestinal *Prevotella 1*. (F) Correlation plot of faecal *D. piger* and small intestinal *Prevotella 2*. (G) Top 10 metabolites that best predicted treatment group allocation allocation (XGBoost predictive modelling algorithm). Percentages are scaled towards the largest, which is set at 100%. Top three metabolites stand out with higher relative importance in the analysis. (H–J) Relative abundance of top three metabolites plotted against time (allogenic: blue and autologous: pink with width of colour band indicating SD). Medians±IQR (P25–P75) are reported. P values were calculated using Mann-Whitney U test between groups at 12 months. 1-myristoyl-2-arachidonoyl-GPC is different between groups at 12 months, p value=0.020. 1-arachidonoyl-GPC is different between groups at 12 months, p value=0.020. (K) Spearman correlation between change in fasting C peptide and change in 1-myristoyl-2-arachidonoyl-GPC. (G) RDA of fasting plasma metabolites over time in T1D compared with healthy donors. T1D, type 1 diabetes.

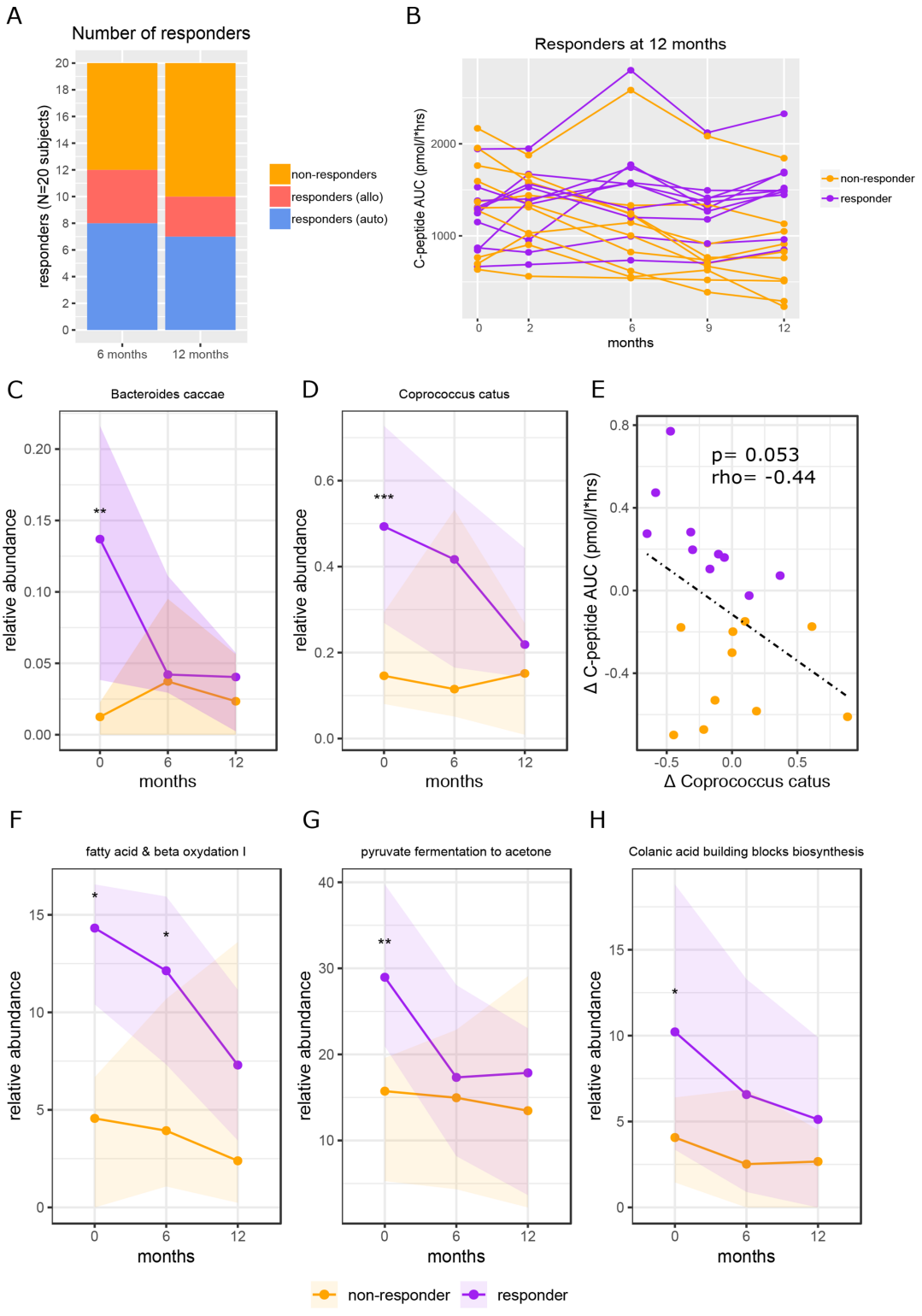

Figure 4 Baseline faecal microbiota and functional pathways in FMT clinical responders versus non-responders. Figure part A shows the number of responders at 6 months and at 12 months and how many subjects were in each treatment group. Response was defined as <10% decline in C peptide AUC compared with baseline. The 12 months responders were used for all analyses. Figure part B shows individual subject lines of C peptide AUC over time. Responders in purple and non-responders in yellow. Figure parts C and D show the abundance of *Bacteroides caccae* and *Coprococcus catus* over time, respectively. P values were calculated using Mann-Whitney U test between groups at each time point. For *B. caccae* at baseline the p value=0.0099, for *C. catus* at baseline the p value=0.00049. Figure part E shows the correlation between delta *C. catus* (0–12 months) and delta C peptide AUC (0–12 months). Spearman's rho (r) is shown, and the p value was calculated using Spearman's rank. Figure part F shows the relative abundance over time of fatty acid and beta oxidation, p value at baseline=0.014, p value at 6 months=0.011; figure part G shows the relative abundance over time of pyruvate fermentation to acetone, p value at baseline=0.0015; figure part H shows the relative abundance of time of the colonic acid building blocks biosynthesis pathways, p value at baseline=0.015. All p values were calculated using Mann-Whitney U test. AUC, area under the curve; FMT, faecal microbiota transplantation.

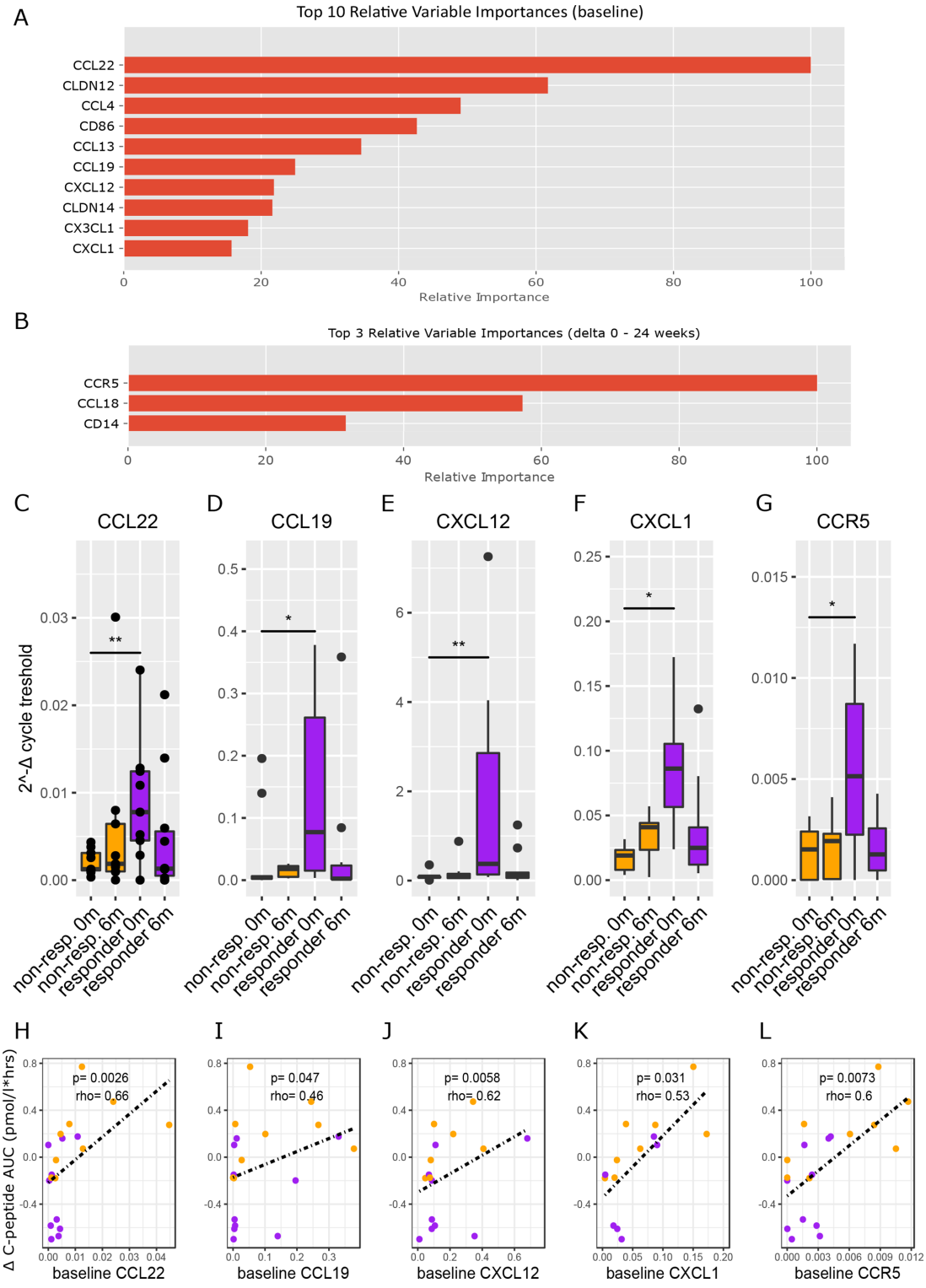

Figure 5 Duodenal gene expression in FMT clinical responders versus non-responders. Figure part A shows the top 10 genes of which baseline expression best differentiated responders from non-responders. Figure part B shows the top three genes of which change in gene expression (0–6 months) best differentiated responders from non-responders. Figure parts C–G show the genes from figure 5A that were significantly different between responders and non-responders at baseline. P values were calculated using Mann-Whitney U test between groups at each time point. Panel C p value=0.0039, panel D p value=0.011, panel E p value=0.0039, panel F p value=0.021, panel G p value=0.015. Figure parts H–L show the Spearman correlations between baseline expression of the genes from figure 5C–G and change in C peptide AUC. AUC, area under the curve; FMT, faecal microbiota transplantation.

biosynthesis pathway (figure 6C). Finally, in clinical responders, preserved beta cell function was characterised by decreases in duodenal *Prevotella 1*, *Prevotella 2*, faecal *C. catus*, metabolite EPL-GPE, the pathway fatty acid and beta oxidation and CD4+ CXCR3+ T cell s, whereas *D. piger* increased (online supplemental figure S12).

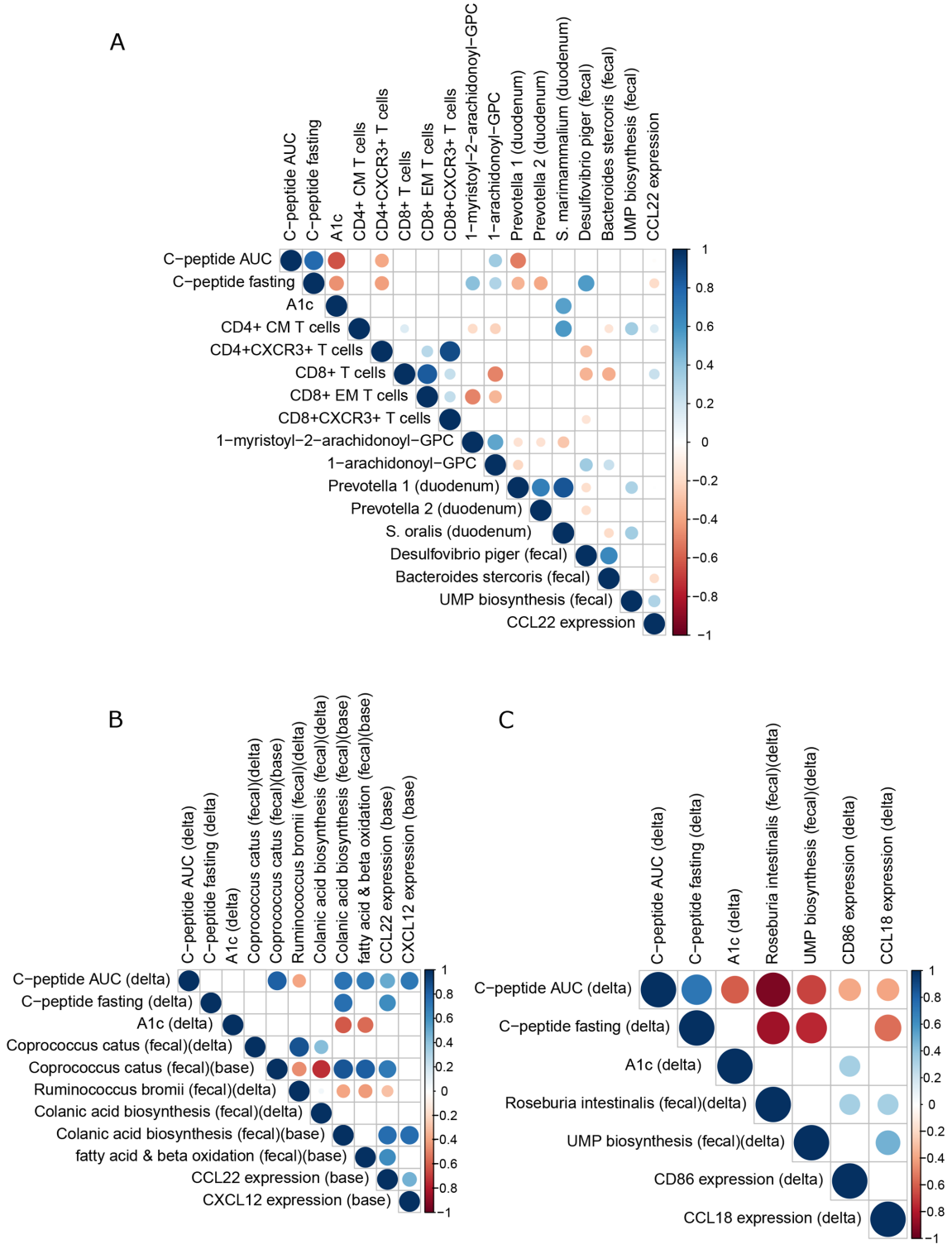

Figure 6 Correlation plots with altered plasma metabolites, bacterial strains and residual beta cell function on FMT. (A) Plot showing Spearman correlations of all subjects pooled (n=20). Only significant (p<0.05) correlations are shown. Red designates a negative correlation and blue a positive correlation. Dot size corresponds to p value (larger is smaller) and dot colour to correlation strength (Spearman's rho). This plot was derived from a larger plot from which all parameters that did not correlate with our primary endpoint and/or any key parameters were removed. (B) As figure part A, for autologous treatment group. (C)aAs figure part A, for the allogenic treatment group. AUC, area under the curve; FMT, faecal microbiota transplantation.

DISCUSSION

We here report for the first time that FMT can have an effect on residual beta cell function in new-onset T1D. This accords with recent observational studies supporting a role for the intestinal microbiota in T1D subjects.[8–12] In contrast to our hypothesis, autologous FMT performed better than healthy donor FMT, while even in the allogenic group, the decline in MMT stimulated C peptide response appeared less than expected in T1D

without treatment in 1 year.[26 27] An appealing explanation would be that beneficial immunological effects of FMT (irrespective of donor source) are more pronounced and durable when the FMT donor microbiota is more immunologically compatible with the host. We suspect that allogenic FMT increases the already present increase in inflammation that is known to occur around the time of diagnosis,[31] by offering immunologically foreign colonic microbiota to which the host is less tolerant to the small intestine (where the T cells are thought to be trained[32]), which may overshadow beneficial effects that occur simultaneously and are caused by different agents. In contrast to animal studies, the beneficial effect of FMT was not associated with changes in SCFA-producing strains.[21] Nevertheless, observations point towards an immunological regulatory role of specific plasma metabolites that are derived from diet and converted by intestinal microbiota.[33]

Preservation of beta cell function by autologous FMT is T cell mediated

A number of studies targeting T cells have shown delayed loss of beta cell function in T1D.[1 3–5 34 35] Our study underscores that beta cell preservation after transplantation of host colonic microecology is T cell mediated, as CD4+ CXCR3+ and CD8+ CXCR3+ T cells were decreased differentially in the responders at 12 months. Beta cells are known to attract autoreactive T cells through the production of ligands (ie, CXCL9, 10 and 11) that bind to CXCR3.[36–38] Also, it is known that the putative immunological changes occur not peripherally but locally in the pancreas and draining lymph nodes, the small intestinal mucosa or the gut-draining lymph nodes.[39] Indeed, altering tone of the regulatory T cells residing in the small intestinal mucosa can prevent T1D.[40 41] Furthermore, we identified that baseline expression of CCL22 in small intestine was a strong predictor of clinical response. It has been previously published that small intestinal CCL22 expression is higher in T1D subjects versus controls,[17] and CCL22 has been previously suggested as novel therapeutic strategy for T1D, for example, protecting against autoimmunity in NOD mice by activating and recruiting regulatory T cells and decreasing the number of CD8+ T cells.[42 43] CCL4 expression was also higher in our responders, while in NOD mice CCL4 is required in protection from T1D by neutralising IL-16[44] and is also required by T cells for IL-4-mediated protection from T1D.[45] Also, small CD86 expression was higher in our clinical responders than in non-responders, which is interesting as CD86 is required for full T cell activation and also a target of Abatacept, which can postpone decline beta cell function in T1D subjects.[4 46]

Preservation of beta cell function is associated with changes in specific gut microbiota strains

In line with previous literature,[47] we propose that *D. piger* dampens autoimmunity in T1D via *plasma 1-arachidonoyl-GPC* thus affecting CXCR3+ T cells. Predictive modelling showed that baseline faecal microbiota taxonomy and metabolic pathways accurately predicted response at 12 months. However, the identified microbes (eg, *B. caccae* and *C. catus*) did not correlate with any of our relevant immune parameters, small intestinal genes or plasma metabolites. This suggests that faecal microbiota composition is consequence rather than cause of the host immunological characteristics that associate with response. The exception to this was *D. piger*, a sulfate-reducing bacterial strain that was previously shown to shape individual responses of gut microbiota to diet.[48] Its beneficial effects may be mediated by its production of hydrogen sulfide, a molecule that was found to have neurostimulatory effects[49] and affect regulatory T cells and immune homeostasis.[50] Moreover, we identified *D. piger* as outstanding faecal microbial predictor of FMT treatment group allocation. Interestingly, this small intestinal bacterial strain was also beneficially associated with change in stimulated C peptide responses on FMT and its abundance increased in the autologous group and in the overall responders. Interestingly, *D. piger* correlated positively with levels of plasma 1-arachidonoyl-GPC (figure 3I), one of our key metabolites that also associated with improved C peptide production. Moreover, *D. piger* and this metabolite correlate negatively with CD4+ CXCR3+ and CD8+ CXCR3+ T cells, which is in line with previous reports in murine T1D.[51] In conclusion, *D. piger* could be a strong candidate to dampen autoimmunity by suppressing these cells through production of A-GPC, for example, through uptake by protruding dendrites of immune cells into the intestinal lumen.[52] Interestingly, *D. piger* was recently cultured from the human intestinal tract, enabling testing this bacterial strain in human T1D.[53] Other bacterial species in the duodenum that best differentiated between treatment groups were two unnamed *Prevotella* spp and S. *oralis*. In this regard, faecal[8] but not duodenal *Prevotella* has been previously linked to T1D. Our explorative integration of multiomics analyses subsequently show that these *Prevotella* spp and *S. oralis* are negatively associated with our key beneficial metabolite MA-GPC, a glycerophospholipid. In this regard, other phospholipids have previously been linked to beta cell function in new-onset T1D.[26] *B. stercoris* correlated positively with *D. piger* and A-GPC and negatively with *S. oralis* and CCL22, but did not correlate positively with C peptide. Intriguingly, *B. stercoris* was recently found to be cross-recognised by ZnT8-reactive CD8+ T cells.[19] Finally, changes in *R. bromii* (autologous FMT group) and *R. intestinalis* (allogenic FMT group) were negatively associated with changes in C peptide, although both strains are generally regarded as beneficial microbes that thrive during fibre-rich diets, produce SCFAs and promote intestinal integrity.

Limitations

First, this exploratory RCT stopped enrolment before the calculated sample size was reached. It is of limited sample size, and it was not powered for secondary clinical endpoints such as A1c. However, it paves the way for larger studies to confirm our findings. Although the driving factors of baseline gut microbiota composition for FMT treatment efficacy in new-onset T1D are currently unknown, we speculate that the level of clinical response might be driven by gut microbial strain composition in the FMT (irrespective of donor source) in combination with host factors such as autoimmunological tone. Whether adding a standard dietary intervention could work synergetic with FMT donors better matched to host immunology to optimise clinical metabolic and immunological response requires further study. Second, we attempted to approximate local effects of our intervention by taking duodenal mucosal biopsies at baseline and after 6 months (thus during the active FMT intervention). However, most relevant immunological effects are expected to occur in the pancreas and the pancreatic lymph nodes, compartments that cannot be sampled in living T1D patients. Third, our earliest biological samples were taken 2 months after first FMT. Therefore, changes that may have occurred sooner but have waned may have been missed. Fourth, our population consisted of only adult subjects with consequently slower onset T1D, which may be immunologically different from earlier onset adolescent T1D.[54] Notwithstanding and awaiting confirmation of this pilot

trial in a larger RCT with adult T1D patients, our study also warrants trials applying FMT in younger T1D subjects. Fifth, although insulin resistance plays a modest role in T1D, we have not quantified it in this study. As shown in previous research, insulin sensitivity can be both increased[23 24] and decreased[25] by donor FMT. However unlikely in a state of beta cell failure and absolute insulin deficiency, it is conceivable that FMT has increased insulin sensitivity thereby counteracting increased C peptide release and obscuring observable benefits. Finally, in future studies, we should include a true placebo control group (eg, lavage and duodenal tube placement without FMT) to compare autologous FMT infusions with the 'natural' course of beta cell function decline in new-onset T1D.

CONCLUSIONS

Faecal transplantation of colon-derived microbiome into the host small and large intestine in patients with new onset T1D effectively prolongs residual beta cell function in our study. From this hypothesis-generating study, we report several important findings. First,several novel bacterial strains including faecal *D. piger* and *B. stercoris* as well as duodenal *Prevotella* spp and *S. oralis* were identified with therapeutic potential. Accordingly, increases in plasma phospholipids and tryptophan derivatives such as 1-myristoyl-2-arachidonoyl-GPC and 1-arachidonoyl-GPC as well as 6-bromotryptophan after FMT associated with beneficial changes in small intestinal CCL22 expression and whole blood immune cell subsets such as CXCR3+ CD4+ T cells. While developing the identified leads for assessment in clinical trials in T1D will be challenging and time consuming, FMT itself appears to be a safe treatment modality that can be readily applied in clinical studies to dissect the causal influences of gut microbiota in pathophysiology of T1D. We therefore hope that our exploratory study will spark larger randomised (allogenic vs autologous vs real placebo) FMT trials with a longer follow-up to confirm and expand on our compelling findings of FMT-based intervention in the progressive loss of beta cell function in human T1D.

Author affiliations
[1]Department of Vascular Medicine, Amsterdam University Medical Centres, Amsterdam, Noord-Holland, The Netherlands
[2]Department of Internal Medicine, LUMC, Leiden, Zuid-Holland, The Netherlands
[3]Diabetes Research Institute, IRCCS San Raffaele Scientific Institute, Milan, Italy
[4]Diabetes Research Institute, San Raffaele Scientific Institute, Milan, Italy
[5]Internal Medicine, OLVG Location West, Amsterdam, North Holland, The Netherlands
[6]Internal Medicine, Rijnstate, Arnhem, Gelderland, The Netherlands
[7]Internal Medicine, OLVG, Location Oost, Amsterdam, Noord-Holland, The Netherlands
[8]Internal Medicine, North West Hospital Group, Alkmaar, Noord-Holland, The Netherlands
[9]Internal Medicine, Groene Hart Hospital, Gouda, Zuid-Holland, The Netherlands
[10]Internal Medicine, Deventer Hospital, Deventer, Overijssel, The Netherlands
[11]Internal Medicine, Hospital Amstelland, Amstelveen, North Holland, The Netherlands
[12]Department of Epidemiology and Biostatistics, Amsterdam University Medical Centres, Amsterdam, Noord-Holland, The Netherlands
[13]Department of Gastroenterology, Academic Medical Center, Amsterdam, The Netherlands
[14]Microbiology, WUR, Wageningen, The Netherlands
[15]Department of Diabetes Immunology, Diabetes & Metabolism Research Institute at the Beckman Research Institute, City of Hope, Duarte, CA, USA

Correction notice This article has been corrected since it published Online First. The author affiliations have been updated.

Acknowledgements We acknowledge MDs/nurses P Geelhoed, T M Vriesendorp, H J Aanstoot, R Zwertbroek, A Pijlman, A W van den Beld, I Wakelkamp, A Muller, A Binnerts, W van Houtum, N Posthuma, D Faber, J de Sonnaville, F A J Verburg, N Smit, C Oldenburg, I Bonapart, K Mahmoud, T Paardekoper, C Pronk and T Claassen for inclusion of patients. We are grateful to Hans Heilig and Steven Aalvink for support in the DNA isolation. H R Buller and B A Hutten are acknowledged as DSMB members. Finally, we respectfully acknowledge our participants who selflessly applied themselves to help completing this burdensome project.

Funding This trial was funded by an AMC MD PhD fellowship grant (to Nieuwdorp) on which PFdG was appointed. VS is supported by a grant from EFSD/JDRF/Lilly 2017. BR is Director of the Expert Center of the Dutch Diabetes Research Foundation and Stichting DON, and Director of the Wanek Family Project for Type 1 Diabetes. WMDV was supported by the Netherlands Organization for Scientific Research (Spinoza Award). MN is supported by a ZONMW-VIDI grant 2013 (016.146.327).

Competing interests MN and WMDV are founders and in the Scientific Advisory Board of Caelus Health, the Netherlands. WMDV is Founder and in the Scientific Advisory Board of A-Mansia, Belgium. MN is in the Scientific Advisory Board of Kaleido Biosciences, USA.

Patient consent for publication Not required.

Ethics approval All study procedures were approved by the institutional review board of the Amsterdam UMC (location AMC).

Provenance and peer review Not commissioned; externally peer reviewed.

Data availability statement No data are available.

ORCID iDs
Jacques Bergman http://orcid.org/0000-0001-7548-6955
Lorenzo Piemonti http://orcid.org/0000-0002-2172-2198
Max Nieuwdorp http://orcid.org/0000-0002-1926-7659

REFERENCES

1 Bougnères PF, Landais P, Boisson C, *et al*. Limited duration of remission of insulin dependency in children with recent overt type I diabetes treated with low-dose cyclosporin. *Diabetes* 1990;39:1264–72.
2 Herold KC, Gitelman SE, Ehlers MR, *et al*. Teplizumab (anti-CD3 mAb) treatment preserves C-peptide responses in patients with new-onset type 1 diabetes in a randomized controlled trial: metabolic and immunologic features at baseline identify a subgroup of responders. *Diabetes* 2013;62:3766–74.
3 Haller MJ, Long SA, Blanchfield JL, *et al*. Low-Dose anti-thymocyte globulin preserves C-peptide and reduces A1c in new onset type 1 diabetes: two year clinical trial data. *Diabetes*.
4 Orban T, Bundy B, Becker DJ, *et al*. Co-Stimulation modulation with abatacept in patients with recent-onset type 1 diabetes: a randomised, double-blind, placebo-controlled trial. *Lancet* 2011;378:412–9.
5 Orban T, Bundy B, Becker DJ, *et al*. Costimulation modulation with abatacept in patients with recent-onset type 1 diabetes: follow-up 1 year after cessation of treatment. *Diabetes Care* 2014;37:1069–75.
6 Roep BO, Wheeler DCS, Peakman M. Antigen-Based immune modulation therapy for type 1 diabetes: the era of precision medicine. *Lancet Diabetes Endocrinol* 2019;7:65–74.
7 Atkinson MA, Roep BO, Posgai A, *et al*. The challenge of modulating β-cell autoimmunity in type 1 diabetes. *Lancet Diabetes Endocrinol* 2019;7:52–64.
8 Brown CT, Davis-Richardson AG, Giongo A, *et al*. Gut microbiome metagenomics analysis suggests a functional model for the development of autoimmunity for type 1 diabetes. *PLoS One* 2011;6:e25792.
9 de Goffau MC, Fuentes S, van den Bogert B, *et al*. Aberrant gut microbiota composition at the onset of type 1 diabetes in young children. *Diabetologia* 2014;57:1569–77.
10 de Goffau MC, Luopajärvi K, Knip M, *et al*. Fecal microbiota composition differs between children with β-cell autoimmunity and those without. *Diabetes* 2013;62:1238–44.
11 Davis-Richardson AG, Triplett EW. A model for the role of gut bacteria in the development of autoimmunity for type 1 diabetes. *Diabetologia* 2015;58:1386–93.
12 de Groot PF, Belzer C, Aydin Ömrüm, *et al*. Distinct fecal and oral microbiota composition in human type 1 diabetes, an observational study. *PLoS One* 2017;12:e0188475.

13 Wen L, Ley RE, Volchkov PY, *et al*. Innate immunity and intestinal microbiota in the development of type 1 diabetes. *Nature* 2008;455:1109–13.
14 Hänninen A, Toivonen R, Pöysti S, *et al*. *Akkermansia muciniphila* induces gut microbiota remodelling and controls islet autoimmunity in NOD mice. *Gut* 2018;67:1445–53.
15 Kriegel MA, Sefik E, Hill JA, *et al*. Naturally transmitted segmented filamentous bacteria segregate with diabetes protection in nonobese diabetic mice. *Proc Natl Acad Sci U S A* 2011;108:11548–53.
16 Korsgren S, Molin Y, Salmela K, *et al*. On the etiology of type 1 diabetes: a new animal model signifying a decisive role for bacteria eliciting an adverse innate immunity response. *Am J Pathol* 2012;181:1735–48.
17 Pellegrini S, Sordi V, Bolla AM, *et al*. Duodenal mucosa of patients with type 1 diabetes shows distinctive inflammatory profile and microbiota. *J Clin Endocrinol Metab* 2017;102:1468–77.
18 Desai MS, Seekatz AM, Koropatkin NM, *et al*. A dietary Fiber-Deprived gut microbiota degrades the colonic mucus barrier and enhances pathogen susceptibility. *Cell* 2016;167:1339–53.
19 Culina S, Lalanne AI, Afonso G, *et al*. Islet-reactive $CD8^+$ T cell frequencies in the pancreas, but not in blood, distinguish type 1 diabetic patients from healthy donors. *Sci Immunol* 2018;3:eaao4013.
20 Hand TW, Dos Santos LM, Bouladoux N, *et al*. Acute gastrointestinal infection induces long-lived microbiota-specific T cell responses. *Science* 2012;337:1553–6.
21 Marino E, Richards JL, McLeod KH, *et al*. Gut microbial metabolites limit the frequency of autoimmune T cells and protect against type 1 diabetes. *Nat Immunol* 2017.
22 de Groot PF, Nikolic T, Imangaliyev S, *et al*. Oral butyrate does not affect innate immunity and islet autoimmunity in individuals with longstanding type 1 diabetes: a randomised controlled trial. *Diabetologia* 2020;63:597–610.
23 Vrieze A, Van Nood E, Holleman F, *et al*. Transfer of intestinal microbiota from lean donors increases insulin sensitivity in individuals with metabolic syndrome. *Gastroenterology* 2012;143:913–6.
24 Kootte RS, Levin E, Salojärvi J, *et al*. Improvement of insulin sensitivity after lean donor feces in metabolic syndrome is driven by baseline intestinal microbiota composition. *Cell Metab* 2017;26:611–9.
25 de Groot P, Scheithauer T, Bakker GJ, *et al*. Donor metabolic characteristics drive effects of faecal microbiota transplantation on recipient insulin sensitivity, energy expenditure and intestinal transit time. *Gut* 2020;69:502–12.
26 Overgaard AJ, Weir JM, Jayawardana K, *et al*. Plasma lipid species at type 1 diabetes onset predict residual beta-cell function after 6 months. *Metabolomics* 2018;14:158.
27 Lachin JM, McGee PL, Greenbaum CJ, *et al*. Sample size requirements for studies of treatment effects on beta-cell function in newly diagnosed type 1 diabetes. *PLoS One* 2011;6:e26471.
28 Chen T, Guestrin C. XGBoost: A Scalable Tree Boosting System. In: *Proceedings of the 22nd ACM SIGKDD International Conference on knowledge discovery and data mining*. New York, NY, USA: ACM, 2016: 785–94.
29 Meinshausen N, Bühlmann P. Stability selection. *J R Stat Soc Ser B* 2010;72:417–73.
30 Aron-Wisnewsky J, Clément K, Nieuwdorp M. Fecal microbiota transplantation: a future therapeutic option for obesity/diabetes? *Curr Diab Rep* 2019;19:51.
31 Kostic AD, Gevers D, Siljander H, *et al*. The dynamics of the human infant gut microbiome in development and in progression toward type 1 diabetes. *Cell Host Microbe* 2015;17:260–73.
32 Esplugues E, Huber S, Gagliani N, *et al*. Control of Th17 cells occurs in the small intestine. *Nature* 2011;475:514–8.
33 Zhang J, Yang G, Wen Y, *et al*. Intestinal microbiota are involved in the immunomodulatory activities of longan polysaccharide. *Mol Nutr Food Res* 2017;61:1700466.
34 Herold KC, Hagopian W, Auger JA, *et al*. Anti-Cd3 monoclonal antibody in new-onset type 1 diabetes mellitus. *N Engl J Med* 2002;346:1692–8.
35 Keymeulen B, Vandemeulebroucke E, Ziegler AG, *et al*. Insulin needs after CD3-antibody therapy in new-onset type 1 diabetes. *N Engl J Med* 2005;352:2598–608.
36 Burke SJ, Karlstad MD, Eder AE, *et al*. Pancreatic β-cell production of CXCR3 ligands precedes diabetes onset. *Biofactors* 2016;42:703–15.
37 Frigerio S, Junt T, Lu B, *et al*. Beta cells are responsible for CXCR3-mediated T-cell infiltration in insulitis. *Nat Med* 2002;8:1414–20.
38 Roep BO, Kleijwegt FS, van Halteren AGS, *et al*. Islet inflammation and CXCL10 in recent-onset type 1 diabetes. *Clin Exp Immunol* 2010;159:338–43.
39 Esterházy D, Canesso MCC, Mesin L, *et al*. Compartmentalized gut lymph node drainage dictates adaptive immune responses. *Nature* 2019;569:126–30.
40 Yu H, Gagliani N, Ishigame H, *et al*. Intestinal type 1 regulatory T cells migrate to periphery to suppress diabetogenic T cells and prevent diabetes development. *Proc Natl Acad Sci U S A* 2017;114:10443–8.
41 Tanoue T, Atarashi K, Honda K. Development and maintenance of intestinal regulatory T cells. *Nat Rev Immunol* 2016;16:295–309.
42 Bischoff L, Alvarez S, Dai DL, *et al*. Cellular mechanisms of CCL22-mediated attenuation of autoimmune diabetes. *J Immunol* 2015;194:3054–64.
43 Montane J, Bischoff L, Soukhatcheva G, *et al*. Prevention of murine autoimmune diabetes by CCL22-mediated Treg recruitment to the pancreatic islets. *J Clin Invest* 2011;121:3024–8.
44 Meagher C, Beilke J, Arreaza G, *et al*. Neutralization of interleukin-16 protects nonobese diabetic mice from autoimmune type 1 diabetes by a CCL4-dependent mechanism. *Diabetes* 2010;59:2862–71.
45 Meagher C, Arreaza G, Peters A, *et al*. Ccl4 protects from type 1 diabetes by altering islet beta-cell-targeted inflammatory responses. *Diabetes* 2007;56:809–17.
46 Orban T, Beam CA, Xu P, *et al*. Reduction in CD4 central memory T-cell subset in costimulation modulator abatacept-treated patients with recent-onset type 1 diabetes is associated with slower C-peptide decline. *Diabetes* 2014;63:3449–57.
47 Alcover A, Alarcón B, Di Bartolo V. Cell biology of T cell receptor expression and regulation. *Annu Rev Immunol* 2018;36:103–25.
48 Rey FE, Gonzalez MD, Cheng J, *et al*. Metabolic niche of a prominent sulfate-reducing human gut bacterium. *Proc Natl Acad Sci U S A* 2013;110:13582–7.
49 Schicho R, Krueger D, Zeller F, *et al*. Hydrogen sulfide is a novel prosecretory neuromodulator in the guinea-pig and human colon. *Gastroenterology* 2006;131:1542–52.
50 Yang R, Qu C, Zhou Y, *et al*. Hydrogen sulfide promotes Tet1- and Tet2-Mediated FOXP3 demethylation to drive regulatory T cell differentiation and maintain immune homeostasis. *Immunity* 2015;43:251–63.
51 Blahnik G, Uchtenhagen H, Chow I-T, *et al*. Analysis of pancreatic beta cell specific CD4+ T cells reveals a predominance of proinsulin specific cells. *Cell Immunol* 2019;335:68–75.
52 Morita N, Umemoto E, Fujita S, *et al*. GPR31-dependent dendrite protrusion of intestinal $CX3CR1^+$ cells by bacterial metabolites. *Nature* 2019;566:110–4.
53 Chen Y-R, Zhou L-Z, Fang S-T, *et al*. Isolation of Desulfovibrio spp. from human gut microbiota using a next-generation sequencing directed culture method. *Lett Appl Microbiol* 2019;68:553–61.
54 Battaglia M, Ahmed S, Anderson MS, *et al*. Introducing the Endotype concept to address the challenge of disease heterogeneity in type 1 diabetes. *Diabetes Care* 2020;43:dc190880

Supplementary methods

Abbreviations

ASV – amplicon sequence variant

AUC – area under the curve

AUROC – area under the receiver-operator curve

CMV - cytomegalovirus

CRP – C-reactive protein

EBV – Epstein-Barr virus

ESBL – extended-spectrum beta lactamase

FACS – fluorescent-activated cell sorting

FMT – fecal microbiota transplantation

GAD – glutamate decarboxylase

HDLc – high density lipoprotein cholesterol

HLA – human leukocyte antigen

LDLc – low density lipoprotein cholesterol

LMM – linear mixed models analysis

LST – lymphocyte stimulation test

MMT – mixed meal test

MWU – Mann-Whitney U test

MRSA **–** methicillin-resistant *Staphylococcus aureus*

PBMCs - Peripheral blood mononuclear cells

PCR – polymerase chain reaction

PPI – preproinsulin

Qdot – quantum dot

ROC – receiver-operator curve

RT qPCR – reverse transcription quantitative PCR

T1D – type 1 diabetes

TG - triglycerides

TT – tetanus toxoid

UPLC-MS/MS - ultra high performance liquid chromatography coupled to tandem mass spectrometry

Fecal donor recruitment and randomization

Fecal donors completed questionnaires regarding dietary and bowel habits, travel history, comorbidity including family history of diabetes mellitus and medication use. They were screened for the presence of infectious diseases as described previously[1]. Furthermore, donors with 1st or 2nd degree relatives with autoimmune diseases (including Coeliac disease, autoimmune thyroid disease, type 1 diabetes and rheumatoid arthritis) were excluded. Blood was screened for human immunodeficiency virus; human T-lymphotropic virus; Hepatitis A, B, and C; cytomegalovirus (CMV); Epstein–Barr virus (EBV); strongyloides; amoebiasis, and lues. Presence of infection resulted in exclusion, although previous and non-active infections with EBV and CMV were allowed. Donors were also excluded if screening of their feces revealed the presence of pathogenic parasites (e.g. blastocystis hominis, dientamoeba fragilis, giardia lamblia), multiresistent bacteria (*Shigella*, *Campylobacter*, *Yersinia*, *MRSA ,ESBL, Salmonella, enteropathogenic E. Coli* and *Clostridium difficile*) or viruses (noro-, rota-, astro-, adeno (40/41/52)-, entero-, parecho- and sapovirus) as previously recommended[2]. After an overnight fast, plasma samples were taken for biochemistry and metabolomics and a morning fecal sample was collected.

FMT procedure

Seven healthy lean donors (of whom 3 were used twice) donated for the allogenic gut microbiota transfer to new onset type 1 diabetes (T1D) patients, and the same donor was used for the three consecutive FMT's in an individual T1D patient.

After admission, a duodenal tube was placed by gastroscopy or CORTRAK enteral access system. Each patient then underwent complete colon lavage with 2-4L of Klean prep® (macrogol) by duodenal tube until the researcher judged that the bowel was properly lavaged (i.e. no solid excrement, but clear fluid) for approximately 3h. Then, between 200 and 300 grams of feces was processed by dilution in 500 ml of 0.9% saline solution and filtered through unfolded cotton gauzes. The filtrate was used for transplantation two hours after the last administration of Klean prep® by duodenal tube in around 30 minutes using 50cc syringes. After a short observation period the patient was sent home.

Study visits

All study visits were performed at Amsterdam UMC, location AMC. Participants were asked to fill out an online nutritional diary for the duration of one week before each study visit to monitor caloric intake including the amount of dietary carbohydrates, fats, proteins and fibers. During the study visits blood pressure, weight and daily insulin use were documented. Fasting blood samples were taken at each visit and upon centrifugation stored at -80°C for subsequent analyses. Whole blood sodium heparin tubes were kept on room temperature and processed within 24 hours for immunological analyses (described under immunology).

Description per study visit

All visits took place after an overnight fast with subjects taking no long acting insulin the night before as previously described (Moran et al., 2013). At each visit blood, fecal and urine sampling and biometric measurements took place. At baseline all patients first underwent gastroduodenoscopy. A small dose of midazolam (2.5 or 5mg) was administered for patient's comfort. Duodenal biopsies were immediately collected in sterile tubes, snap-frozen in liquid nitrogen and stored at -80°C, followed by nasoduodenal tube placement. Then at least 2 hours later, a standardized 2h mixed meal test (MMT)(Nestlé sustacal boost®) was performed as previously described[3] to study residual Beta-

cell function. At 2, 9 and 12 months, patients again underwent a mixed-meal test for residual Beta-cell C-peptide secretion. After the 2 hour MMT, a duodenal tube was placed by means of CORTRAK enteral access, bowel cleansing for 6 hours was performed and the fecal transplant procedures were repeated. At 6 months, patients underwent gastroduodenoscopy and biopsies were taken from the duodenum and again thereafter, the mixed-meal test was performed. Of note, the similar daily schedule was used in all patients to minimize variation in measurements between subjects.

Mixed meal test

Starting the evening before each mixed meal test, T1D patients interrupted their long-acting insulin injections as previously published [3]. After an overnight fast and without taking their short-acting morning insulin dose, a mixed meal test was performed with Boost High Protein (Nestlé Nutrition, Vervey, Switzerland) at 6 ml/kg body weight with a maximum of 360 ml per person as previously described[4]. Subsequent blood sampling for stimulated C-peptide was performed at -10, 0, 15, 30, 45, 60, 90 and 120 minutes. Area under the curve (AUC) was derived according to the trapezoidal rule.

Adaptive T-cell Immunity

Whole blood samples were processed within 24 hours after sampling. Peripheral blood mononuclear cells (PBMC's) were used for measurement of immune response. Granulocytes were isolated for DNA-extraction and human leukocyte antigen (HLA) typing.

Isolation of Peripheral blood mononuclear cells (PBMC's)

PBMC's were isolated using Ficoll-density gradient centrifugation (ficoll 5.7%, amidotrizoaat 9%, *Pharmacy Leiden University Medical Centre*). After centrifuging, the interphase containing PBMC's was harvest and washed 3 times using PBS. PBMC's were suspended in 2 ml Iscove's modified

Dulbecco's Medium (IMDM, *Lonza*) supplemented with L-glutamine, penicillin-streptomycin (Pen Strep) and 15% Human serum and counted.

Lymphocyte Stimulation Test (LST)

T-cell proliferation in response to antigenic stimulation was performed as described previously (Kracht, Nature Medicine 2017). Cells were incubated in conditioned medium alone or in the presence of autoantigen proteins glutamate decarboxylase (GAD65), preproinsulin (PPI), insulinoma antigen-1 (IA-2) and a defective ribosomal product of proinsulin mRNA (DRiP) generated by stressed Beta cells[5]. For controls, cells were stimulated with Interleukin-2 (IL-2) or cultured with tetanus toxoid (TT). Cells were incubated for 5 days, after which ^{3}H-thymidine (50µl, 10 µCi/ml) was added for the last 18 hours of the culture.

Fluorescent-activated cell sorting (FACS) analyses and Quantum dot (Qdot)

For phenotyping and quantification of autoreactive CD8+ T-cell s, PBMC were stained with fluorescent antibodies according to a standard, independently validated protocol as described previously [6]. Stained cells were measured using FACS-Canto (phenotyping) and LSR-II (Q-dot) machines (Becton&Dickinson). Phenotyping data were analyzed using FlowJo software (TreeStar) using the gating strategy (supplementary figure 1) or as described previously for Qdot analyses [6].

Plasma metabolites

Fasting plasma targeted metabolite measurements were done by Metabolon (Durham, NC), using ultra high performance liquid chromatography coupled to tandem mass spectrometry (UPLC-MS/MS), as previously described [7]. Raw data was normalized to account for inter-day differences. Then, the levels of each metabolite were rescaled to set the median equal to 1 across all samples. Missing values, generally due to the sample measurement falling below the limit of detection, were then imputed with the minimum observed value for the respective metabolite.

Biochemistry

Glucose and C-reactive protein (CRP, Roche, Switzerland) were determined in fasted plasma samples. C-peptide was measured by radioimmunoassay (Millipore, Amsterdam, The Netherlands). Total cholesterol, high density lipoprotein cholesterol (HDLc), and triglycerides (TG) were determined in EDTA-containing plasma using commercially available enzymatic assays (Randox, Antrim, UK and DiaSys, Germany). All analyses were performed using a Selectra autoanalyzer (Sopachem, The Netherlands). Low density lipoprotein cholesterol (LDLc) was calculated using the Friedewald formula. Calprotectin was determined in feces using a commercial ELISA (Bühlmann, Switzerland). Hba1c was measured by HPLC (Tosoh G8, Tosoh Bioscience)

Fecal sample shotgun sequencing and metagenomic pipeline

Fecal microbiota were analysed using shotgun sequencing on donor and patient samples taken at 0, 6 and 12 months after initiation of study. DNA extraction from fecal samples for shotgun metagenomics was performed as previously described[8]. Subsequently, shotgun metagenomic sequencing was performed (Clinical Microbiomics, Copenhagen, Denmark). Before sequencing, the quality of the DNA samples was evaluated using agarose gel electrophoresis, NanoDrop 2000 spectrophotometry and Qubit 2.0 fluorometer quantitation. The genomic DNA was randomly sheared into fragments of around 350 bp. The fragmented DNA was used for library construction using NEBNext Ultra Library Prep Kit for Illumina (New England Biolabs). The prepared DNA libraries were evaluated using Qubit 2.0 fluorometer quantitation and Agilent 2100 Bioanalyzer for the fragment size distribution. Real time quantitative PCR (qPCR) was used to determine the concentration of the final library before sequencing. The library was sequenced on an Illumina HiSeq platform to produce 2 x 150 bp paired-end reads. Raw reads were quality filtered using Trimmomatic (v0.38), removing adapters, trimming the first 5 bp, and then quality trimming reads using a sliding

window of 4 bp and a minimum Q-score of 15. Reads that were shorter than 70 bp after trimming were discarded. Surviving paired reads were mapped against the human genome (GRCh37_hg19) with bowtie2 (v2.3.4.3) in order to remove human reads. Finally, the remaining quality filtered, non-human reads were sub-sampled to 20 million reads per sample and processed using Metaphlan2[9] (v2.7.7) to infer metagenomic microbial species composition and Humann2[10] (v0.11.2) to extract gene counts and functional pathways. In brief, reads were mapped using bowtie2 against microbial pangenomes; unmapped reads were translated and mapped against the full Uniref90 protein database using diamond (v0.8.38). Pathway collection was performed using the MetaCyc database.

Small intestinal microbiota analyses

Biopsies were added to a bead-beating tube with 300 µl Stool Transport and Recovery (STAR) buffer, 0.25 g of sterilized zirconia beads (0.1 mm). 6 µl of Proteinase K (20mg/ml; QIAGEN, Venlo, The Netherlands) was added and incubated for 1hr at 55 °C. The biopsies were then homogenized by bead-beating three times (60 s × 5.5 ms) followed by incubation for 15 min at 95 °C at 1000 rpm. Samples were then centrifuged for 5 min at 4 °C and 14,000 g and supernatants transferred to sterile tubes. Pellets were re-processed using 200 µl STAR buffer and both supernatants were pooled. DNA purification was performed with a customized kit (AS1220; Promega) using 250 µl of the final supernatant pool. DNA was eluted in 50 µl of DNAse- RNAse-free water and its concentration measured using a DS-11 FX+ Spectrophotometer/Fluorometer (DeNovix Inc., Wilmington, USA) with the Qubit™ dsDNA BR Assay kit (Thermo Scientific, Landsmeer, The Netherlands). The V5-V6 region of 16S ribosomal RNA (rRNA) gene was amplified in duplicate PCR reactions for each sample in a total reaction volume of 50 µl. A first step PCR using the 27F and the 1369R primer were used for primary enrichment. 1µl of 10uM primer, 1 µl dNTPs mixture, 0.5 µl Phusion Green Hot Start II High-Fidelity DNA Polymerase (2 U/µl; Thermo Scientific, Landsmeer, The Netherlands), 10 µl 5× Phusion Green HF Buffer, and 36.5 µl DNAse- RNAse-free water. The amplification program included 30 s of initial denaturation step at 98°C, followed by 5 cycles of denaturation at 98 oC for 30 s, annealing at 52 °C

for 40 s, elongation at 72 °C for 90 s, and a final extension step at 72 °C for 7 min. On the PCR product a nested PCR was performed using the master mix containing 1 µl of a unique barcoded primer, 784F-n and 1064R-n (10 µM each per reaction), 1 µl dNTPs mixture, 0.5 µl Phusion Green Hot Start II High-Fidelity DNA Polymerase (2 U/µl; Thermo Scientific, Landsmeer, The Netherlands), 10 µl 5× Phusion Green HF Buffer, and 36.5 µl DNAse- RNAse-free water. The amplification program included 30 s of initial denaturation step at 98°C, followed by 5 cycles of denaturation at 98 °C for 10 s, annealing at 42 °C for 10 s, elongation at 72 °C for 10 s, and a final extension step at 72 °C for 7 min. The PCR product was visualised in 1% agarose gel (~280 bp) and purified with CleanPCR kit (CleanNA, Alphen aan den Rijn, The Netherlands). The concentration of the purified PCR product was measured with Qubit dsDNA BR Assay Kit (Invitrogen, California, USA) and 200 ng of microbial DNA from each sample were pooled for the creation of the final amplicon library which was sequenced (150 bp, paired-end) on the Illumina HiSeq. 2500 platform (GATC Biotech, Constance, Germany).

Raw reads were demultiplexed using the Je software suite (v2.0.) allowing no mismatches in the barcodes. After removing the barcodes, linker and primers, reads were mapped against the human genome using bowtie2 in order to remove human reads. Surviving microbial forward and reverse reads were pipelined separately using DADA2[11] (v1.12.1). Amplicon Sequence Variants (ASVs) inferred from the reverse reads were reverse-complemented and matched against ASVs inferred from the forwards reads. Only non-chimeric forward reads ASVs that matched reverse-complemented reverse reads ASVs were kept. ASV sample counts were inferred from the forward reads. ASV taxonomy was assigned using DADA2 and the SILVA (v132) database. The resulting ASV table and taxonomy assignments were integrated using the phyloseq R package (v1.28.0) and rarefied to 60000 counts per sample.

Duodenal gene expression

Fresh biopsy samples were snap frozen, stored at −80°C and processed as previously published (Pellegrini et al., 2017). Prior to RNA extraction, biopsies were transferred into 500 µl lysis buffer

(mirVana Isolation Kit, Ambion, Austin, TX), homogenized with Tissue Ruptor (Qiagen, Hilden, Germany) and frozen again. Total RNA was extracted with mirVana Kit following manufacturer's instruction and quantified by spectrophotometer lecture (Epoch, Gen5 software; BioTek, Winooski, VT). OD A260/A280 ratio ≥2.0 and *GAPDH* Ct<28 in Taqman single assay identified acceptable quality RNA samples. For reverse transcription PCR, after DNAse treatment (Turbo DNAse, Invitrogen), 5 µg of RNA were retro-transcribed in a 21 µl reaction volume with SuperScript IV RT (Invitrogen) following manufacturer's instructions. Predesigned TaqMan Arrays Human Inflammation Panel and Human Cell Junction Panel (Applied Biosystems, Foster City, CA) were used for gene expression study. A list of genes is reported in supplementary table 1. PCR runs and fluorescence detection were carried out in a 7900 Real-Time PCR System (Applied Biosystems) at the following temperature conditions: 50° C for 2 minutes, 95°C for 10 minutes and 40 cycles of 95° C for 15 seconds and 60° C for 1 minute. Results were expressed as fold changes (2^-ΔCt method) over a mean of expression of the selected best reference genes: 5 housekeeping (HK) genes for Human Inflammation panel l (β-*actin*, β-*2 Microglobulin*, *GAPDH, RPLP0* and *UBC)* and 4 housekeeping genes for Human Cell Junction Panel (β-*2 Microglobulin*, *GAPDH, RPLP0* and *UBC*).

Statistical analysis

For baseline differences between groups, unpaired Student's t-test or the Mann-Whitney U test (MWU) were used dependent on the distribution of the data. Accordingly, data are expressed as mean ± the standard deviation or the median with interquartile range. Post-prandial results (e.g. c-peptide) are described as area under the curves (AUC) for the 2-hour post-prandial follow-up, calculated by using the trapezoidal method. For correlation analyses, Spearman's Rank test was used (as all parameters were non-parametric). For comparison of the primary end point a linear mixed model (LMM) was used (lme4 package in R), where 'allocation' and 'time point' were fixed effects and 'patient entry number' was a random effect. The p value for the interaction between 'allocation' and 'time point' was reported. Additionally, parameters were compared between groups at various

time points using MWU with multiplicity correction. A p-value < 0.05 was considered statistically significant.

Missing values

One study participant retracted informed consent after the first visit. This participant was not included in our analyses. All other study participants completed all study visits, therefore missing values are limited. Most missing data points were caused by laboratory problems such as inability to extract DNA or failure to properly process or harvest immune cells. These missing data are considered to be missing completely at random (MCAR). The exception to this is that one subject refused the second gastroduodenoscopy, therefore his duodenal biopsies (small intestinal microbiota and gene expression) after treatment are missing (1 in 20 cases or 5%). This subject has received autologous FMT. We do not assume that having received autologous treatment rather than allogenic (donor) faeces, metabolism or gene expression are in any way related to this person refusing the second gastroscopy, therefore we consider these data to be 'missing at random'(MAR). Key variables fasting C-peptide, C-peptide AUC, A1c and weight are complete (0% missing). The immunological parameters mentioned in the text and figures (main figure 6 and supplementary figure 3) are all based on complete data sets i.e. no missing values (CD4+ CM T cells, CD8+ T cells, CD8+CXCR3+ T cells and CD4+CXCR3+ T cells). Most gene expression data in the manuscript and main and supplemental figures (CCL22, CLDN12, CCL4, CD86, CCL19, CLDN 14, CCR5, CCL18, CD14) is 95% complete (see above). For CCL13 one extra baseline measurement is missing, for CXCL12 one 'after treatment' time point is missing, for CXCL1 two baseline and 1 after treatment time point is missing. Some immunological analyses have suffered from missing data, e.g. the lymphocyte stimulation tests (LST) analyses (1 to 4/20 (5-20%) of cases depending on the parameter). However, these data are not mentioned in the figures (there was no statistically significant difference between the groups). The fecal microbiota dataset is complete (complete case analysis). The missing values in the metabolite

data were imputated (see paragraph on metabolite analysis), therefore complete case analysis was performed. No other data have been imputated.

Machine learning and follow-up statistical analyses

This technique was used on duodenal microbial composition (perform RT-qPCR on biopsies), on fecal microbiota composition and metabolic pathway abundance (Shotgun sequencing), on plasma metabolite levels and on duodenal gene expression levels data. To predict treatment groups, we used the relative change (delta) of each parameter between 0 and 12 months. For duodenal microbes and duodenal gene expression, we used delta 0 vs 6 months as no 12 months' time point was available. For prediction of responders vs non-responders baseline values, delta 0 vs 6 months and delta 0 vs 12 months were used. Each analysis produced a ranked list of the top 30 most discriminative features. We selected the top parameters from each analysis that accurately (i.e., areau under the receiver-operator curve (AUROC)≥0.8) or moderately (AUROC > 0.7) predicted group allocation for closer study, using an arbitrary cut off. This cut off was generally a relative importance of around 30% or higher (for an example of this see figure 2C, from which the top 4 features were selected). Then, we visualized the change in time of the selected parameters (Wilcoxon's signed rank tests) and studied between-group differences (MWU) at each time point and finally, using Spearman's rank test, we correlated these parameters with our primary end point and with other key parameters that were identified in this way. For the most important analyses supplementary figures showing the top 30 selected features are presented.

Analysis of responders and non-responders irrespective of treatment group

We investigated whether baseline characteristics of T1D patients can predict response to FMT therapy at 12 months follow-up and which bacterial strains and plasma metabolites were associated with this response. Clinical response was defined as <10% decline in Beta-cell function compared to baseline at 12 months follow-up, which is significantly less than the expected natural 12 months decline of 20% in beta cell function [4,12]. We chose responders at 12 months for our analyses because our primary end point (MMT stimulated C-peptide) was significantly different at 12 (but not at 6) months. At 12 months follow-up, clinical response sustained in 10 subjects of whom 3 had received allogenic and 7 had received autologous FMT (see Figure 4A-B). We next used predictive modelling to determine which parameters (either their baseline values or delta 0-12 month values) were predictors of clinical response to FMT.

Patient and public involvement

This research was done without patient involvement. Patients were not invited to comment on the study design and were not consulted to develop patient relevant outcomes or interpret the results. Patients were not invited to contribute to the writing or editing of this document for readability or accuracy.

References

1 van Nood E, Vrieze A, Nieuwdorp M, *et al.* Duodenal infusion of donor feces for recurrent Clostridium difficile. *N Engl J Med* 2013;**368**:407–15. doi:10.1056/NEJMoa1205037

2 Cammarota G, Ianiro G, Tilg H, *et al.* European consensus conference on faecal microbiota transplantation in clinical practice. *Gut* 2017;**66**:569–80. doi:10.1136/gutjnl-2016-313017

3 Moran A, Bundy B, Becker DJ, *et al.* Interleukin-1 antagonism in type 1 diabetes of recent onset: two multicentre, randomised, double-blind, placebo-controlled trials. *Lancet (London,*

England) 2013;**381**:1905–15. doi:10.1016/S0140-6736(13)60023-9

4 Lachin JM, McGee PL, Greenbaum CJ, *et al.* Sample size requirements for studies of treatment effects on beta-cell function in newly diagnosed type 1 diabetes. *PLoS One* 2011;**6**:e26471. doi:10.1371/journal.pone.0026471

5 Kracht MJL, van Lummel M, Nikolic T, *et al.* Autoimmunity against a defective ribosomal insulin gene product in type 1 diabetes. *Nat Med* 2017;**23**:501–7. doi:10.1038/nm.4289

6 Velthuis JH, Unger WW, Abreu JRF, *et al.* Simultaneous detection of circulating autoreactive CD8+ T-cells specific for different islet cell-associated epitopes using combinatorial MHC multimers. *Diabetes* 2010;**59**:1721–30. doi:10.2337/db09-1486

7 Koh A, Molinaro A, Stahlman M, *et al.* Microbially Produced Imidazole Propionate Impairs Insulin Signaling through mTORC1. *Cell* 2018;**175**:947-961.e17. doi:10.1016/j.cell.2018.09.055

8 Vrieze A, Van Nood E, Holleman F, *et al.* Transfer of intestinal microbiota from lean donors increases insulin sensitivity in individuals with metabolic syndrome. *Gastroenterology* 2012;**143**:913-6.e7. doi:10.1053/j.gastro.2012.06.031

9 Truong DT, Franzosa EA, Tickle TL, *et al.* MetaPhlAn2 for enhanced metagenomic taxonomic profiling. Nat. Methods. 2015;**12**:902–3. doi:10.1038/nmeth.3589

10 Franzosa EA, McIver LJ, Rahnavard G, *et al.* Species-level functional profiling of metagenomes and metatranscriptomes. *Nat Methods* 2018;**15**:962–8. doi:10.1038/s41592-018-0176-y

11 Callahan BJ, McMurdie PJ, Rosen MJ, *et al.* DADA2: High-resolution sample inference from Illumina amplicon data. *Nat Methods* 2016;**13**:581–3. doi:10.1038/nmeth.3869

12 Overgaard AJ, Weir JM, Jayawardana K, *et al.* Plasma lipid species at type 1 diabetes onset predict residual beta-cell function after 6 months. *Metabolomics* 2018;**14**:158. doi:10.1007/s11306-018-1456-3

332

333

334

Supplementary table 1

Genecard Cell Junctions			Genecard Inflammation		
Gene code	Gene name	Gene type	Gene code	Gene name	Gene type
GAPDH-Hs99999905_m1	glyceraldehyde-3-phosphate dehydrogenase	housekeeping	GAPDH-Hs99999905_m1	glyceraldehyde-3-phosphate dehydrogenase	housekeeping
CAV1-Hs00971716_m1	caveolin 1	target	ACTB-Hs99999903_m1	actin beta	housekeeping
CAV2-Hs00184597_m1	caveolin 2	target	ALOX5-Hs00167536_m1	arachidonate 5-lipoxygenase	target
CAV3-Hs00154292_m1	caveolin 3	target	B2M-Hs99999907_m1	beta-2-microglobulin	housekeeping
CDH1-Hs01023894_m1	cadherin 1	target	HSPA5-Hs00607129_gH	heat shock protein family A (Hsp70) member 5	target
CDH2-Hs00983056_m1	cadherin 2	target	CARD9-Hs00364485_m1	caspase recruitment domain family member 9	target
CLDN1-Hs00221623_m1	claudin 1	target	ACKR2-Hs00174299_m1	atypical chemokine receptor 2	target
CLDN10-Hs00734479_m1	claudin 10	target	CCL11-Hs00237013_m1	C-C motif chemokine ligand 11	target
CLDN11-Hs00194440_m1	claudin 11	target	CCL13-Hs00234646_m1	C-C motif chemokine ligand 13	target
CLDN12-Hs00273258_s1	claudin 12	target	CCL15-CCL14;CCL15-Hs00263142_m1	CCL15-CCL14, C-C motif chemokine ligand 15	target
CLDN14-Hs00273267_s1	claudin 14	target	CCL16-Hs00171123_m1	C-C motif chemokine ligand 16	target
CLDN15-Hs00204982_m1	claudin 15	target	CCL17-Hs00171074_m1	C-C motif chemokine ligand 17	target
CLDN16-Hs01070692_m1	claudin 16	target	CCL18-Hs00268113_m1	C-C motif chemokine ligand 18	target
CLDN17-Hs01043467_s1	claudin 17	target	CCL19-Hs00171149_m1	C-C motif chemokine ligand 19	target
CLDN18-Hs00212584_m1	claudin 18	target	CCL1-Hs00171072_m1	C-C motif chemokine ligand 1	target
CLDN19-Hs00961709_m1	claudin 19	target	CCL2-Hs00234140_m1	C-C motif chemokine ligand 2	target
CLDN2-Hs00252666_s1	claudin 2	target	CCL20-Hs00171125_m1	C-C motif chemokine ligand 20	target
CLDN3-Hs00265816_s1	claudin 3	target	CCL21-Hs00171076_m1	C-C motif chemokine ligand 21	target
CLDN4-Hs00976831_s1	claudin 4	target	CCL22-Hs00171080_m1	C-C motif chemokine ligand 22	target
CLDN5-Hs00533949_s1	claudin 5	target	CCL25-Hs00171144_m1	C-C motif chemokine ligand 25	target
CLDN6-Hs00607528_s1	claudin 6	target	CCL26-Hs00171146_m1	C-C motif chemokine ligand 26	target
CLDN7-Hs00600772_m1	claudin 7	target	UBC-Hs00824723_m1	ubiquitin C	housekeeping
CLDN8-Hs04186769_s1	claudin 8	target	CCL3-Hs00234142_m1	C-C motif chemokine ligand 3	target
CLDN9-Hs00253134_s1	claudin 9	target	CCL4-Hs99999148_m1	C-C motif chemokine ligand 4	target
DLL1-Hs00194509_m1	delta like canonical Notch ligand 1	target	CCL5-Hs00174575_m1	C-C motif chemokine ligand 5	target
DSC1-Hs00245189_m1	desmocollin 1	target	CCL7-Hs00171147_m1	C-C motif chemokine ligand 7	target
DSC2-Hs00951428_m1	desmocollin 2	target	CCL8-Hs00271615_m1	C-C motif chemokine ligand 8	target
DSC3-Hs00170032_m1	desmocollin 3	target	CCR1-Hs00174298_m1	C-C motif chemokine receptor 1	target
DSG1-Hs00355084_m1	desmoglein 1	target	CCR2-Hs00356601_m1	C-C motif chemokine receptor 2	target
DSG2-Hs00170071_m1	desmoglein 2	target	CCR3-Hs00266213_s1	C-C motif chemokine receptor 3	target
DSG3-Hs00951897_m1	desmoglein 3	target	CCR4-Hs99999919_m1	C-C motif chemokine receptor 4	target
DSG4-Hs00698286_m1	desmoglein 4	target	CCR5-Hs00152917_m1	C-C motif chemokine receptor 5	target
DSP-Hs00950591_m1	desmoplakin	target	CCR6-Hs00171121_m1	C-C motif chemokine receptor 6	target
DST-Hs00156137_m1	dystonin	target	CCR7-Hs00171054_m1	C-C motif chemokine receptor 7	target
ESAM-Hs00332781_m1	endothelial cell adhesion molecule	target	CCR8-Hs00174764_m1	C-C motif chemokine receptor 8	target
F11R-Hs00170991_m1	F11 receptor	target	CD14-Hs02621496_s1	CD14 molecule	target
GJA1-Hs00748445_s1	gap junction protein alpha 1	target	CD28-Hs01007422_m1	CD28 molecule	target
GJA3-Hs00254296_s1	gap junction protein alpha 3	target	CD68-Hs00154355_m1	CD68 molecule	target
GJA4-Hs00704917_s1	gap junction protein alpha 4	target	CD80-Hs01045161_m1	CD80 molecule	target
GJA5-Hs00270952_s1	gap junction protein alpha 5	target	CD86-Hs01567026_m1	CD86 molecule	target
GJA8-Hs00270960_s1	gap junction protein alpha 8	target	CHGA-Hs00900375_m1	chromogranin A	target
GJB1-Hs00939759_s1	gap junction protein beta 1	target	DDIT3-Hs00358796_g1	DNA damage inducible transcript 3	target
GJB2-Hs00269615_s1	gap junction protein beta 2	target	PTGS2-Hs00153133_m1	prostaglandin-endoperoxide synthase 2	target
GJB3-Hs02378125_s1	gap junction protein beta 3	target	CSF1-Hs00174164_m1	colony stimulating factor 1	target
GJB4-Hs00920816_s1	gap junction protein beta 4	target	CTLA4-Hs00175480_m1	cytotoxic T-lymphocyte associated protein 4	target
GJB5-Hs01921450_s1	gap junction protein beta 5	target	CX3CL1-Hs00171086_m1	C-X3-C motif chemokine ligand 1	target
GJB6-Hs00922742_s1	gap junction protein beta 6	target	CX3CR1-Hs00365842_m1	C-X3-C motif chemokine receptor 1	target
GJC2-Hs00252713_s1	gap junction protein gamma 2	target	CXCL10-Hs00171042_m1	C-X-C motif chemokine ligand 10	target
GJD2-Hs00950432_m1	gap junction protein delta 2	target	CXCL12-Hs00171022_m1	C-X-C motif chemokine ligand 12	target
GJC3-Hs01384570_m1	gap junction protein gamma 3	target	CXCL1-Hs00236937_m1	C-X-C motif chemokine ligand 1	target
ICAM1-Hs00164932_m1	intercellular adhesion molecule 1	target	CXCL9-Hs00171065_m1	C-X-C motif chemokine ligand 9	target
ICAM2-Hs00609563_m1	intercellular adhesion molecule 2	target	CXCR1-Hs00174146_m1	C-X-C motif chemokine receptor 1	target
ITGA1-Hs00235006_m1	integrin subunit alpha 1	target	CXCR2-Hs00174304_m1	C-X-C motif chemokine receptor 2	target
ITGA2-Hs00158127_m1	integrin subunit alpha 2	target	CXCR3-Hs00171041_m1	C-X-C motif chemokine receptor 3	target
ITGA3-Hs01076873_m1	integrin subunit alpha 3	target	CXCR4-Hs00237052_m1	C-X-C motif chemokine receptor 4	target
ITGA4-Hs00168433_m1	integrin subunit alpha 4	target	CXCR6-Hs00174843_m1	C-X-C motif chemokine receptor 6	target
ITGA5-Hs01547673_m1	integrin subunit alpha 5	target	ACKR3-Hs00604567_m1	atypical chemokine receptor 3	target
ITGA6-Hs01041011_m1	integrin subunit alpha 6	target	FCGR3B;FCGR3A-Hs00275547_m1	Fc fragment of IgG receptor IIIb,Fc fragment of IgG receptor IIIa	target
ITGA7-Hs00174397_m1	integrin subunit alpha 7	target	GAD2-Hs00609534_m1	glutamate decarboxylase 2	target
ITGA8-Hs00233321_m1	integrin subunit alpha 8	target	HCK-Hs01067403_m1	HCK proto-oncogene, Src family tyrosine kinase	target
ITGA9-Hs00979865_m1	integrin subunit alpha 9	target	PTPRN-Hs01090891_g1	protein tyrosine phosphatase, receptor type N	target
ITGAL-Hs00158218_m1	integrin subunit alpha L	target	IDO1-Hs00984148_m1	indoleamine 2,3-dioxygenase 1	target
ITGAM-Hs00355885_m1	integrin subunit alpha M	target	IFNG-Hs00174143_m1	interferon gamma	target
ITGAV-Hs00233808_m1	integrin subunit alpha V	target	IL10-Hs00174086_m1	interleukin 10	target
ITGB1-Hs00559595_m1	integrin subunit beta 1	target	IL12A-Hs00168405_m1	interleukin 12A	target
ITGB2-Hs00164957_m1	integrin subunit beta 2	target	RPLP0-Hs99999902_m1	ribosomal protein lateral stalk subunit P0	housekeeping
ITGB3-Hs01001469_m1	integrin subunit beta 3	target	IL12B-Hs00233688_m1	interleukin 12B	target
ITGB4-Hs00236216_m1	integrin subunit beta 4	target	IL15-Hs00542562_m1	interleukin 15	target
ITGB5-Hs00174435_m1	integrin subunit beta 5	target	IL15RA-Hs00542602_g1	interleukin 15 receptor subunit alpha	target
ITGB6-Hs00168458_m1	integrin subunit beta 6	target	IL17A-Hs00174383_m1	interleukin 17A	target
JAM2-Hs01022006_m1	junctional adhesion molecule 2	target	IL1R1-Hs00991010_m1	interleukin 1 receptor type 1	target
JAM3-Hs00230289_m1	junctional adhesion molecule 3	target	IL1B-Hs00174097_m1	interleukin 1 beta	target
JUP-Hs00158408_m1	junction plakoglobin	target	IL2-Hs00174114_m1	interleukin 2	target
NOTCH1-Hs01062014_m1	notch 1	target	IL22-Hs01574154_m1	interleukin 22	target
NOTCH2-Hs01050702_m1	notch 2	target	IL4-Hs00174122_m1	interleukin 4	target
NOTCH3-Hs01128541_m1	notch 3	target	IL4R-Hs00166237_m1	interleukin 4 receptor	target
NOTCH4-Hs00965889_m1	notch 4	target	IL6-Hs00174131_m1	interleukin 6	target
OCLN-Hs00170162_m1	occludin	target	CXCL8-Hs00174103_m1	C-X-C motif chemokine ligand 8	target
PLEC-Hs00356986_g1	plectin	target	INS-Hs02741908_m1	insulin	target
NECTIN1-Hs01591978_m1	nectin cell adhesion molecule 1	target	LAG3-Hs00958444_g1	lymphocyte activating 3	target
NECTIN2-Hs01071562_m1	nectin cell adhesion molecule 2	target	LST1-Hs00705788_s1	leukocyte specific transcript 1	target
NECTIN3-Hs00210043_m1	nectin cell adhesion molecule 3	target	CIITA-Hs00172106_m1	class II, major histocompatibility complex, transactivator	target
TJP1-Hs01551861_m1	tight junction protein 1	target	MIF-Hs00236988_g1	macrophage migration inhibitory factor	target
TJP2-Hs00910543_m1	tight junction protein 2	target	NOD2-Hs00223394_m1	nucleotide binding oligomerization domain containing 2	target
TJP3-Hs00274276_m1	tight junction protein 3	target	NOS2-Hs00167257_m1	nitric oxide synthase 2	target
HPRT1-Hs99999909_m1	hypoxanthine phosphoribosyltransferase 1	housekeeping	PDCD1-Hs01550088_m1	programmed cell death 1	target
GUSB-Hs99999908_m1	glucuronidase beta	housekeeping	CD274-Hs00204257_m1	CD274 molecule	target
ACTB-Hs99999903_m1	actin beta	housekeeping	PTX3-Hs00173615_m1	pentraxin 3	target
B2M-Hs99999907_m1	beta-2-microglobulin	housekeeping	SIGIRR-Hs00222347_m1	single Ig and TIR domain containing	target
HMBS-Hs00609297_m1	hydroxymethylbilane synthase	housekeeping	TMEM173-Hs00736955_g1	transmembrane protein 173	target
IPO8-Hs00183533_m1	importin 8	housekeeping	SYP-Hs00300531_m1	synaptophysin	target
PGK1-Hs99999906_m1	phosphoglycerate kinase 1	housekeeping	TNF-Hs00174128_m1	tumor necrosis factor	target
RPLP0-Hs99999902_m1	ribosomal protein lateral stalk subunit P0	housekeeping	TSPAN7-Hs00190284_m1	tetraspanin 7	target
TBP-Hs99999910_m1	TATA-box binding protein	housekeeping	VEGFA-Hs00900054_m1	vascular endothelial growth factor A	target
TFRC-Hs99999911_m1	transferrin receptor	housekeeping	C10orf54-Hs00735289_m1	chromosome 10 open reading frame 54	target
UBC-Hs00824723_m1	ubiquitin C	housekeeping	KCNJ8-Hs00958961_m1	potassium voltage-gated channel subfamily J member 8	target

Parameter	Groups	Delta or baseline	AUC ± CI	1st most predictive variable	2nd	3rd
Metabolites	Tx groups	Δ 0 – 12M	0.79 ± 0.23	1-myristoyl-2-arachidonoyl-GPC	1-(1-enyl-palmitoyl)-2-linoleoyl-GPE	1-arachidonoyl-GPC
	R12	Baseline	0.70 ± 0.28	7-hydroxyoctanoate	N-acetylphenylalanine	2-methylcitrate/homocitrate
		Δ 0 – 12M	0.74 ± 0.25	7-hydroxyoctanoate	14 or 15-methylpalmitate	5-methylthioadenosine
Small intestinal microbes	Tx groups	Δ 0 – 12M	0.89 ± 0.18	Prevotella 1	Prevotella 2	Streptococcus oralis
	R12	Baseline	0.72 ± 0.27	Undibacterium oligocarboniphilum	Nesterenkonia flava	Shewanella colwelliana
		Δ 0 – 6M	0.60 ± 0.29	Neisseria animalis	Tenuibacillus multivorans	Streptococcus mitis
Fecal microbes (taxonomy)	Tx groups	Δ 0 – 6M	0.58 ± 0.24	Desulfovibrio piger	Bacteroidales bacterium ph8	Ruminococcus callidus
		Δ 0 – 12M	0.72 ± 0.24	Desulfovibrio piger	Eubacterium ventriosum	Sutterella wadsworthensis
	R12	Baseline	0.93 ± 0.14	Coprococcus catus	Bacteroides caccae	Paraprevotella unclassified
		Δ 0 – 6M	0.78 ± 0.23	Lachnospiraceae bacterium 8 1 57FAA	Collinsella aerofaciens	Holdemania unclassified
		Δ 0 – 12M	0.76 ± 0.23	Bacteroidales bacterium ph8	Actinomyces viscosus	Bacteroides thetaiotaomicron
Fecal microbes (metabolic pathways)	Tx groups	Δ 0 – 6M	0.75 ± 0.24	GDP-mannose biosynthesis	dTDP-L-rhamnose biosynthesis I	seleno-amino acid biosynthesis
		Δ 0 – 12M	0.68 ± 0.27	seleno-amino acid biosynthesis	UMP biosynthesis	superpathway of UDP-glucose-derived O-antigen building blocks biosynthesis
	R12	Baseline	0.85 ± 0.22	fatty acid β-oxidation I	pyruvate fermentation to acetone	colanic acid building blocks biosynthesis
		Δ 0 – 6M	0.70 ± 0.27	glycogen biosynthesis I (from ADP-D-Glucose)	phosphatidylcholine acyl editing	L-lysine biosynthesis II
		Δ 0 – 12M	0.69 ± 0.22	creatinine degradation I	Bifidobacterium shunt	glycolysis III (from glucose)
Duodenal gene expression	Tx groups	Δ 0 – 6M	0.61 ± 0.24	CCL18	CXCR1	CXCR4
	R12	Baseline	0.83 ± 0.21	CCL22	CLDN12	CCL4
		Δ 0 – 6M	0.73 ± 0.24	CCR5	CCL18	CD14

Supplementary table 2: AUCs. This table provides an overview of all predictive modeling analyses that we have performed. It shows what parameter was studied, in which group the analysis was done, whether baseline or delta values were used, how well the predictive model performed (measured asAUROC) and what were the top 3 predictive parameters from that analysis. The highest AUC from each category in bold. Tx: treatment, R12: responders versus non-responders at 12 months, Baseline: for this analysis, the baseline value of the parameters were used, Δ 0 – 12M: for this analysis, the delta's between baseline and 12 months were used. AUROC: area under the receiver-operator curve ± confidence interval.

S1

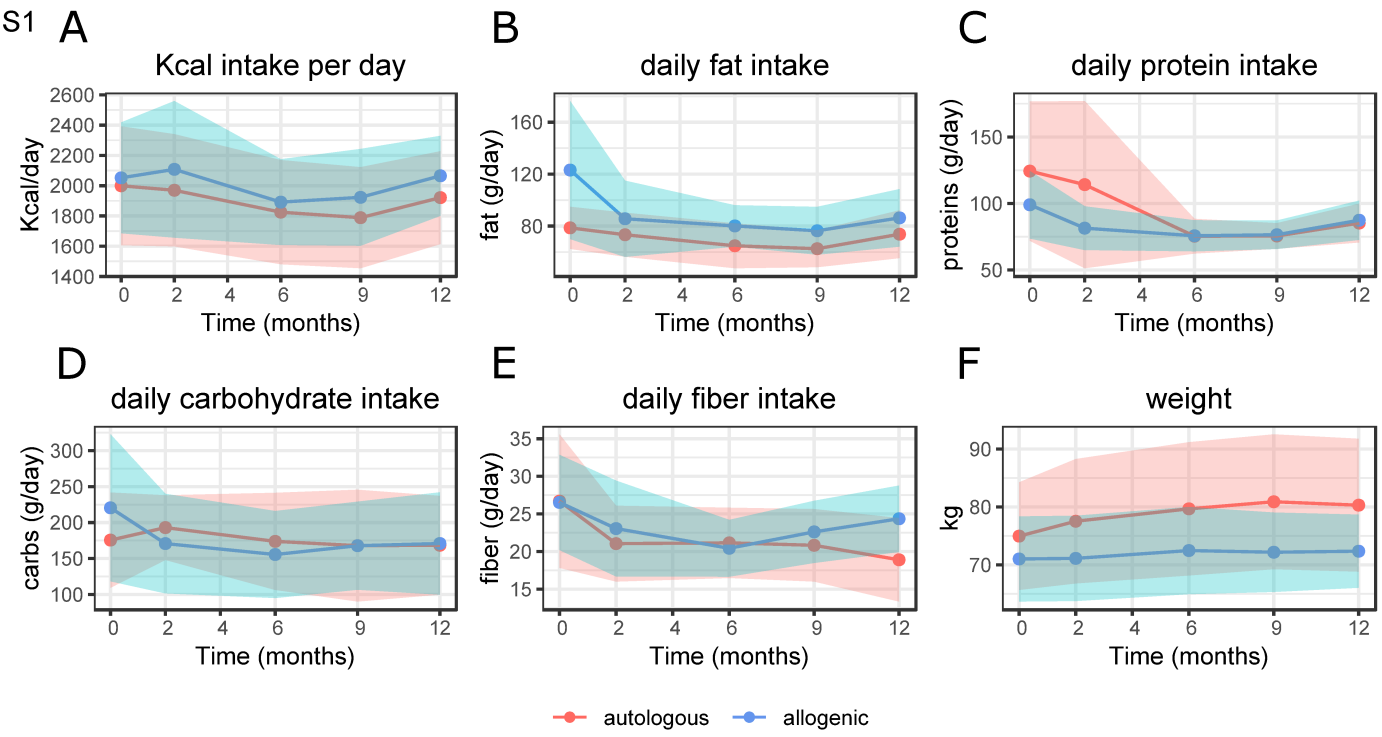
A
Kcal intake per day
Kcal/day
2600
2400
2200
2000
1800
1600
1400
0 2 4 6 9 12
Time (months)
B
daily fat intake
fat (g/day)
160
120
80
0 2 4 6 9 12
Time (months)
C
daily protein intake
proteins (g/day)
150
100
50
0 2 4 6 9 12
Time (months)
D
daily carbohydrate intake
carbs (g/day)
300
250
200
150
100
0 2 4 6 9 12
Time (months)
E
daily fiber intake
fiber (g/day)
35
30
25
20
15
0 2 4 6 9 12
Time (months)
F
weight
kg
90
80
70
0 2 4 6 9 12
Time (months)
autologous
allogenic

S2

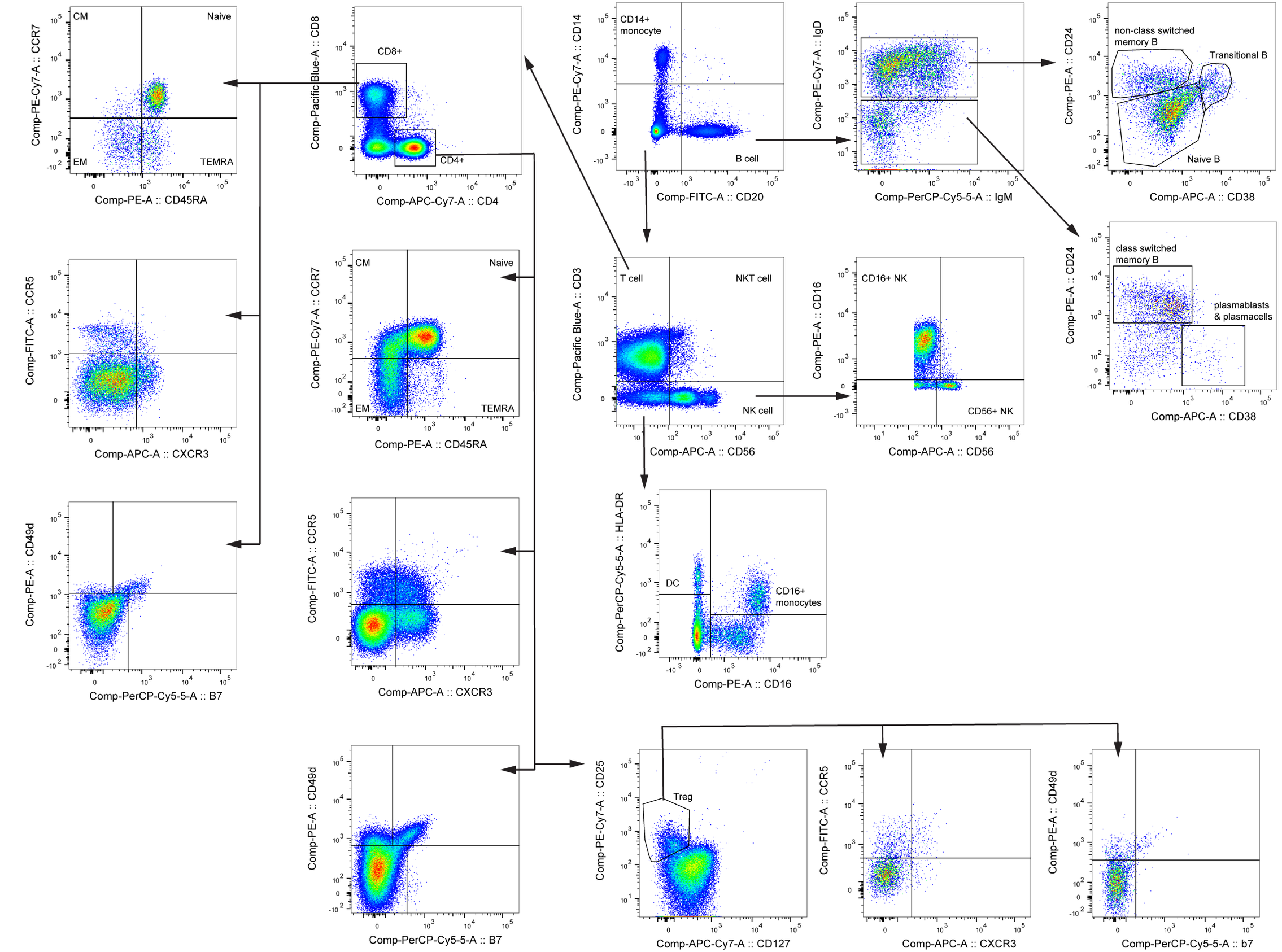
CM
Naive
EM
TEMRA
Comp-PE-Cy7-A :: CCR7
Comp-PE-A :: CD45RA
Comp-Pacific Blue-A :: CD8
CD8+
CD4+
Comp-APC-Cy7-A :: CD4
Comp-FITC-A :: CCR5
Comp-APC-A :: CXCR3
Comp-PE-A :: CD49d
Comp-PerCP-Cy5-5-A :: B7
CD14+ monocyte
B cell
Comp-PE-Cy7-A :: CD14
Comp-FITC-A :: CD20
Comp-PE-Cy7-A :: IgD
Comp-PerCP-Cy5-5-A :: IgM
non-class switched memory B
Transitional B
Naive B
Comp-PE-A :: CD24
Comp-APC-A :: CD38
class switched memory B
plasmablasts & plasmacells
T cell
NK cell
Comp-Pacific Blue-A :: CD3
Comp-APC-A :: CD56
CD16+ NK
CD56+ NK
Comp-PE-A :: CD16
DC
CD16+ monocytes
Comp-PerCP-Cy5-5-A :: HLA-DR
Comp-PE-A :: CD16
Treg
Comp-PE-Cy7-A :: CD25
Comp-APC-Cy7-A :: CD127
Comp-FITC-A :: CCR5
Comp-APC-A :: CXCR3
Comp-PE-A :: CD49d
Comp-PerCP-Cy5-5-A :: b7

S3

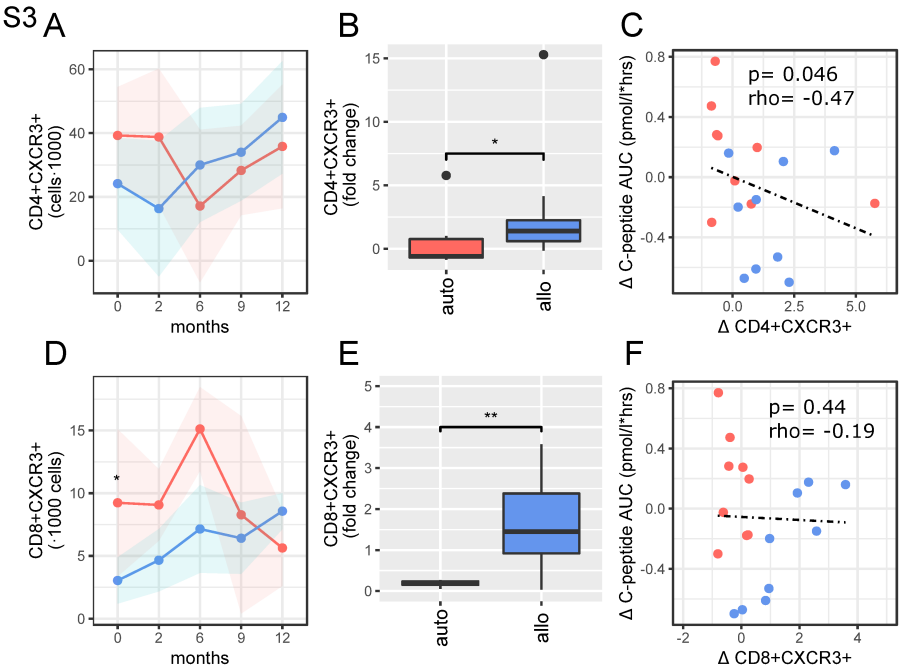
A
CD4+CXCR3+ (cells·1000)
months
B
CD4+CXCR3+ (fold change)
auto
allo
C
p= 0.046
rho= -0.47
Δ C-peptide AUC (pmol/l*hrs)
Δ CD4+CXCR3+
D
CD8+CXCR3+ (·1000 cells)
months
E
CD8+CXCR3+ (fold change)
auto
allo
F
p= 0.44
rho= -0.19
Δ C-peptide AUC (pmol/l*hrs)
Δ CD8+CXCR3+

S4

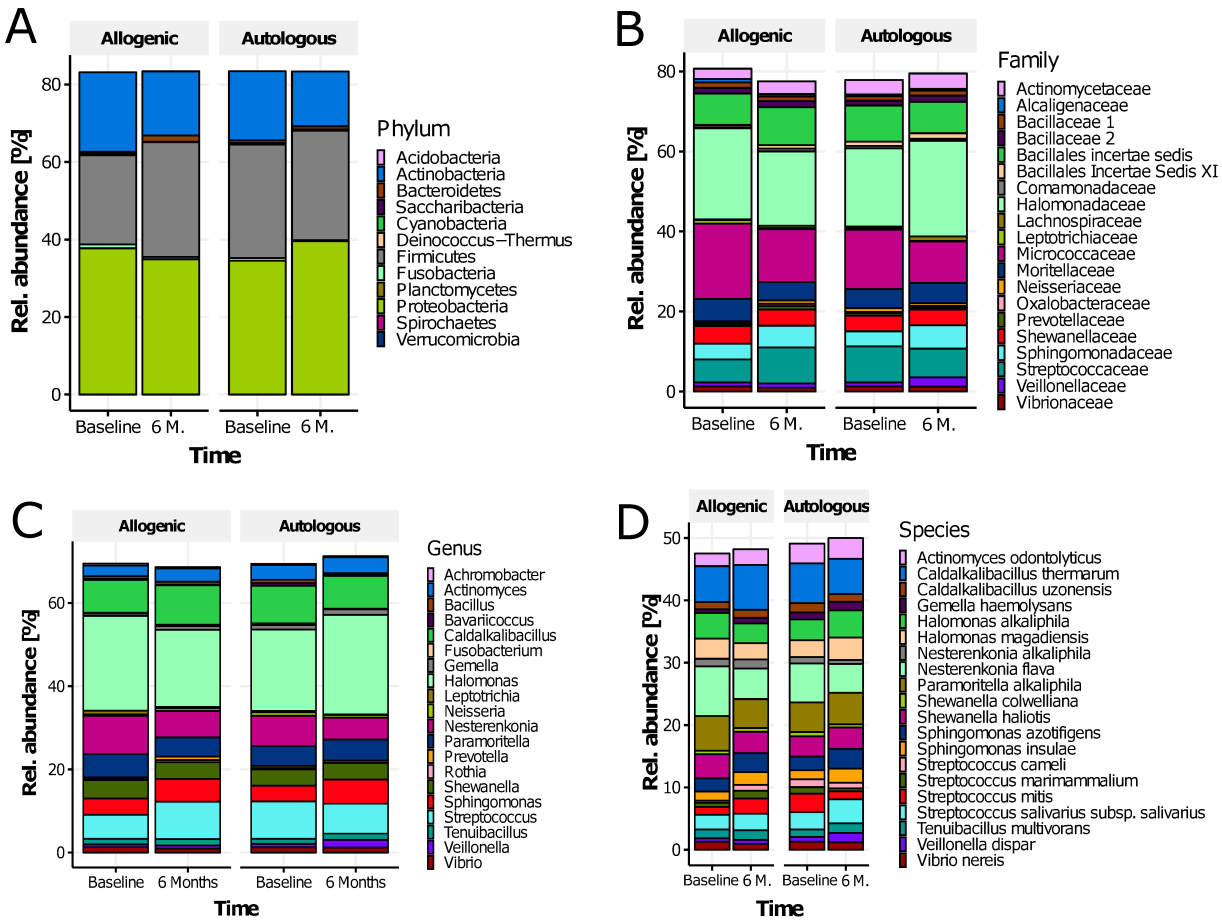
A
Allogenic
Autologous
Rel. abundance [%]
Baseline 6 M. Baseline 6 M.
Time
Phylum
Acidobacteria
Actinobacteria
Bacteroidetes
Saccharibacteria
Cyanobacteria
Deinococcus–Thermus
Firmicutes
Fusobacteria
Planctomycetes
Proteobacteria
Spirochaetes
Verrucomicrobia
B
Allogenic
Autologous
Rel. abundance [%]
Baseline 6 M. Baseline 6 M.
Time
Family
Actinomycetaceae
Alcaligenaceae
Bacillaceae 1
Bacillaceae 2
Bacillales incertae sedis
Bacillales Incertae Sedis XI
Comamonadaceae
Halomonadaceae
Lachnospiraceae
Leptotrichiaceae
Micrococcaceae
Moritellaceae
Neisseriaceae
Oxalobacteraceae
Prevotellaceae
Shewanellaceae
Sphingomonadaceae
Streptococcaceae
Veillonellaceae
Vibrionaceae
C
Allogenic
Autologous
Rel. abundance [%]
Baseline 6 Months Baseline 6 Months
Time
Genus
Achromobacter
Actinomyces
Bacillus
Bavariicoccus
Caldalkalibacillus
Fusobacterium
Gemella
Halomonas
Leptotrichia
Neisseria
Nesterenkonia
Paramoritella
Prevotella
Rothia
Shewanella
Sphingomonas
Streptococcus
Tenuibacillus
Veillonella
Vibrio
D
Allogenic
Autologous
Rel. abundance [%]
Baseline 6 M. Baseline 6 M.
Time
Species
Actinomyces odontolyticus
Caldalkalibacillus thermarum
Caldalkalibacillus uzonensis
Gemella haemolysans
Halomonas alkaliphila
Halomonas magadiensis
Nesterenkonia alkaliphila
Nesterenkonia flava
Paramoritella alkaliphila
Shewanella colwelliana
Shewanella haliotis
Sphingomonas azotifigens
Sphingomonas insulae
Streptococcus cameli
Streptococcus marimammalium
Streptococcus mitis
Streptococcus salivarius subsp. salivarius
Tenuibacillus multivorans
Veillonella dispar
Vibrio nereis

S5

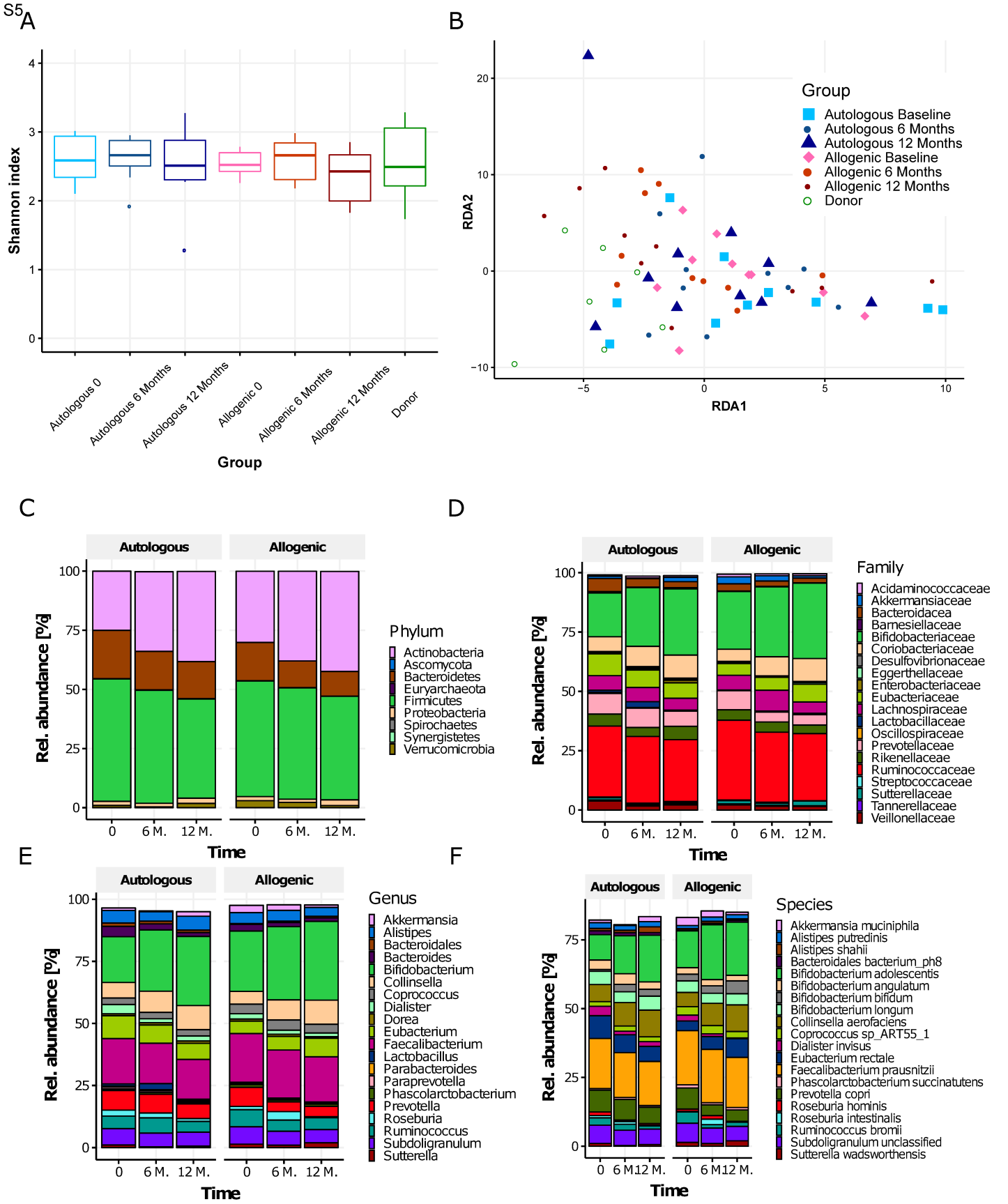
A
Shannon index
Group
Autologous 0
Autologous 6 Months
Autologous 12 Months
Allogenic 0
Allogenic 6 Months
Allogenic 12 Months
Donor
B
RDA1
RDA2
Group
Autologous Baseline
Autologous 6 Months
Autologous 12 Months
Allogenic Baseline
Allogenic 6 Months
Allogenic 12 Months
Donor
C
Autologous
Allogenic
Rel. abundance [%]
Time
Phylum
Actinobacteria
Ascomycota
Bacteroidetes
Euryarchaeota
Firmicutes
Proteobacteria
Spirochaetes
Synergistetes
Verrucomicrobia
D
Family
Acidaminococcaceae
Akkermansiaceae
Bacteroidacea
Barnesiellaceae
Bifidobacteriaceae
Coriobacteriaceae
Desulfovibrionaceae
Eggerthellaceae
Enterobacteriaceae
Eubacteriaceae
Lachnospiraceae
Lactobacillaceae
Oscillospiraceae
Prevotellaceae
Rikenellaceae
Ruminococcaceae
Streptococcaceae
Sutterellaceae
Tannerellaceae
Veillonellaceae
E
Genus
Akkermansia
Alistipes
Bacteroidales
Bacteroides
Bifidobacterium
Collinsella
Coprococcus
Dialister
Dorea
Eubacterium
Faecalibacterium
Lactobacillus
Parabacteroides
Paraprevotella
Phascolarctobacterium
Prevotella
Roseburia
Ruminococcus
Subdoligranulum
Sutterella
F
Species
Akkermansia muciniphila
Alistipes putredinis
Alistipes shahii
Bacteroidales bacterium_ph8
Bifidobacterium adolescentis
Bifidobacterium angulatum
Bifidobacterium bifidum
Bifidobacterium longum
Collinsella aerofaciens
Coprococcus sp_ART55_1
Dialister invisus
Eubacterium rectale
Faecalibacterium prausnitzii
Phascolarctobacterium succinatutens
Prevotella copri
Roseburia hominis
Roseburia intestinalis
Ruminococcus bromii
Subdoligranulum unclassified
Sutterella wadsworthensis

S6 A

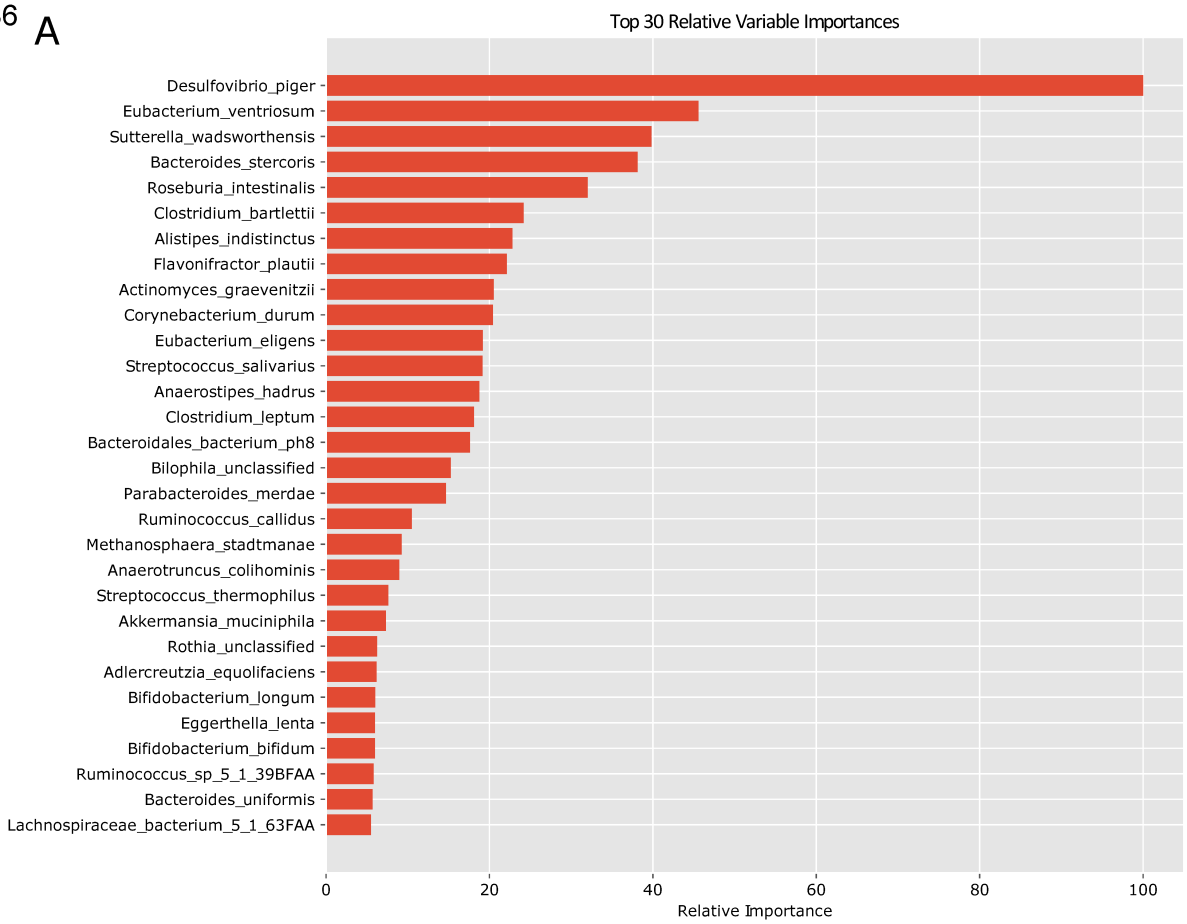
Top 30 Relative Variable Importances
Desulfovibrio_piger
Eubacterium_ventriosum
Sutterella_wadsworthensis
Bacteroides_stercoris
Roseburia_intestinalis
Clostridium_bartlettii
Alistipes_indistinctus
Flavonifractor_plautii
Actinomyces_graevenitzii
Corynebacterium_durum
Eubacterium_eligens
Streptococcus_salivarius
Anaerostipes_hadrus
Clostridium_leptum
Bacteroidales_bacterium_ph8
Bilophila_unclassified
Parabacteroides_merdae
Ruminococcus_callidus
Methanosphaera_stadtmanae
Anaerotruncus_colihominis
Streptococcus_thermophilus
Akkermansia_muciniphila
Rothia_unclassified
Adlercreutzia_equolifaciens
Bifidobacterium_longum
Eggerthella_lenta
Bifidobacterium_bifidum
Ruminococcus_sp_5_1_39BFAA
Bacteroides_uniformis
Lachnospiraceae_bacterium_5_1_63FAA
0
20
40
60
80
100
Relative Importance

B

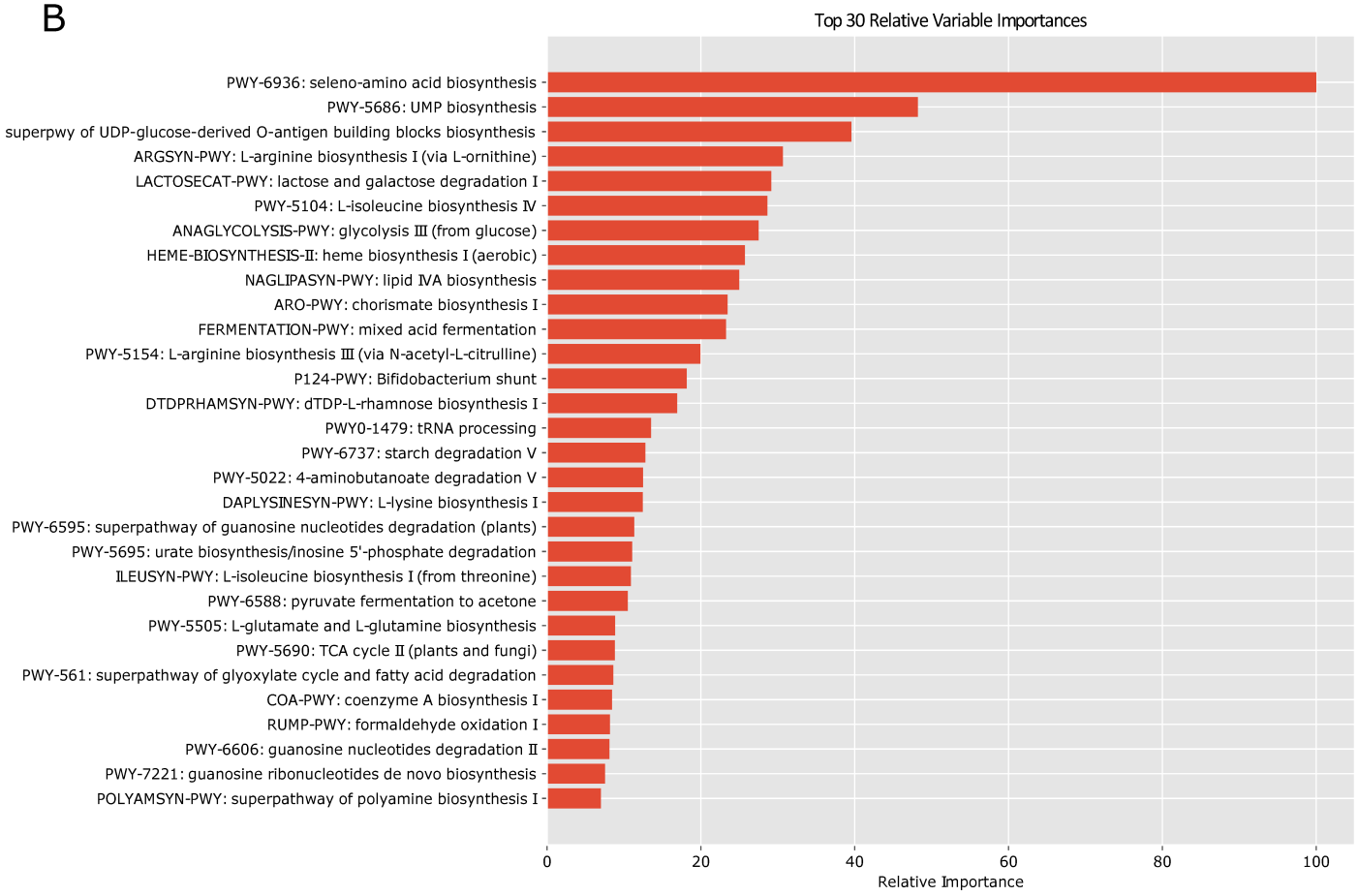
Top 30 Relative Variable Importances
PWY-6936: seleno-amino acid biosynthesis
PWY-5686: UMP biosynthesis
superpwy of UDP-glucose-derived O-antigen building blocks biosynthesis
ARGSYN-PWY: L-arginine biosynthesis I (via L-ornithine)
LACTOSECAT-PWY: lactose and galactose degradation I
PWY-5104: L-isoleucine biosynthesis IV
ANAGLYCOLYSIS-PWY: glycolysis III (from glucose)
HEME-BIOSYNTHESIS-II: heme biosynthesis I (aerobic)
NAGLIPASYN-PWY: lipid IVA biosynthesis
ARO-PWY: chorismate biosynthesis I
FERMENTATION-PWY: mixed acid fermentation
PWY-5154: L-arginine biosynthesis III (via N-acetyl-L-citrulline)
P124-PWY: Bifidobacterium shunt
DTDPRHAMSYN-PWY: dTDP-L-rhamnose biosynthesis I
PWY0-1479: tRNA processing
PWY-6737: starch degradation V
PWY-5022: 4-aminobutanoate degradation V
DAPLYSINESYN-PWY: L-lysine biosynthesis I
PWY-6595: superpathway of guanosine nucleotides degradation (plants)
PWY-5695: urate biosynthesis/inosine 5'-phosphate degradation
ILEUSYN-PWY: L-isoleucine biosynthesis I (from threonine)
PWY-6588: pyruvate fermentation to acetone
PWY-5505: L-glutamate and L-glutamine biosynthesis
PWY-5690: TCA cycle II (plants and fungi)
PWY-561: superpathway of glyoxylate cycle and fatty acid degradation
COA-PWY: coenzyme A biosynthesis I
RUMP-PWY: formaldehyde oxidation I
PWY-6606: guanosine nucleotides degradation II
PWY-7221: guanosine ribonucleotides de novo biosynthesis
POLYAMSYN-PWY: superpathway of polyamine biosynthesis I
0
20
40
60
80
100
Relative Importance

S7

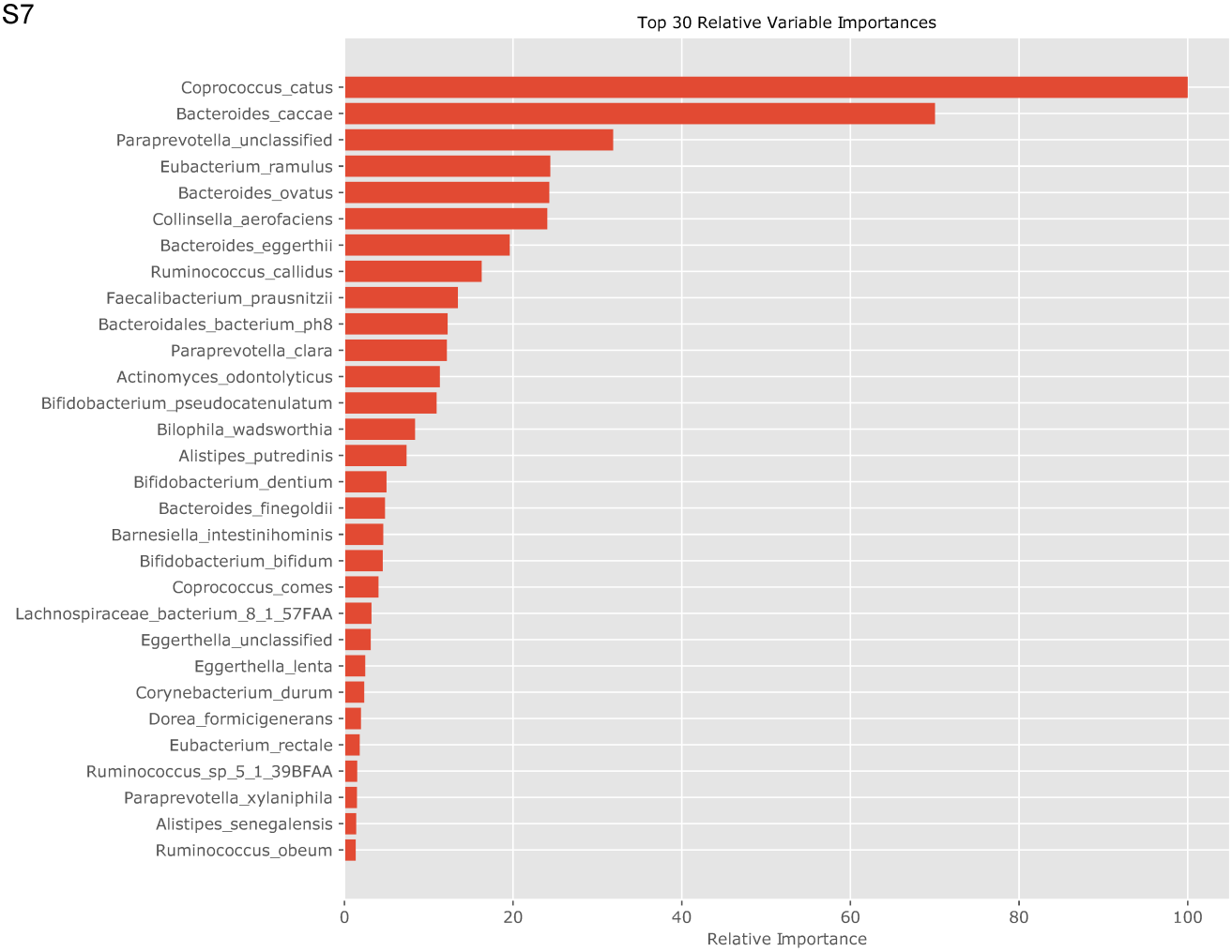
Top 30 Relative Variable Importances
Coprococcus_catus
Bacteroides_caccae
Paraprevotella_unclassified
Eubacterium_ramulus
Bacteroides_ovatus
Collinsella_aerofaciens
Bacteroides_eggerthii
Ruminococcus_callidus
Faecalibacterium_prausnitzii
Bacteroidales_bacterium_ph8
Paraprevotella_clara
Actinomyces_odontolyticus
Bifidobacterium_pseudocatenulatum
Bilophila_wadsworthia
Alistipes_putredinis
Bifidobacterium_dentium
Bacteroides_finegoldii
Barnesiella_intestinihominis
Bifidobacterium_bifidum
Coprococcus_comes
Lachnospiraceae_bacterium_8_1_57FAA
Eggerthella_unclassified
Eggerthella_lenta
Corynebacterium_durum
Dorea_formicigenerans
Eubacterium_rectale
Ruminococcus_sp_5_1_39BFAA
Paraprevotella_xylaniphila
Alistipes_senegalensis
Ruminococcus_obeum
0
20
40
60
80
100
Relative Importance

S8

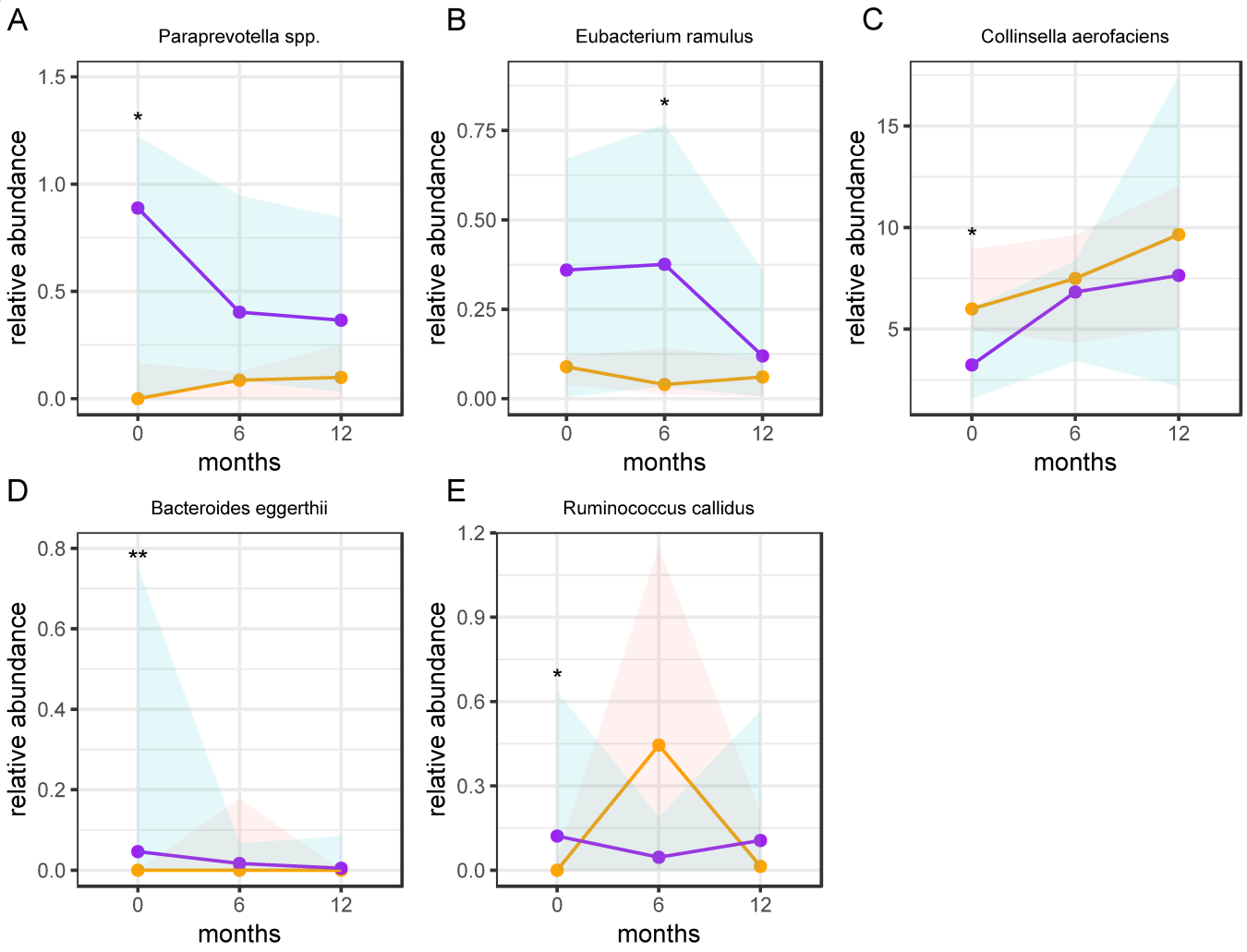
A
Paraprevotella spp.
relative abundance
1.5
1.0
0.5
0.0
*
0
6
12
months
B
Eubacterium ramulus
relative abundance
0.75
0.50
0.25
0.00
*
0
6
12
months
C
Collinsella aerofaciens
relative abundance
15
10
5
*
0
6
12
months
D
Bacteroides eggerthii
relative abundance
0.8
0.6
0.4
0.2
0.0
**
0
6
12
months
E
Ruminococcus callidus
relative abundance
1.2
0.9
0.6
0.3
0.0
*
0
6
12
months

S9

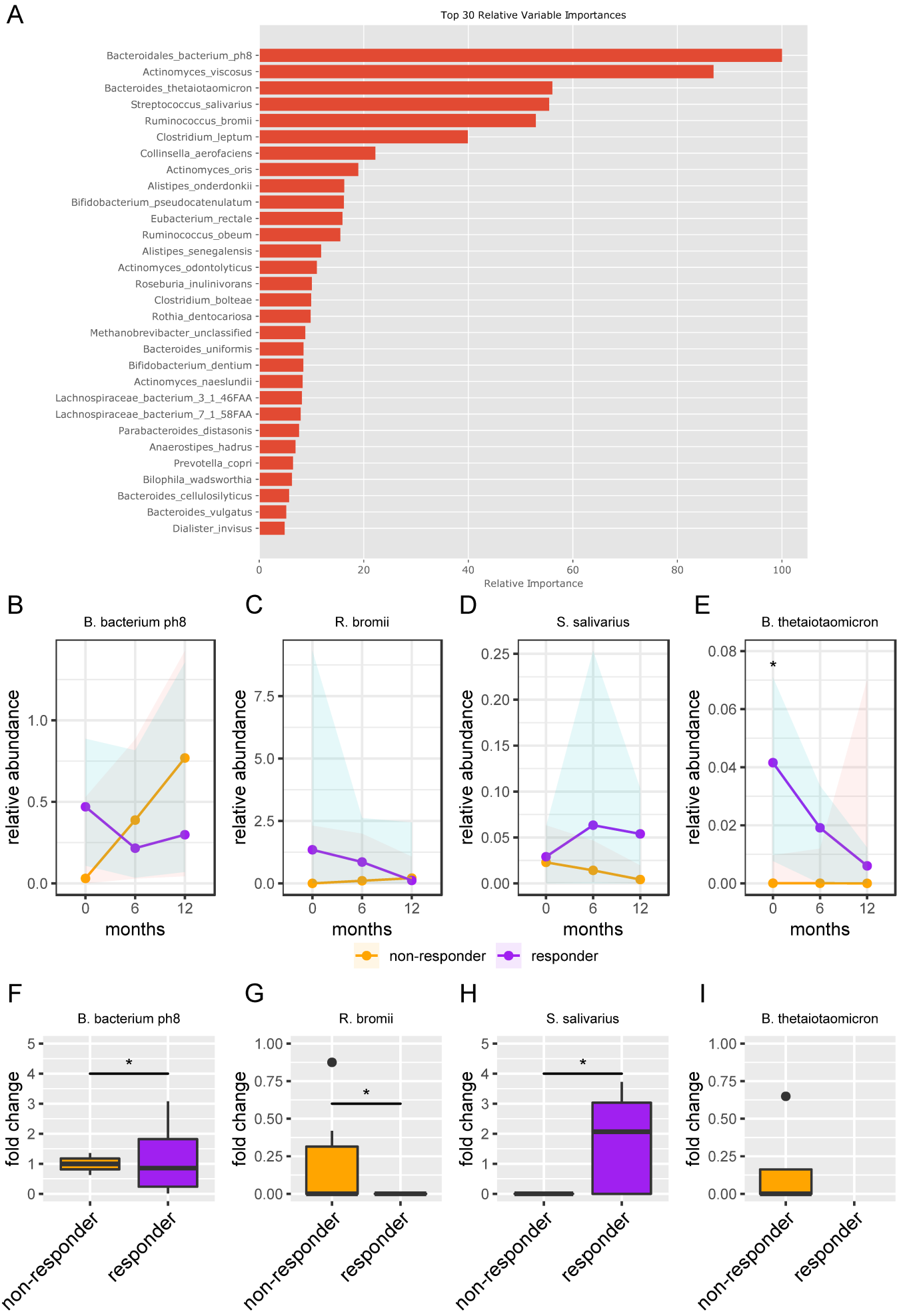
A
Top 30 Relative Variable Importances
Bacteroidales_bacterium_ph8
Actinomyces_viscosus
Bacteroides_thetaiotaomicron
Streptococcus_salivarius
Ruminococcus_bromii
Clostridium_leptum
Collinsella_aerofaciens
Actinomyces_oris
Alistipes_onderdonkii
Bifidobacterium_pseudocatenulatum
Eubacterium_rectale
Ruminococcus_obeum
Alistipes_senegalensis
Actinomyces_odontolyticus
Roseburia_inulinivorans
Clostridium_bolteae
Rothia_dentocariosa
Methanobrevibacter_unclassified
Bacteroides_uniformis
Bifidobacterium_dentium
Actinomyces_naeslundii
Lachnospiraceae_bacterium_3_1_46FAA
Lachnospiraceae_bacterium_7_1_58FAA
Parabacteroides_distasonis
Anaerostipes_hadrus
Prevotella_copri
Bilophila_wadsworthia
Bacteroides_cellulosilyticus
Bacteroides_vulgatus
Dialister_invisus
0
20
40
60
80
100
Relative Importance
B
B. bacterium ph8
C
R. bromii
D
S. salivarius
E
B. thetaiotaomicron
relative abundance
months
non-responder
responder
F
G
H
I
fold change
*

S10

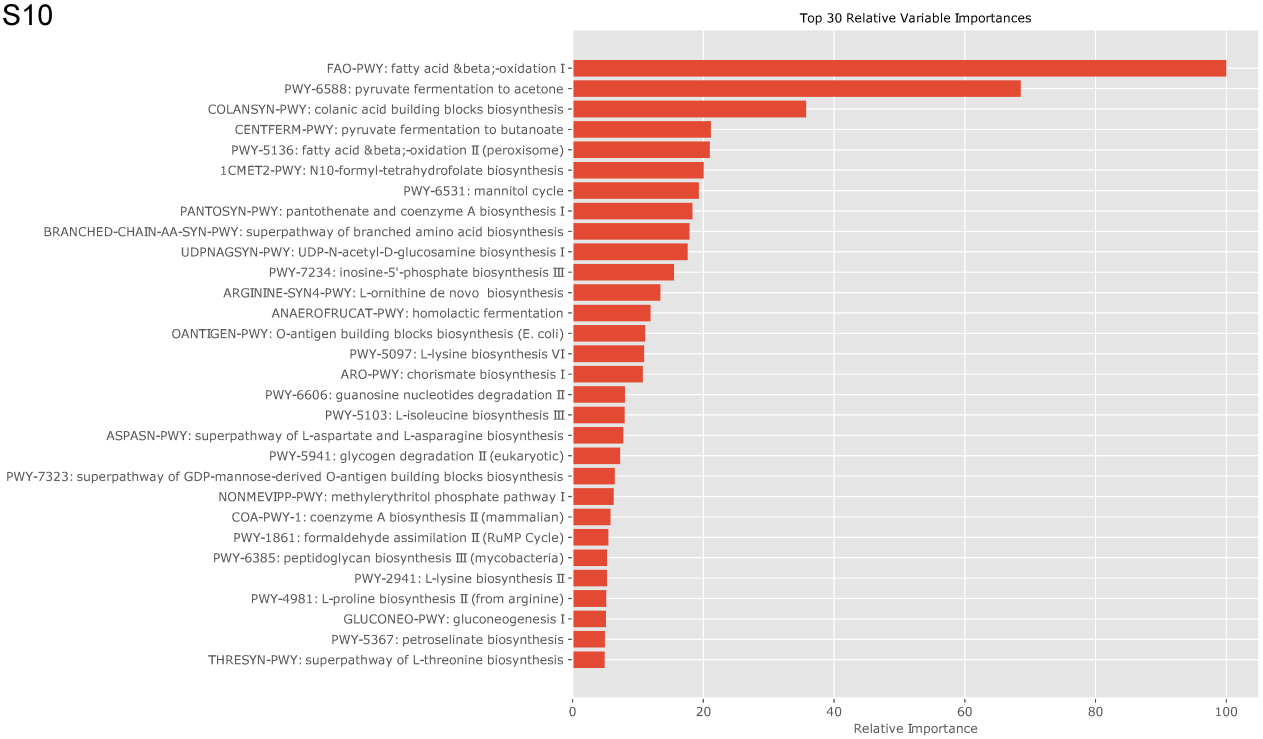
Top 30 Relative Variable Importances
FAO-PWY: fatty acid β-oxidation I
PWY-6588: pyruvate fermentation to acetone
COLANSYN-PWY: colanic acid building blocks biosynthesis
CENTFERM-PWY: pyruvate fermentation to butanoate
PWY-5136: fatty acid β-oxidation II (peroxisome)
1CMET2-PWY: N10-formyl-tetrahydrofolate biosynthesis
PWY-6531: mannitol cycle
PANTOSYN-PWY: pantothenate and coenzyme A biosynthesis I
BRANCHED-CHAIN-AA-SYN-PWY: superpathway of branched amino acid biosynthesis
UDPNAGSYN-PWY: UDP-N-acetyl-D-glucosamine biosynthesis I
PWY-7234: inosine-5'-phosphate biosynthesis III
ARGININE-SYN4-PWY: L-ornithine de novo biosynthesis
ANAEROFRUCAT-PWY: homolactic fermentation
OANTIGEN-PWY: O-antigen building blocks biosynthesis (E. coli)
PWY-5097: L-lysine biosynthesis VI
ARO-PWY: chorismate biosynthesis I
PWY-6606: guanosine nucleotides degradation II
PWY-5103: L-isoleucine biosynthesis III
ASPASN-PWY: superpathway of L-aspartate and L-asparagine biosynthesis
PWY-5941: glycogen degradation II (eukaryotic)
PWY-7323: superpathway of GDP-mannose-derived O-antigen building blocks biosynthesis
NONMEVIPP-PWY: methylerythritol phosphate pathway I
COA-PWY-1: coenzyme A biosynthesis II (mammalian)
PWY-1861: formaldehyde assimilation II (RuMP Cycle)
PWY-6385: peptidoglycan biosynthesis III (mycobacteria)
PWY-2941: L-lysine biosynthesis II
PWY-4981: L-proline biosynthesis II (from arginine)
GLUCONEO-PWY: gluconeogenesis I
PWY-5367: petroselinate biosynthesis
THRESYN-PWY: superpathway of L-threonine biosynthesis
0
20
40
60
80
100
Relative Importance

S11

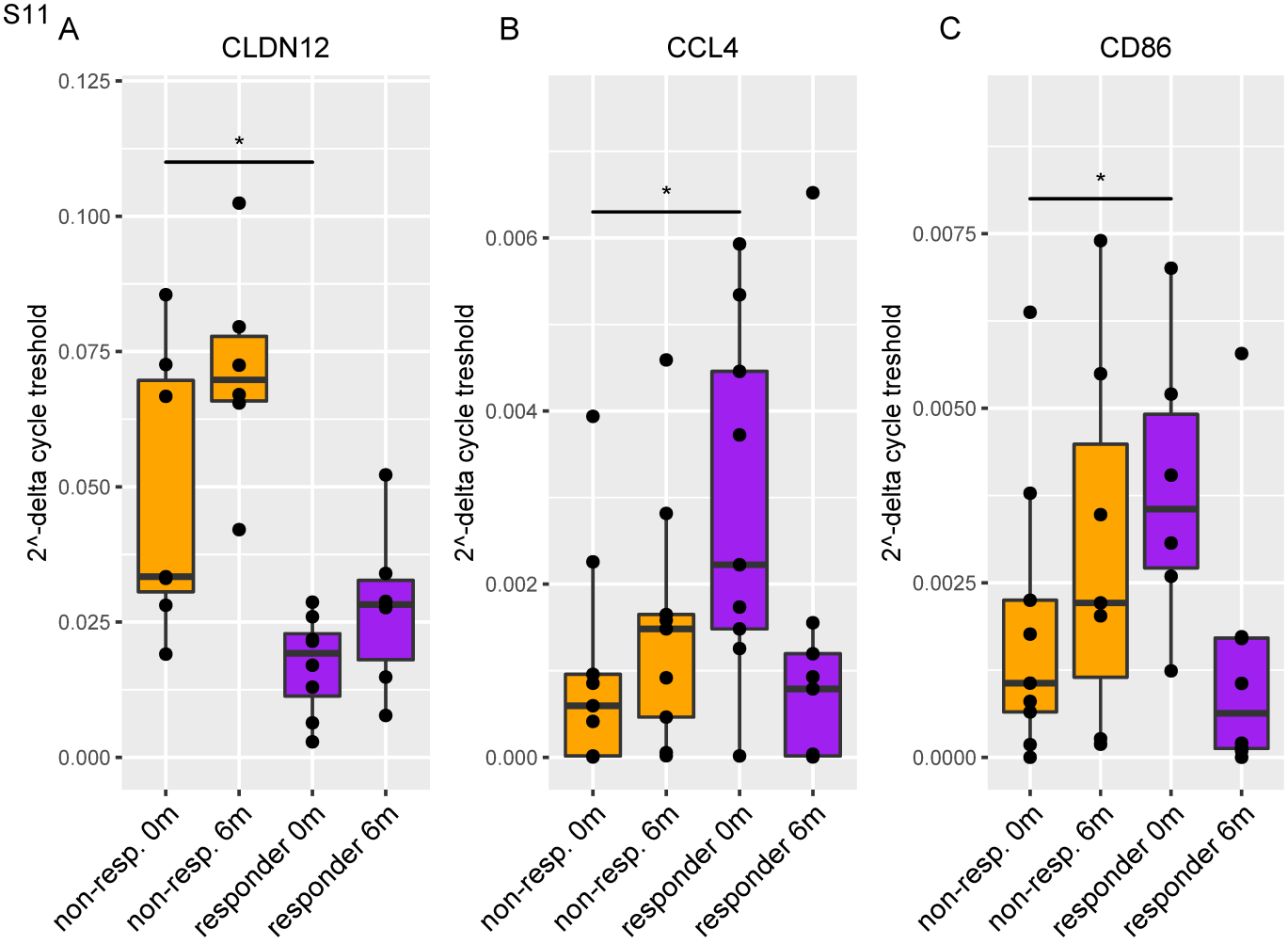
A
CLDN12
B
CCL4
C
CD86
2^-delta cycle treshold
0.125
0.100
0.075
0.050
0.025
0.000
0.006
0.004
0.002
0.0075
0.0050
0.0025
0.0000
*
non-resp. 0m
non-resp. 6m
responder 0m
responder 6m

S12

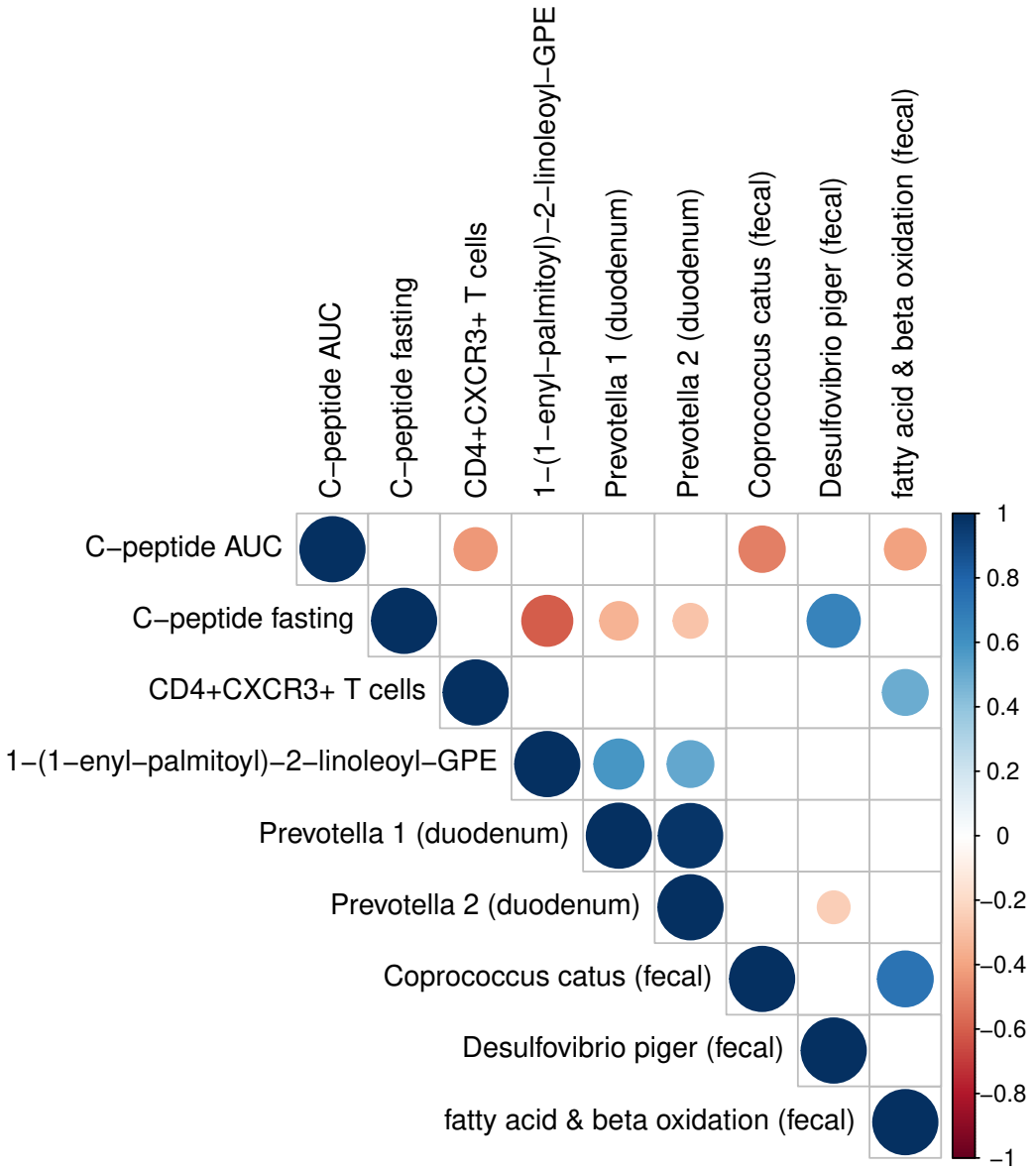
C–peptide AUC
C–peptide fasting
CD4+CXCR3+ T cells
1–(1–enyl–palmitoyl)–2–linoleoyl–GPE
Prevotella 1 (duodenum)
Prevotella 2 (duodenum)
Coprococcus catus (fecal)
Desulfovibrio piger (fecal)
fatty acid & beta oxidation (fecal)
1
0.8
0.6
0.4
0.2
0
–0.2
–0.4
–0.6
–0.8
–1

Cell type	Autologous (n=10)	Allogenic (N=10)	P value
Dendritic cells	17123	14529	0.07
Total monocytes	119555	73615	0.39
CD16 pos monocytes	7395	5539	0.07
CD14 pos monocytes	93804	72016	0.44
B cells	105975	172553	0.22
Naive B	61851	105175	0.22
non CS memory B	21187	20716	0.39
Transitional B	4463	3089	0.07
CS memory B	16577	21048	0.30
plasmablasts and plasmacells	3548	2826	0.07
NK cells	112375	123638	0.75
CD16 pos NK	95077	94477	0.82
CD56 NK	12090	18402	0.62
NKT cells	11571	11847	0.69
T cells	629591	588006	0.44
CD4 T pos cells	251710	228152	0.39
CD4 pos Naive T cells	120264	63899	1.00
CD4 pos CM	73353	46334	0.62
CD4 pos EM	36782	59531	0.75
CD4 TEMRA	7228	4172	0.50
CD4 pos B7 pos	5262	3544	0.34
CD4 pos CCR5 pos	11380	10425	0.15
CD4 CXCR3	39267	24162	0.06
CD8 pos	85578	67805	0.96
CD8 pos Naive	49335	28281	0.13
CD8 pos CM	7266	6906	0.34
CD8 pos EM	14732	6080	0.16
CD8 TEMRA	7688	5519	0.39
CD8 pos B7 pos	2413	1091	0.09
CD8 pos CCR5 pos	5141	3240	0.77
CD8 CXCR3	9237	3039	0.89
nTreg	8005	6190	0.30
Treg B7 pos	1070	339	0.96
Treg CCR5 pos	969	319	0.75
Treg CXCR3	847	303	0.62

Supplementary table 3: Number of Whole blood immune cells per group at baseline. p-values were calculated using Mann-Whitney U test.

Supplementary methods

Abbreviations

ASV – amplicon sequence variant

AUC – area under the curve

AUROC – area under the receiver-operator curve

CMV - cytomegalovirus

CRP – C-reactive protein

EBV – Epstein-Barr virus

ESBL – extended-spectrum beta lactamase

FACS – fluorescent-activated cell sorting

FMT – fecal microbiota transplantation

GAD – glutamate decarboxylase

HDLc – high density lipoprotein cholesterol

HLA – human leukocyte antigen

LDLc – low density lipoprotein cholesterol

LMM – linear mixed models analysis

LST – lymphocyte stimulation test

MMT – mixed meal test

MWU – Mann-Whitney U test

MRSA **–** methicillin-resistant *Staphylococcus aureus*

PBMCs - Peripheral blood mononuclear cells

PCR – polymerase chain reaction

PPI – preproinsulin

Qdot – quantum dot

ROC – receiver-operator curve

RT qPCR – reverse transcription quantitative PCR

T1D – type 1 diabetes

TG - triglycerides

TT – tetanus toxoid

UPLC-MS/MS - ultra high performance liquid chromatography coupled to tandem mass spectrometry

Fecal donor recruitment and randomization

Fecal donors completed questionnaires regarding dietary and bowel habits, travel history, comorbidity including family history of diabetes mellitus and medication use. They were screened for the presence of infectious diseases as described previously[1]. Furthermore, donors with 1st or 2nd degree relatives with autoimmune diseases (including Coeliac disease, autoimmune thyroid disease, type 1 diabetes and rheumatoid arthritis) were excluded. Blood was screened for human immunodeficiency virus; human T-lymphotropic virus; Hepatitis A, B, and C; cytomegalovirus (CMV); Epstein–Barr virus (EBV); strongyloides; amoebiasis, and lues. Presence of infection resulted in exclusion, although previous and non-active infections with EBV and CMV were allowed. Donors were also excluded if screening of their feces revealed the presence of pathogenic parasites (e.g. blastocystis hominis, dientamoeba fragilis, giardia lamblia), multiresistent bacteria (*Shigella*, *Campylobacter*, *Yersinia*, *MRSA ,ESBL, Salmonella, enteropathogenic E. Coli* and *Clostridium difficile*) or viruses (noro-, rota-, astro-, adeno (40/41/52)-, entero-, parecho- and sapovirus) as previously recommended[2]. After an overnight fast, plasma samples were taken for biochemistry and metabolomics and a morning fecal sample was collected.

FMT procedure

Seven healthy lean donors (of whom 3 were used twice) donated for the allogenic gut microbiota transfer to new onset type 1 diabetes (T1D) patients, and the same donor was used for the three consecutive FMT's in an individual T1D patient.

After admission, a duodenal tube was placed by gastroscopy or CORTRAK enteral access system. Each patient then underwent complete colon lavage with 2-4L of Klean prep® (macrogol) by duodenal tube until the researcher judged that the bowel was properly lavaged (i.e. no solid excrement, but clear fluid) for approximately 3h. Then, between 200 and 300 grams of feces was processed by dilution in 500 ml of 0.9% saline solution and filtered through unfolded cotton gauzes. The filtrate was used for transplantation two hours after the last administration of Klean prep® by duodenal tube in around 30 minutes using 50cc syringes. After a short observation period the patient was sent home.

Study visits

All study visits were performed at Amsterdam UMC, location AMC. Participants were asked to fill out an online nutritional diary for the duration of one week before each study visit to monitor caloric intake including the amount of dietary carbohydrates, fats, proteins and fibers. During the study visits blood pressure, weight and daily insulin use were documented. Fasting blood samples were taken at each visit and upon centrifugation stored at -80°C for subsequent analyses. Whole blood sodium heparin tubes were kept on room temperature and processed within 24 hours for immunological analyses (described under immunology).

Description per study visit

All visits took place after an overnight fast with subjects taking no long acting insulin the night before as previously described (Moran et al., 2013). At each visit blood, fecal and urine sampling and biometric measurements took place. At baseline all patients first underwent gastroduodenoscopy. A small dose of midazolam (2.5 or 5mg) was administered for patient's comfort. Duodenal biopsies were immediately collected in sterile tubes, snap-frozen in liquid nitrogen and stored at -80°C, followed by nasoduodenal tube placement. Then at least 2 hours later, a standardized 2h mixed meal test (MMT)(Nestlé sustacal boost®) was performed as previously described[3] to study residual Beta-

cell function. At 2, 9 and 12 months, patients again underwent a mixed-meal test for residual Beta-cell C-peptide secretion. After the 2 hour MMT, a duodenal tube was placed by means of CORTRAK enteral access, bowel cleansing for 6 hours was performed and the fecal transplant procedures were repeated. At 6 months, patients underwent gastroduodenoscopy and biopsies were taken from the duodenum and again thereafter, the mixed-meal test was performed. Of note, the similar daily schedule was used in all patients to minimize variation in measurements between subjects.

Mixed meal test

Starting the evening before each mixed meal test, T1D patients interrupted their long-acting insulin injections as previously published [3]. After an overnight fast and without taking their short-acting morning insulin dose, a mixed meal test was performed with Boost High Protein (Nestlé Nutrition, Vervey, Switzerland) at 6 ml/kg body weight with a maximum of 360 ml per person as previously described[4]. Subsequent blood sampling for stimulated C-peptide was performed at -10, 0, 15, 30, 45, 60, 90 and 120 minutes. Area under the curve (AUC) was derived according to the trapezoidal rule.

Adaptive T-cell Immunity

Whole blood samples were processed within 24 hours after sampling. Peripheral blood mononuclear cells (PBMC's) were used for measurement of immune response. Granulocytes were isolated for DNA-extraction and human leukocyte antigen (HLA) typing.

Isolation of Peripheral blood mononuclear cells (PBMC's)

PBMC's were isolated using Ficoll-density gradient centrifugation (ficoll 5.7%, amidotrizoaat 9%, *Pharmacy Leiden University Medical Centre*). After centrifuging, the interphase containing PBMC's was harvest and washed 3 times using PBS. PBMC's were suspended in 2 ml Iscove's modified

Dulbecco's Medium (IMDM, *Lonza*) supplemented with L-glutamine, penicillin-streptomycin (Pen Strep) and 15% Human serum and counted.

Lymphocyte Stimulation Test (LST)

T-cell proliferation in response to antigenic stimulation was performed as described previously (Kracht, Nature Medicine 2017). Cells were incubated in conditioned medium alone or in the presence of autoantigen proteins glutamate decarboxylase (GAD65), preproinsulin (PPI), insulinoma antigen-1 (IA-2) and a defective ribosomal product of proinsulin mRNA (DRiP) generated by stressed Beta cells[5]. For controls, cells were stimulated with Interleukin-2 (IL-2) or cultured with tetanus toxoid (TT). Cells were incubated for 5 days, after which ^{3}H-thymidine (50µl, 10 µCi/ml) was added for the last 18 hours of the culture.

Fluorescent-activated cell sorting (FACS) analyses and Quantum dot (Qdot)

For phenotyping and quantification of autoreactive CD8+ T-cell s, PBMC were stained with fluorescent antibodies according to a standard, independently validated protocol as described previously [6]. Stained cells were measured using FACS-Canto (phenotyping) and LSR-II (Q-dot) machines (Becton&Dickinson). Phenotyping data were analyzed using FlowJo software (TreeStar) using the gating strategy (supplementary figure 1) or as described previously for Qdot analyses [6].

Plasma metabolites

Fasting plasma targeted metabolite measurements were done by Metabolon (Durham, NC), using ultra high performance liquid chromatography coupled to tandem mass spectrometry (UPLC-MS/MS), as previously described [7]. Raw data was normalized to account for inter-day differences. Then, the levels of each metabolite were rescaled to set the median equal to 1 across all samples. Missing values, generally due to the sample measurement falling below the limit of detection, were then imputed with the minimum observed value for the respective metabolite.

Biochemistry

Glucose and C-reactive protein (CRP, Roche, Switzerland) were determined in fasted plasma samples. C-peptide was measured by radioimmunoassay (Millipore, Amsterdam, The Netherlands). Total cholesterol, high density lipoprotein cholesterol (HDLc), and triglycerides (TG) were determined in EDTA-containing plasma using commercially available enzymatic assays (Randox, Antrim, UK and DiaSys, Germany). All analyses were performed using a Selectra autoanalyzer (Sopachem, The Netherlands). Low density lipoprotein cholesterol (LDLc) was calculated using the Friedewald formula. Calprotectin was determined in feces using a commercial ELISA (Bühlmann, Switzerland). Hba1c was measured by HPLC (Tosoh G8, Tosoh Bioscience)

Fecal sample shotgun sequencing and metagenomic pipeline

Fecal microbiota were analysed using shotgun sequencing on donor and patient samples taken at 0, 6 and 12 months after initiation of study. DNA extraction from fecal samples for shotgun metagenomics was performed as previously described[8]. Subsequently, shotgun metagenomic sequencing was performed (Clinical Microbiomics, Copenhagen, Denmark). Before sequencing, the quality of the DNA samples was evaluated using agarose gel electrophoresis, NanoDrop 2000 spectrophotometry and Qubit 2.0 fluorometer quantitation. The genomic DNA was randomly sheared into fragments of around 350 bp. The fragmented DNA was used for library construction using NEBNext Ultra Library Prep Kit for Illumina (New England Biolabs). The prepared DNA libraries were evaluated using Qubit 2.0 fluorometer quantitation and Agilent 2100 Bioanalyzer for the fragment size distribution. Real time quantitative PCR (qPCR) was used to determine the concentration of the final library before sequencing. The library was sequenced on an Illumina HiSeq platform to produce 2 x 150 bp paired-end reads. Raw reads were quality filtered using Trimmomatic (v0.38), removing adapters, trimming the first 5 bp, and then quality trimming reads using a sliding

window of 4 bp and a minimum Q-score of 15. Reads that were shorter than 70 bp after trimming were discarded. Surviving paired reads were mapped against the human genome (GRCh37_hg19) with bowtie2 (v2.3.4.3) in order to remove human reads. Finally, the remaining quality filtered, non-human reads were sub-sampled to 20 million reads per sample and processed using Metaphlan2[9] (v2.7.7) to infer metagenomic microbial species composition and Humann2[10] (v0.11.2) to extract gene counts and functional pathways. In brief, reads were mapped using bowtie2 against microbial pangenomes; unmapped reads were translated and mapped against the full Uniref90 protein database using diamond (v0.8.38). Pathway collection was performed using the MetaCyc database.

Small intestinal microbiota analyses

Biopsies were added to a bead-beating tube with 300 µl Stool Transport and Recovery (STAR) buffer, 0.25 g of sterilized zirconia beads (0.1 mm). 6 µl of Proteinase K (20mg/ml; QIAGEN, Venlo, The Netherlands) was added and incubated for 1hr at 55 °C. The biopsies were then homogenized by bead-beating three times (60 s × 5.5 ms) followed by incubation for 15 min at 95 °C at 1000 rpm. Samples were then centrifuged for 5 min at 4 °C and 14,000 g and supernatants transferred to sterile tubes. Pellets were re-processed using 200 µl STAR buffer and both supernatants were pooled. DNA purification was performed with a customized kit (AS1220; Promega) using 250 µl of the final supernatant pool. DNA was eluted in 50 µl of DNAse- RNAse-free water and its concentration measured using a DS-11 FX+ Spectrophotometer/Fluorometer (DeNovix Inc., Wilmington, USA) with the Qubit™ dsDNA BR Assay kit (Thermo Scientific, Landsmeer, The Netherlands). The V5-V6 region of 16S ribosomal RNA (rRNA) gene was amplified in duplicate PCR reactions for each sample in a total reaction volume of 50 µl. A first step PCR using the 27F and the 1369R primer were used for primary enrichment. 1µl of 10uM primer, 1 µl dNTPs mixture, 0.5 µl Phusion Green Hot Start II High-Fidelity DNA Polymerase (2 U/µl; Thermo Scientific, Landsmeer, The Netherlands), 10 µl 5× Phusion Green HF Buffer, and 36.5 µl DNAse- RNAse-free water. The amplification program included 30 s of initial denaturation step at 98°C, followed by 5 cycles of denaturation at 98 oC for 30 s, annealing at 52 °C

for 40 s, elongation at 72 °C for 90 s, and a final extension step at 72 °C for 7 min. On the PCR product a nested PCR was performed using the master mix containing 1 µl of a unique barcoded primer, 784F-n and 1064R-n (10 µM each per reaction), 1 µl dNTPs mixture, 0.5 µl Phusion Green Hot Start II High-Fidelity DNA Polymerase (2 U/µl; Thermo Scientific, Landsmeer, The Netherlands), 10 µl 5× Phusion Green HF Buffer, and 36.5 µl DNAse- RNAse-free water. The amplification program included 30 s of initial denaturation step at 98°C, followed by 5 cycles of denaturation at 98 °C for 10 s, annealing at 42 °C for 10 s, elongation at 72 °C for 10 s, and a final extension step at 72 °C for 7 min. The PCR product was visualised in 1% agarose gel (~280 bp) and purified with CleanPCR kit (CleanNA, Alphen aan den Rijn, The Netherlands). The concentration of the purified PCR product was measured with Qubit dsDNA BR Assay Kit (Invitrogen, California, USA) and 200 ng of microbial DNA from each sample were pooled for the creation of the final amplicon library which was sequenced (150 bp, paired-end) on the Illumina HiSeq. 2500 platform (GATC Biotech, Constance, Germany).

Raw reads were demultiplexed using the Je software suite (v2.0.) allowing no mismatches in the barcodes. After removing the barcodes, linker and primers, reads were mapped against the human genome using bowtie2 in order to remove human reads. Surviving microbial forward and reverse reads were pipelined separately using DADA2[11] (v1.12.1). Amplicon Sequence Variants (ASVs) inferred from the reverse reads were reverse-complemented and matched against ASVs inferred from the forwards reads. Only non-chimeric forward reads ASVs that matched reverse-complemented reverse reads ASVs were kept. ASV sample counts were inferred from the forward reads. ASV taxonomy was assigned using DADA2 and the SILVA (v132) database. The resulting ASV table and taxonomy assignments were integrated using the phyloseq R package (v1.28.0) and rarefied to 60000 counts per sample.

Duodenal gene expression

Fresh biopsy samples were snap frozen, stored at −80°C and processed as previously published (Pellegrini et al., 2017). Prior to RNA extraction, biopsies were transferred into 500 µl lysis buffer

(mirVana Isolation Kit, Ambion, Austin, TX), homogenized with Tissue Ruptor (Qiagen, Hilden, Germany) and frozen again. Total RNA was extracted with mirVana Kit following manufacturer's instruction and quantified by spectrophotometer lecture (Epoch, Gen5 software; BioTek, Winooski, VT). OD A260/A280 ratio ≥2.0 and *GAPDH* Ct<28 in Taqman single assay identified acceptable quality RNA samples. For reverse transcription PCR, after DNAse treatment (Turbo DNAse, Invitrogen), 5 µg of RNA were retro-transcribed in a 21 µl reaction volume with SuperScript IV RT (Invitrogen) following manufacturer's instructions. Predesigned TaqMan Arrays Human Inflammation Panel and Human Cell Junction Panel (Applied Biosystems, Foster City, CA) were used for gene expression study. A list of genes is reported in supplementary table 1. PCR runs and fluorescence detection were carried out in a 7900 Real-Time PCR System (Applied Biosystems) at the following temperature conditions: 50° C for 2 minutes, 95°C for 10 minutes and 40 cycles of 95° C for 15 seconds and 60° C for 1 minute. Results were expressed as fold changes (2^-ΔCt method) over a mean of expression of the selected best reference genes: 5 housekeeping (HK) genes for Human Inflammation panel l (β-*actin*, β-*2 Microglobulin*, *GAPDH, RPLP0* and *UBC)* and 4 housekeeping genes for Human Cell Junction Panel (β-*2 Microglobulin*, *GAPDH, RPLP0* and *UBC*).

Statistical analysis

For baseline differences between groups, unpaired Student's t-test or the Mann-Whitney U test (MWU) were used dependent on the distribution of the data. Accordingly, data are expressed as mean ± the standard deviation or the median with interquartile range. Post-prandial results (e.g. c-peptide) are described as area under the curves (AUC) for the 2-hour post-prandial follow-up, calculated by using the trapezoidal method. For correlation analyses, Spearman's Rank test was used (as all parameters were non-parametric). For comparison of the primary end point a linear mixed model (LMM) was used (lme4 package in R), where 'allocation' and 'time point' were fixed effects and 'patient entry number' was a random effect. The p value for the interaction between 'allocation' and 'time point' was reported. Additionally, parameters were compared between groups at various

time points using MWU with multiplicity correction. A p-value < 0.05 was considered statistically significant.

Missing values

One study participant retracted informed consent after the first visit. This participant was not included in our analyses. All other study participants completed all study visits, therefore missing values are limited. Most missing data points were caused by laboratory problems such as inability to extract DNA or failure to properly process or harvest immune cells. These missing data are considered to be missing completely at random (MCAR). The exception to this is that one subject refused the second gastroduodenoscopy, therefore his duodenal biopsies (small intestinal microbiota and gene expression) after treatment are missing (1 in 20 cases or 5%). This subject has received autologous FMT. We do not assume that having received autologous treatment rather than allogenic (donor) faeces, metabolism or gene expression are in any way related to this person refusing the second gastroscopy, therefore we consider these data to be 'missing at random'(MAR). Key variables fasting C-peptide, C-peptide AUC, A1c and weight are complete (0% missing). The immunological parameters mentioned in the text and figures (main figure 6 and supplementary figure 3) are all based on complete data sets i.e. no missing values (CD4+ CM T cells, CD8+ T cells, CD8+CXCR3+ T cells and CD4+CXCR3+ T cells). Most gene expression data in the manuscript and main and supplemental figures (CCL22, CLDN12, CCL4, CD86, CCL19, CLDN 14, CCR5, CCL18, CD14) is 95% complete (see above). For CCL13 one extra baseline measurement is missing, for CXCL12 one 'after treatment' time point is missing, for CXCL1 two baseline and 1 after treatment time point is missing. Some immunological analyses have suffered from missing data, e.g. the lymphocyte stimulation tests (LST) analyses (1 to 4/20 (5-20%) of cases depending on the parameter). However, these data are not mentioned in the figures (there was no statistically significant difference between the groups). The fecal microbiota dataset is complete (complete case analysis). The missing values in the metabolite

data were imputated (see paragraph on metabolite analysis), therefore complete case analysis was performed. No other data have been imputated.

Machine learning and follow-up statistical analyses

This technique was used on duodenal microbial composition (perform RT-qPCR on biopsies), on fecal microbiota composition and metabolic pathway abundance (Shotgun sequencing), on plasma metabolite levels and on duodenal gene expression levels data. To predict treatment groups, we used the relative change (delta) of each parameter between 0 and 12 months. For duodenal microbes and duodenal gene expression, we used delta 0 vs 6 months as no 12 months' time point was available. For prediction of responders vs non-responders baseline values, delta 0 vs 6 months and delta 0 vs 12 months were used. Each analysis produced a ranked list of the top 30 most discriminative features. We selected the top parameters from each analysis that accurately (i.e., areau under the receiver-operator curve (AUROC)≥0.8) or moderately (AUROC > 0.7) predicted group allocation for closer study, using an arbitrary cut off. This cut off was generally a relative importance of around 30% or higher (for an example of this see figure 2C, from which the top 4 features were selected). Then, we visualized the change in time of the selected parameters (Wilcoxon's signed rank tests) and studied between-group differences (MWU) at each time point and finally, using Spearman's rank test, we correlated these parameters with our primary end point and with other key parameters that were identified in this way. For the most important analyses supplementary figures showing the top 30 selected features are presented.

Analysis of responders and non-responders irrespective of treatment group

We investigated whether baseline characteristics of T1D patients can predict response to FMT therapy at 12 months follow-up and which bacterial strains and plasma metabolites were associated with this response. Clinical response was defined as <10% decline in Beta-cell function compared to baseline at 12 months follow-up, which is significantly less than the expected natural 12 months decline of 20% in beta cell function [4,12]. We chose responders at 12 months for our analyses because our primary end point (MMT stimulated C-peptide) was significantly different at 12 (but not at 6) months. At 12 months follow-up, clinical response sustained in 10 subjects of whom 3 had received allogenic and 7 had received autologous FMT (see Figure 4A-B). We next used predictive modelling to determine which parameters (either their baseline values or delta 0-12 month values) were predictors of clinical response to FMT.

Patient and public involvement

This research was done without patient involvement. Patients were not invited to comment on the study design and were not consulted to develop patient relevant outcomes or interpret the results. Patients were not invited to contribute to the writing or editing of this document for readability or accuracy.

References

1 van Nood E, Vrieze A, Nieuwdorp M, *et al.* Duodenal infusion of donor feces for recurrent Clostridium difficile. *N Engl J Med* 2013;**368**:407–15. doi:10.1056/NEJMoa1205037

2 Cammarota G, Ianiro G, Tilg H, *et al.* European consensus conference on faecal microbiota transplantation in clinical practice. *Gut* 2017;**66**:569–80. doi:10.1136/gutjnl-2016-313017

3 Moran A, Bundy B, Becker DJ, *et al.* Interleukin-1 antagonism in type 1 diabetes of recent onset: two multicentre, randomised, double-blind, placebo-controlled trials. *Lancet (London,*

England) 2013;**381**:1905–15. doi:10.1016/S0140-6736(13)60023-9

4 Lachin JM, McGee PL, Greenbaum CJ, *et al.* Sample size requirements for studies of treatment effects on beta-cell function in newly diagnosed type 1 diabetes. *PLoS One* 2011;**6**:e26471. doi:10.1371/journal.pone.0026471

5 Kracht MJL, van Lummel M, Nikolic T, *et al.* Autoimmunity against a defective ribosomal insulin gene product in type 1 diabetes. *Nat Med* 2017;**23**:501–7. doi:10.1038/nm.4289

6 Velthuis JH, Unger WW, Abreu JRF, *et al.* Simultaneous detection of circulating autoreactive CD8+ T-cells specific for different islet cell-associated epitopes using combinatorial MHC multimers. *Diabetes* 2010;**59**:1721–30. doi:10.2337/db09-1486

7 Koh A, Molinaro A, Stahlman M, *et al.* Microbially Produced Imidazole Propionate Impairs Insulin Signaling through mTORC1. *Cell* 2018;**175**:947-961.e17. doi:10.1016/j.cell.2018.09.055

8 Vrieze A, Van Nood E, Holleman F, *et al.* Transfer of intestinal microbiota from lean donors increases insulin sensitivity in individuals with metabolic syndrome. *Gastroenterology* 2012;**143**:913-6.e7. doi:10.1053/j.gastro.2012.06.031

9 Truong DT, Franzosa EA, Tickle TL, *et al.* MetaPhlAn2 for enhanced metagenomic taxonomic profiling. Nat. Methods. 2015;**12**:902–3. doi:10.1038/nmeth.3589

10 Franzosa EA, McIver LJ, Rahnavard G, *et al.* Species-level functional profiling of metagenomes and metatranscriptomes. *Nat Methods* 2018;**15**:962–8. doi:10.1038/s41592-018-0176-y

11 Callahan BJ, McMurdie PJ, Rosen MJ, *et al.* DADA2: High-resolution sample inference from Illumina amplicon data. *Nat Methods* 2016;**13**:581–3. doi:10.1038/nmeth.3869

12 Overgaard AJ, Weir JM, Jayawardana K, *et al.* Plasma lipid species at type 1 diabetes onset predict residual beta-cell function after 6 months. *Metabolomics* 2018;**14**:158. doi:10.1007/s11306-018-1456-3

332

333

334

Supplementary table 1

Genecard Cell Junctions			Genecard Inflammation		
Gene code	Gene name	Gene type	Gene code	Gene name	Gene type
GAPDH-Hs99999905_m1	glyceraldehyde-3-phosphate dehydrogenase	housekeeping	GAPDH-Hs99999905_m1	glyceraldehyde-3-phosphate dehydrogenase	housekeeping
CAV1-Hs00971716_m1	caveolin 1	target	ACTB-Hs99999903_m1	actin beta	housekeeping
CAV2-Hs00184597_m1	caveolin 2	target	ALOX5-Hs00167536_m1	arachidonate 5-lipoxygenase	target
CAV3-Hs00154292_m1	caveolin 3	target	B2M-Hs99999907_m1	beta-2-microglobulin	housekeeping
CDH1-Hs01023894_m1	cadherin 1	target	HSPA5-Hs00607129_gH	heat shock protein family A (Hsp70) member 5	target
CDH2-Hs00983056_m1	cadherin 2	target	CARD9-Hs00364485_m1	caspase recruitment domain family member 9	target
CLDN1-Hs00221623_m1	claudin 1	target	ACKR2-Hs00174299_m1	atypical chemokine receptor 2	target
CLDN10-Hs00734479_m1	claudin 10	target	CCL11-Hs00237013_m1	C-C motif chemokine ligand 11	target
CLDN11-Hs00194440_m1	claudin 11	target	CCL13-Hs00234646_m1	C-C motif chemokine ligand 13	target
CLDN12-Hs00273258_s1	claudin 12	target	CCL15-CCL14;CCL15-Hs00263142_m1	CCL15-CCL14, C-C motif chemokine ligand 15	target
CLDN14-Hs00273267_s1	claudin 14	target	CCL16-Hs00171123_m1	C-C motif chemokine ligand 16	target
CLDN15-Hs00204982_m1	claudin 15	target	CCL17-Hs00171074_m1	C-C motif chemokine ligand 17	target
CLDN16-Hs01070692_m1	claudin 16	target	CCL18-Hs00268113_m1	C-C motif chemokine ligand 18	target
CLDN17-Hs01043467_s1	claudin 17	target	CCL19-Hs00171149_m1	C-C motif chemokine ligand 19	target
CLDN18-Hs00212584_m1	claudin 18	target	CCL1-Hs00171072_m1	C-C motif chemokine ligand 1	target
CLDN19-Hs00961709_m1	claudin 19	target	CCL2-Hs00234140_m1	C-C motif chemokine ligand 2	target
CLDN2-Hs00252666_s1	claudin 2	target	CCL20-Hs00171125_m1	C-C motif chemokine ligand 20	target
CLDN3-Hs00265816_s1	claudin 3	target	CCL21-Hs00171076_m1	C-C motif chemokine ligand 21	target
CLDN4-Hs00976831_s1	claudin 4	target	CCL22-Hs00171080_m1	C-C motif chemokine ligand 22	target
CLDN5-Hs00533949_s1	claudin 5	target	CCL25-Hs00171144_m1	C-C motif chemokine ligand 25	target
CLDN6-Hs00607528_s1	claudin 6	target	CCL26-Hs00171146_m1	C-C motif chemokine ligand 26	target
CLDN7-Hs00600772_m1	claudin 7	target	UBC-Hs00824723_m1	ubiquitin C	housekeeping
CLDN8-Hs04186769_s1	claudin 8	target	CCL3-Hs00234142_m1	C-C motif chemokine ligand 3	target
CLDN9-Hs00253134_s1	claudin 9	target	CCL4-Hs99999148_m1	C-C motif chemokine ligand 4	target
DLL1-Hs00194509_m1	delta like canonical Notch ligand 1	target	CCL5-Hs00174575_m1	C-C motif chemokine ligand 5	target
DSC1-Hs00245189_m1	desmocollin 1	target	CCL7-Hs00171147_m1	C-C motif chemokine ligand 7	target
DSC2-Hs00951428_m1	desmocollin 2	target	CCL8-Hs00271615_m1	C-C motif chemokine ligand 8	target
DSC3-Hs00170032_m1	desmocollin 3	target	CCR1-Hs00174298_m1	C-C motif chemokine receptor 1	target
DSG1-Hs00355084_m1	desmoglein 1	target	CCR2-Hs00356601_m1	C-C motif chemokine receptor 2	target
DSG2-Hs00170071_m1	desmoglein 2	target	CCR3-Hs00266213_s1	C-C motif chemokine receptor 3	target
DSG3-Hs00951897_m1	desmoglein 3	target	CCR4-Hs99999919_m1	C-C motif chemokine receptor 4	target
DSG4-Hs00698286_m1	desmoglein 4	target	CCR5-Hs00152917_m1	C-C motif chemokine receptor 5	target
DSP-Hs00950591_m1	desmoplakin	target	CCR6-Hs00171121_m1	C-C motif chemokine receptor 6	target
DST-Hs00156137_m1	dystonin	target	CCR7-Hs00171054_m1	C-C motif chemokine receptor 7	target
ESAM-Hs00332781_m1	endothelial cell adhesion molecule	target	CCR8-Hs00174764_m1	C-C motif chemokine receptor 8	target
F11R-Hs00170991_m1	F11 receptor	target	CD14-Hs02621496_s1	CD14 molecule	target
GJA1-Hs00748445_s1	gap junction protein alpha 1	target	CD28-Hs01007422_m1	CD28 molecule	target
GJA3-Hs00254296_s1	gap junction protein alpha 3	target	CD68-Hs00154355_m1	CD68 molecule	target
GJA4-Hs00704917_s1	gap junction protein alpha 4	target	CD80-Hs01045161_m1	CD80 molecule	target
GJA5-Hs00270952_s1	gap junction protein alpha 5	target	CD86-Hs01567026_m1	CD86 molecule	target
GJA8-Hs00270960_s1	gap junction protein alpha 8	target	CHGA-Hs00900375_m1	chromogranin A	target
GJB1-Hs00939759_s1	gap junction protein beta 1	target	DDIT3-Hs00358796_g1	DNA damage inducible transcript 3	target
GJB2-Hs00269615_s1	gap junction protein beta 2	target	PTGS2-Hs00153133_m1	prostaglandin-endoperoxide synthase 2	target
GJB3-Hs02378125_s1	gap junction protein beta 3	target	CSF1-Hs00174164_m1	colony stimulating factor 1	target
GJB4-Hs00920816_s1	gap junction protein beta 4	target	CTLA4-Hs00175480_m1	cytotoxic T-lymphocyte associated protein 4	target
GJB5-Hs01921450_s1	gap junction protein beta 5	target	CX3CL1-Hs00171086_m1	C-X3-C motif chemokine ligand 1	target
GJB6-Hs00922742_s1	gap junction protein beta 6	target	CX3CR1-Hs00365842_m1	C-X3-C motif chemokine receptor 1	target
GJC2-Hs00252713_s1	gap junction protein gamma 2	target	CXCL10-Hs00171042_m1	C-X-C motif chemokine ligand 10	target
GJD2-Hs00950432_m1	gap junction protein delta 2	target	CXCL12-Hs00171022_m1	C-X-C motif chemokine ligand 12	target
GJC3-Hs01384570_m1	gap junction protein gamma 3	target	CXCL1-Hs00236937_m1	C-X-C motif chemokine ligand 1	target
ICAM1-Hs00164932_m1	intercellular adhesion molecule 1	target	CXCL9-Hs00171065_m1	C-X-C motif chemokine ligand 9	target
ICAM2-Hs00609563_m1	intercellular adhesion molecule 2	target	CXCR1-Hs00174146_m1	C-X-C motif chemokine receptor 1	target
ITGA1-Hs00235006_m1	integrin subunit alpha 1	target	CXCR2-Hs00174304_m1	C-X-C motif chemokine receptor 2	target
ITGA2-Hs00158127_m1	integrin subunit alpha 2	target	CXCR3-Hs00171041_m1	C-X-C motif chemokine receptor 3	target
ITGA3-Hs01076873_m1	integrin subunit alpha 3	target	CXCR4-Hs00237052_m1	C-X-C motif chemokine receptor 4	target
ITGA4-Hs00168433_m1	integrin subunit alpha 4	target	CXCR6-Hs00174843_m1	C-X-C motif chemokine receptor 6	target
ITGA5-Hs01547673_m1	integrin subunit alpha 5	target	ACKR3-Hs00604567_m1	atypical chemokine receptor 3	target
ITGA6-Hs01041011_m1	integrin subunit alpha 6	target	FCGR3B;FCGR3A-Hs00275547_m1	Fc fragment of IgG receptor IIIb,Fc fragment of IgG receptor IIIa	target
ITGA7-Hs00174397_m1	integrin subunit alpha 7	target	GAD2-Hs00609534_m1	glutamate decarboxylase 2	target
ITGA8-Hs00233321_m1	integrin subunit alpha 8	target	HCK-Hs01067403_m1	HCK proto-oncogene, Src family tyrosine kinase	target
ITGA9-Hs00979865_m1	integrin subunit alpha 9	target	PTPRN-Hs01090891_g1	protein tyrosine phosphatase, receptor type N	target
ITGAL-Hs00158218_m1	integrin subunit alpha L	target	IDO1-Hs00984148_m1	indoleamine 2,3-dioxygenase 1	target
ITGAM-Hs00355885_m1	integrin subunit alpha M	target	IFNG-Hs00174143_m1	interferon gamma	target
ITGAV-Hs00233808_m1	integrin subunit alpha V	target	IL10-Hs00174086_m1	interleukin 10	target
ITGB1-Hs00559595_m1	integrin subunit beta 1	target	IL12A-Hs00168405_m1	interleukin 12A	target
ITGB2-Hs00164957_m1	integrin subunit beta 2	target	RPLP0-Hs99999902_m1	ribosomal protein lateral stalk subunit P0	housekeeping
ITGB3-Hs01001469_m1	integrin subunit beta 3	target	IL12B-Hs00233688_m1	interleukin 12B	target
ITGB4-Hs00236216_m1	integrin subunit beta 4	target	IL15-Hs00542562_m1	interleukin 15	target
ITGB5-Hs00174435_m1	integrin subunit beta 5	target	IL15RA-Hs00542602_g1	interleukin 15 receptor subunit alpha	target
ITGB6-Hs00168458_m1	integrin subunit beta 6	target	IL17A-Hs00174383_m1	interleukin 17A	target
JAM2-Hs01022006_m1	junctional adhesion molecule 2	target	IL1R1-Hs00991010_m1	interleukin 1 receptor type 1	target
JAM3-Hs00230289_m1	junctional adhesion molecule 3	target	IL1B-Hs00174097_m1	interleukin 1 beta	target
JUP-Hs00158408_m1	junction plakoglobin	target	IL2-Hs00174114_m1	interleukin 2	target
NOTCH1-Hs01062014_m1	notch 1	target	IL22-Hs01574154_m1	interleukin 22	target
NOTCH2-Hs01050702_m1	notch 2	target	IL4-Hs00174122_m1	interleukin 4	target
NOTCH3-Hs01128541_m1	notch 3	target	IL4R-Hs00166237_m1	interleukin 4 receptor	target
NOTCH4-Hs00965889_m1	notch 4	target	IL6-Hs00174131_m1	interleukin 6	target
OCLN-Hs00170162_m1	occludin	target	CXCL8-Hs00174103_m1	C-X-C motif chemokine ligand 8	target
PLEC-Hs00356986_g1	plectin	target	INS-Hs02741908_m1	insulin	target
NECTIN1-Hs01591978_m1	nectin cell adhesion molecule 1	target	LAG3-Hs00958444_g1	lymphocyte activating 3	target
NECTIN2-Hs01071562_m1	nectin cell adhesion molecule 2	target	LST1-Hs00705788_s1	leukocyte specific transcript 1	target
NECTIN3-Hs00210043_m1	nectin cell adhesion molecule 3	target	CIITA-Hs00172106_m1	class II, major histocompatibility complex, transactivator	target
TJP1-Hs01551861_m1	tight junction protein 1	target	MIF-Hs00236988_g1	macrophage migration inhibitory factor	target
TJP2-Hs00910543_m1	tight junction protein 2	target	NOD2-Hs00223394_m1	nucleotide binding oligomerization domain containing 2	target
TJP3-Hs00274276_m1	tight junction protein 3	target	NOS2-Hs00167257_m1	nitric oxide synthase 2	target
HPRT1-Hs99999909_m1	hypoxanthine phosphoribosyltransferase 1	housekeeping	PDCD1-Hs01550088_m1	programmed cell death 1	target
GUSB-Hs99999908_m1	glucuronidase beta	housekeeping	CD274-Hs00204257_m1	CD274 molecule	target
ACTB-Hs99999903_m1	actin beta	housekeeping	PTX3-Hs00173615_m1	pentraxin 3	target
B2M-Hs99999907_m1	beta-2-microglobulin	housekeeping	SIGIRR-Hs00222347_m1	single Ig and TIR domain containing	target
HMBS-Hs00609297_m1	hydroxymethylbilane synthase	housekeeping	TMEM173-Hs00736955_g1	transmembrane protein 173	target
IPO8-Hs00183533_m1	importin 8	housekeeping	SYP-Hs00300531_m1	synaptophysin	target
PGK1-Hs99999906_m1	phosphoglycerate kinase 1	housekeeping	TNF-Hs00174128_m1	tumor necrosis factor	target
RPLP0-Hs99999902_m1	ribosomal protein lateral stalk subunit P0	housekeeping	TSPAN7-Hs00190284_m1	tetraspanin 7	target
TBP-Hs99999910_m1	TATA-box binding protein	housekeeping	VEGFA-Hs00900054_m1	vascular endothelial growth factor A	target
TFRC-Hs99999911_m1	transferrin receptor	housekeeping	C10orf54-Hs00735289_m1	chromosome 10 open reading frame 54	target
UBC-Hs00824723_m1	ubiquitin C	housekeeping	KCNJ8-Hs00958961_m1	potassium voltage-gated channel subfamily J member 8	target

Parameter	Groups	Delta or baseline	AUC ± CI	1st most predictive variable	2nd	3rd
Metabolites	Tx groups	Δ 0 – 12M	0.79 ± 0.23	1-myristoyl-2-arachidonoyl-GPC	1-(1-enyl-palmitoyl)-2-linoleoyl-GPE	1-arachidonoyl-GPC
	R12	Baseline	0.70 ± 0.28	7-hydroxyoctanoate	N-acetylphenylalanine	2-methylcitrate/homocitrate
		Δ 0 – 12M	0.74 ± 0.25	7-hydroxyoctanoate	14 or 15-methylpalmitate	5-methylthioadenosine
Small intestinal microbes	Tx groups	Δ 0 – 12M	0.89 ± 0.18	Prevotella 1	Prevotella 2	Streptococcus oralis
	R12	Baseline	0.72 ± 0.27	Undibacterium oligocarboniphilum	Nesterenkonia flava	Shewanella colwelliana
		Δ 0 – 6M	0.60 ± 0.29	Neisseria animalis	Tenuibacillus multivorans	Streptococcus mitis
Fecal microbes (taxonomy)	Tx groups	Δ 0 – 6M	0.58 ± 0.24	Desulfovibrio piger	Bacteroidales bacterium ph8	Ruminococcus callidus
		Δ 0 – 12M	0.72 ± 0.24	Desulfovibrio piger	Eubacterium ventriosum	Sutterella wadsworthensis
	R12	Baseline	0.93 ± 0.14	Coprococcus catus	Bacteroides caccae	Paraprevotella unclassified
		Δ 0 – 6M	0.78 ± 0.23	Lachnospiraceae bacterium 8 1 57FAA	Collinsella aerofaciens	Holdemania unclassified
		Δ 0 – 12M	0.76 ± 0.23	Bacteroidales bacterium ph8	Actinomyces viscosus	Bacteroides thetaiotaomicron
Fecal microbes (metabolic pathways)	Tx groups	Δ 0 – 6M	0.75 ± 0.24	GDP-mannose biosynthesis	dTDP-L-rhamnose biosynthesis I	seleno-amino acid biosynthesis
		Δ 0 – 12M	0.68 ± 0.27	seleno-amino acid biosynthesis	UMP biosynthesis	superpathway of UDP-glucose-derived O-antigen building blocks biosynthesis
	R12	Baseline	0.85 ± 0.22	fatty acid β-oxidation I	pyruvate fermentation to acetone	colanic acid building blocks biosynthesis
		Δ 0 – 6M	0.70 ± 0.27	glycogen biosynthesis I (from ADP-D-Glucose)	phosphatidylcholine acyl editing	L-lysine biosynthesis II
		Δ 0 – 12M	0.69 ± 0.22	creatinine degradation I	Bifidobacterium shunt	glycolysis III (from glucose)
Duodenal gene expression	Tx groups	Δ 0 – 6M	0.61 ± 0.24	CCL18	CXCR1	CXCR4
	R12	Baseline	0.83 ± 0.21	CCL22	CLDN12	CCL4
		Δ 0 – 6M	0.73 ± 0.24	CCR5	CCL18	CD14

Supplementary table 2: AUCs. This table provides an overview of all predictive modeling analyses that we have performed. It shows what parameter was studied, in which group the analysis was done, whether baseline or delta values were used, how well the predictive model performed (measured asAUROC) and what were the top 3 predictive parameters from that analysis. The highest AUC from each category in bold. Tx: treatment, R12: responders versus non-responders at 12 months, Baseline: for this analysis, the baseline value of the parameters were used, Δ 0 – 12M: for this analysis, the delta's between baseline and 12 months were used. AUROC: area under the receiver-operator curve ± confidence interval.

S1

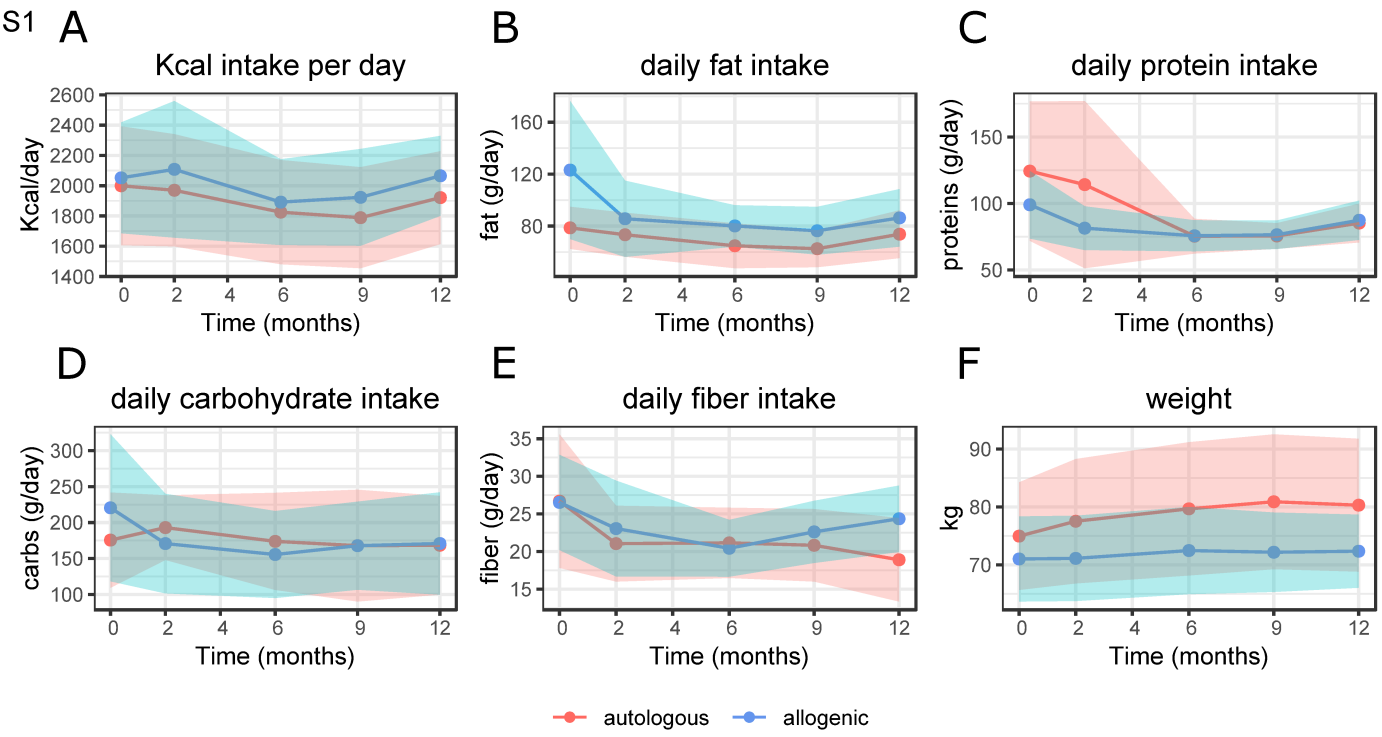
A
Kcal intake per day
Kcal/day
2600
2400
2200
2000
1800
1600
1400
0 2 4 6 9 12
Time (months)
B
daily fat intake
fat (g/day)
160
120
80
0 2 4 6 9 12
Time (months)
C
daily protein intake
proteins (g/day)
150
100
50
0 2 4 6 9 12
Time (months)
D
daily carbohydrate intake
carbs (g/day)
300
250
200
150
100
0 2 4 6 9 12
Time (months)
E
daily fiber intake
fiber (g/day)
35
30
25
20
15
0 2 4 6 9 12
Time (months)
F
weight
kg
90
80
70
0 2 4 6 9 12
Time (months)
autologous
allogenic

S2

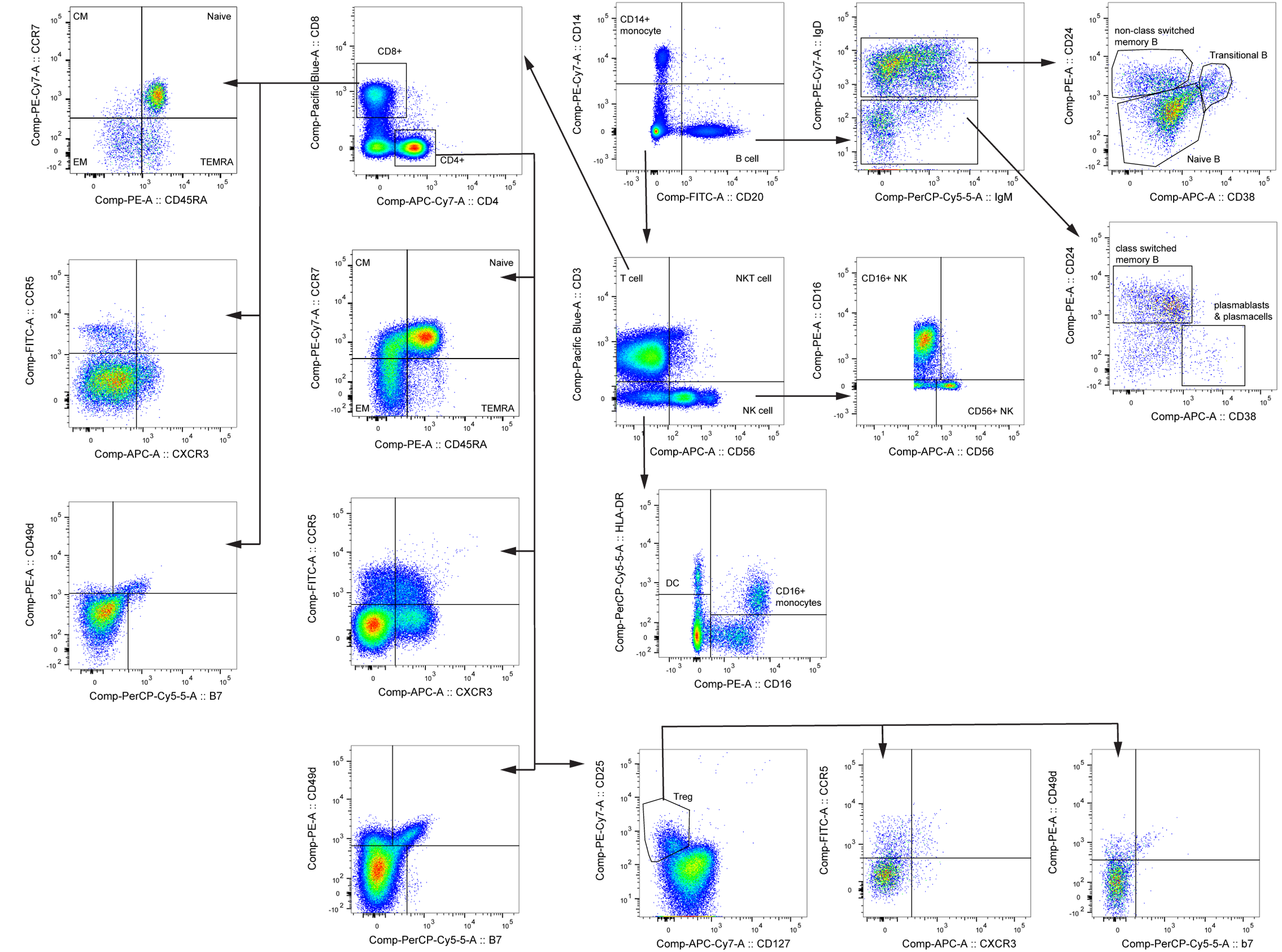
CM
Naive
EM
TEMRA
Comp-PE-Cy7-A :: CCR7
Comp-PE-A :: CD45RA
Comp-Pacific Blue-A :: CD8
CD8+
CD4+
Comp-APC-Cy7-A :: CD4
Comp-FITC-A :: CCR5
Comp-APC-A :: CXCR3
Comp-PE-A :: CD49d
Comp-PerCP-Cy5-5-A :: B7
CD14+ monocyte
B cell
Comp-PE-Cy7-A :: CD14
Comp-FITC-A :: CD20
Comp-PE-Cy7-A :: IgD
Comp-PerCP-Cy5-5-A :: IgM
non-class switched memory B
Transitional B
Naive B
Comp-PE-A :: CD24
Comp-APC-A :: CD38
class switched memory B
plasmablasts & plasmacells
T cell
NK cell
Comp-Pacific Blue-A :: CD3
Comp-APC-A :: CD56
CD16+ NK
CD56+ NK
Comp-PE-A :: CD16
DC
CD16+ monocytes
Comp-PerCP-Cy5-5-A :: HLA-DR
Comp-PE-A :: CD16
Treg
Comp-PE-Cy7-A :: CD25
Comp-APC-Cy7-A :: CD127
Comp-FITC-A :: CCR5
Comp-APC-A :: CXCR3
Comp-PE-A :: CD49d
Comp-PerCP-Cy5-5-A :: b7

S3

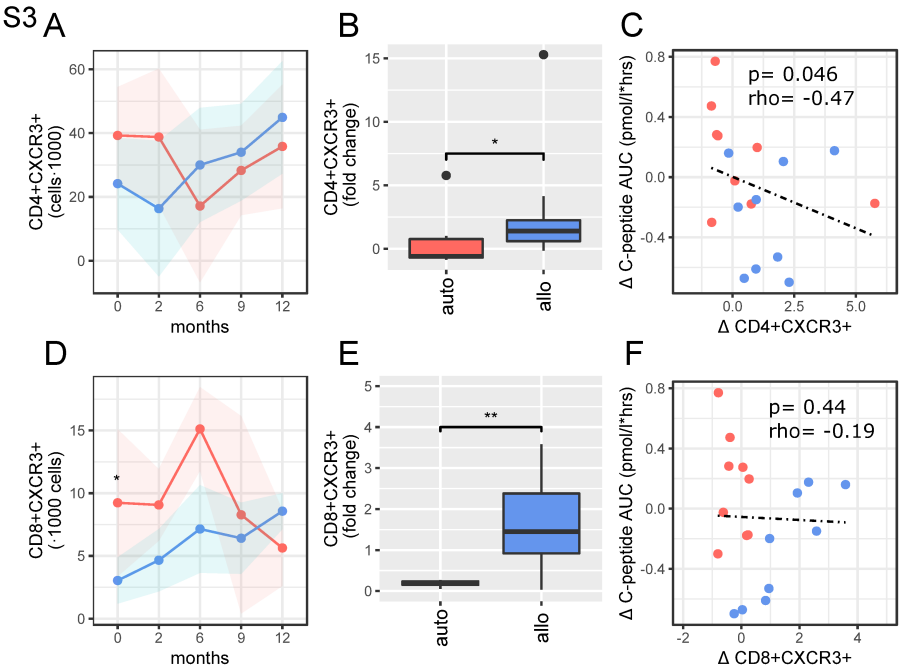
A
CD4+CXCR3+ (cells·1000)
months
B
CD4+CXCR3+ (fold change)
auto
allo
C
p= 0.046
rho= -0.47
Δ C-peptide AUC (pmol/l*hrs)
Δ CD4+CXCR3+
D
CD8+CXCR3+ (·1000 cells)
months
E
CD8+CXCR3+ (fold change)
auto
allo
F
p= 0.44
rho= -0.19
Δ C-peptide AUC (pmol/l*hrs)
Δ CD8+CXCR3+

S4

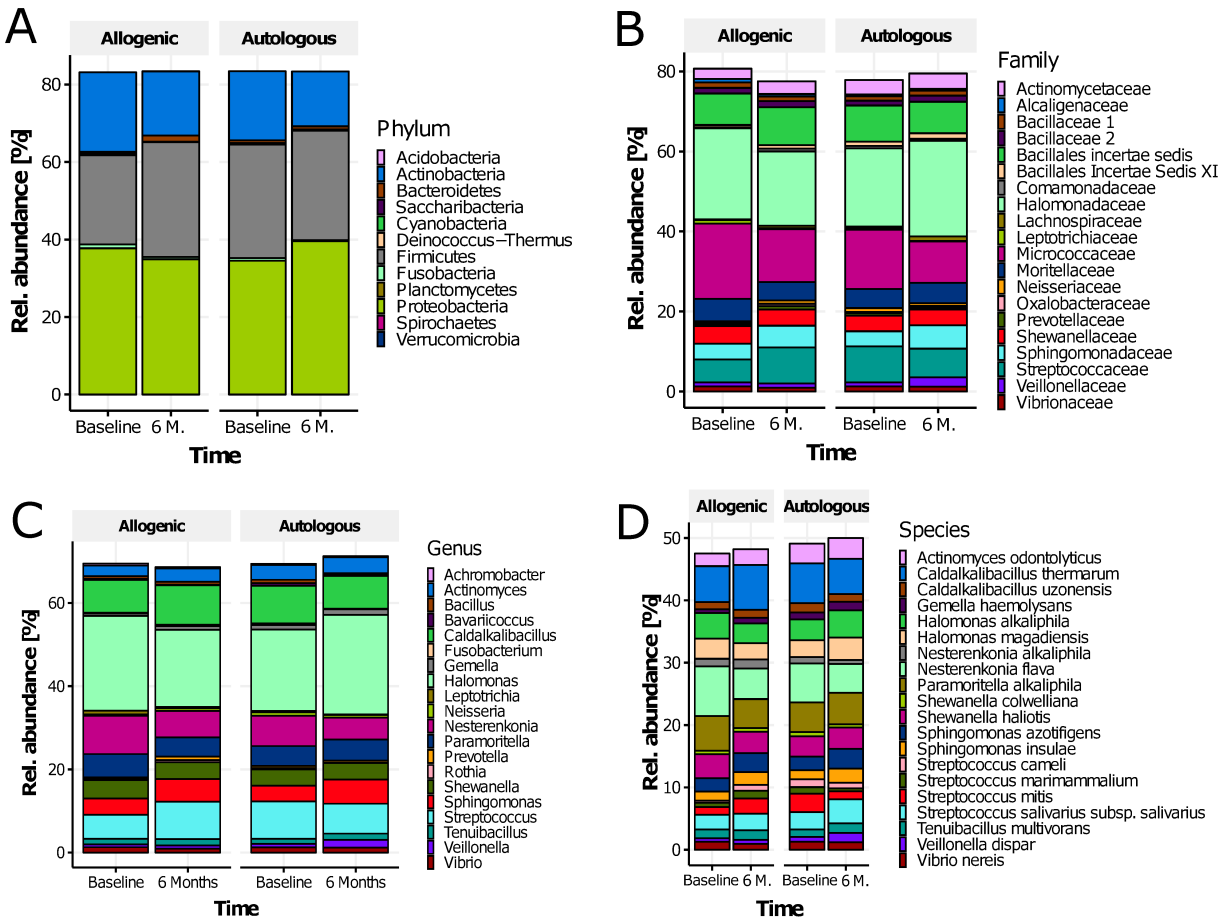
A
Allogenic
Autologous
Rel. abundance [%]
Baseline 6 M. Baseline 6 M.
Time
Phylum
Acidobacteria
Actinobacteria
Bacteroidetes
Saccharibacteria
Cyanobacteria
Deinococcus–Thermus
Firmicutes
Fusobacteria
Planctomycetes
Proteobacteria
Spirochaetes
Verrucomicrobia
B
Allogenic
Autologous
Rel. abundance [%]
Baseline 6 M. Baseline 6 M.
Time
Family
Actinomycetaceae
Alcaligenaceae
Bacillaceae 1
Bacillaceae 2
Bacillales incertae sedis
Bacillales Incertae Sedis XI
Comamonadaceae
Halomonadaceae
Lachnospiraceae
Leptotrichiaceae
Micrococcaceae
Moritellaceae
Neisseriaceae
Oxalobacteraceae
Prevotellaceae
Shewanellaceae
Sphingomonadaceae
Streptococcaceae
Veillonellaceae
Vibrionaceae
C
Allogenic
Autologous
Rel. abundance [%]
Baseline 6 Months Baseline 6 Months
Time
Genus
Achromobacter
Actinomyces
Bacillus
Bavariicoccus
Caldalkalibacillus
Fusobacterium
Gemella
Halomonas
Leptotrichia
Neisseria
Nesterenkonia
Paramoritella
Prevotella
Rothia
Shewanella
Sphingomonas
Streptococcus
Tenuibacillus
Veillonella
Vibrio
D
Allogenic
Autologous
Rel. abundance [%]
Baseline 6 M. Baseline 6 M.
Time
Species
Actinomyces odontolyticus
Caldalkalibacillus thermarum
Caldalkalibacillus uzonensis
Gemella haemolysans
Halomonas alkaliphila
Halomonas magadiensis
Nesterenkonia alkaliphila
Nesterenkonia flava
Paramoritella alkaliphila
Shewanella colwelliana
Shewanella haliotis
Sphingomonas azotifigens
Sphingomonas insulae
Streptococcus cameli
Streptococcus marimammalium
Streptococcus mitis
Streptococcus salivarius subsp. salivarius
Tenuibacillus multivorans
Veillonella dispar
Vibrio nereis

S5

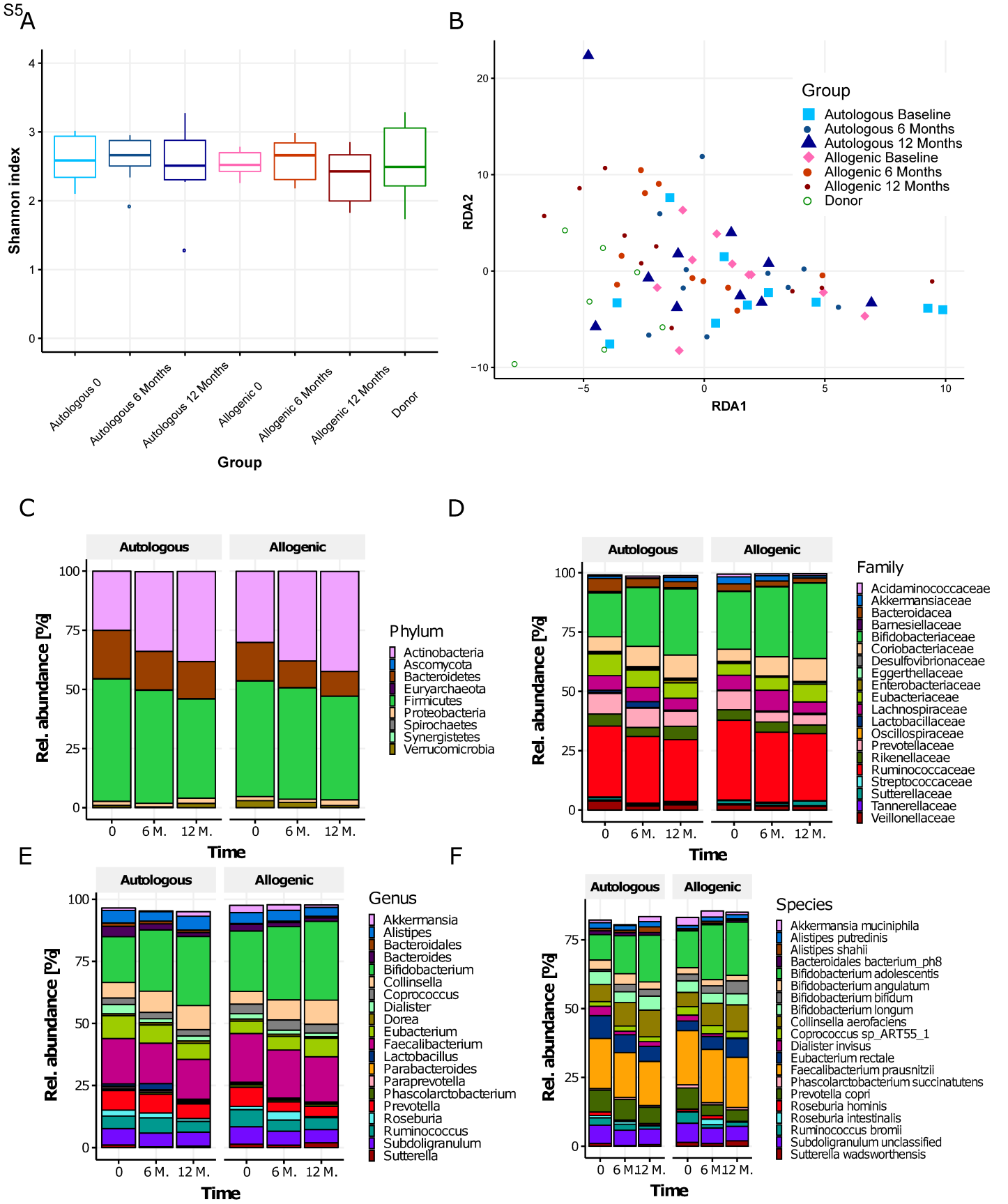
A
Shannon index
Group
Autologous 0
Autologous 6 Months
Autologous 12 Months
Allogenic 0
Allogenic 6 Months
Allogenic 12 Months
Donor
B
RDA1
RDA2
Group
Autologous Baseline
Autologous 6 Months
Autologous 12 Months
Allogenic Baseline
Allogenic 6 Months
Allogenic 12 Months
Donor
C
Autologous
Allogenic
Rel. abundance [%]
Time
Phylum
Actinobacteria
Ascomycota
Bacteroidetes
Euryarchaeota
Firmicutes
Proteobacteria
Spirochaetes
Synergistetes
Verrucomicrobia
D
Family
Acidaminococcaceae
Akkermansiaceae
Bacteroidacea
Barnesiellaceae
Bifidobacteriaceae
Coriobacteriaceae
Desulfovibrionaceae
Eggerthellaceae
Enterobacteriaceae
Eubacteriaceae
Lachnospiraceae
Lactobacillaceae
Oscillospiraceae
Prevotellaceae
Rikenellaceae
Ruminococcaceae
Streptococcaceae
Sutterellaceae
Tannerellaceae
Veillonellaceae
E
Genus
Akkermansia
Alistipes
Bacteroidales
Bacteroides
Bifidobacterium
Collinsella
Coprococcus
Dialister
Dorea
Eubacterium
Faecalibacterium
Lactobacillus
Parabacteroides
Paraprevotella
Phascolarctobacterium
Prevotella
Roseburia
Ruminococcus
Subdoligranulum
Sutterella
F
Species
Akkermansia muciniphila
Alistipes putredinis
Alistipes shahii
Bacteroidales bacterium_ph8
Bifidobacterium adolescentis
Bifidobacterium angulatum
Bifidobacterium bifidum
Bifidobacterium longum
Collinsella aerofaciens
Coprococcus sp_ART55_1
Dialister invisus
Eubacterium rectale
Faecalibacterium prausnitzii
Phascolarctobacterium succinatutens
Prevotella copri
Roseburia hominis
Roseburia intestinalis
Ruminococcus bromii
Subdoligranulum unclassified
Sutterella wadsworthensis

S6 A

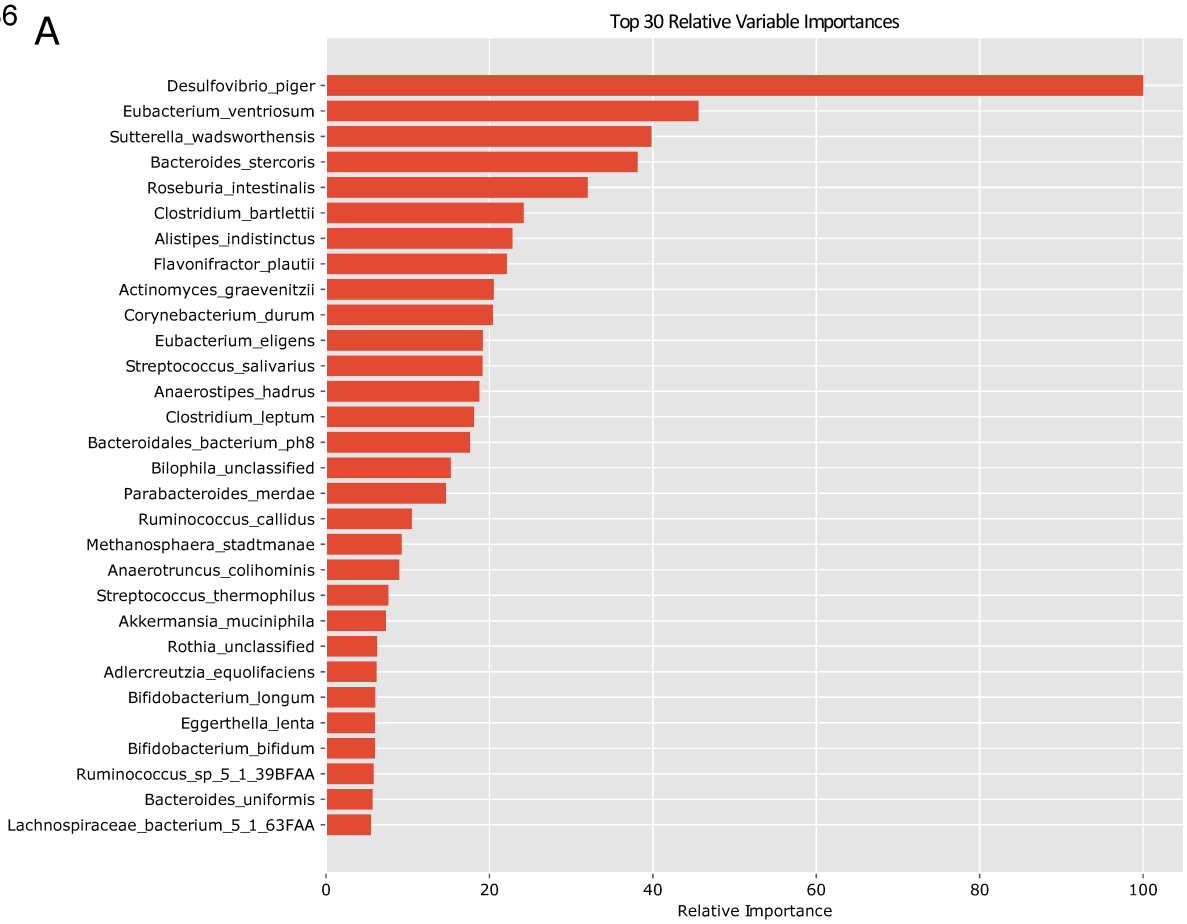
Top 30 Relative Variable Importances
Desulfovibrio_piger
Eubacterium_ventriosum
Sutterella_wadsworthensis
Bacteroides_stercoris
Roseburia_intestinalis
Clostridium_bartlettii
Alistipes_indistinctus
Flavonifractor_plautii
Actinomyces_graevenitzii
Corynebacterium_durum
Eubacterium_eligens
Streptococcus_salivarius
Anaerostipes_hadrus
Clostridium_leptum
Bacteroidales_bacterium_ph8
Bilophila_unclassified
Parabacteroides_merdae
Ruminococcus_callidus
Methanosphaera_stadtmanae
Anaerotruncus_colihominis
Streptococcus_thermophilus
Akkermansia_muciniphila
Rothia_unclassified
Adlercreutzia_equolifaciens
Bifidobacterium_longum
Eggerthella_lenta
Bifidobacterium_bifidum
Ruminococcus_sp_5_1_39BFAA
Bacteroides_uniformis
Lachnospiraceae_bacterium_5_1_63FAA
0
20
40
60
80
100
Relative Importance

B

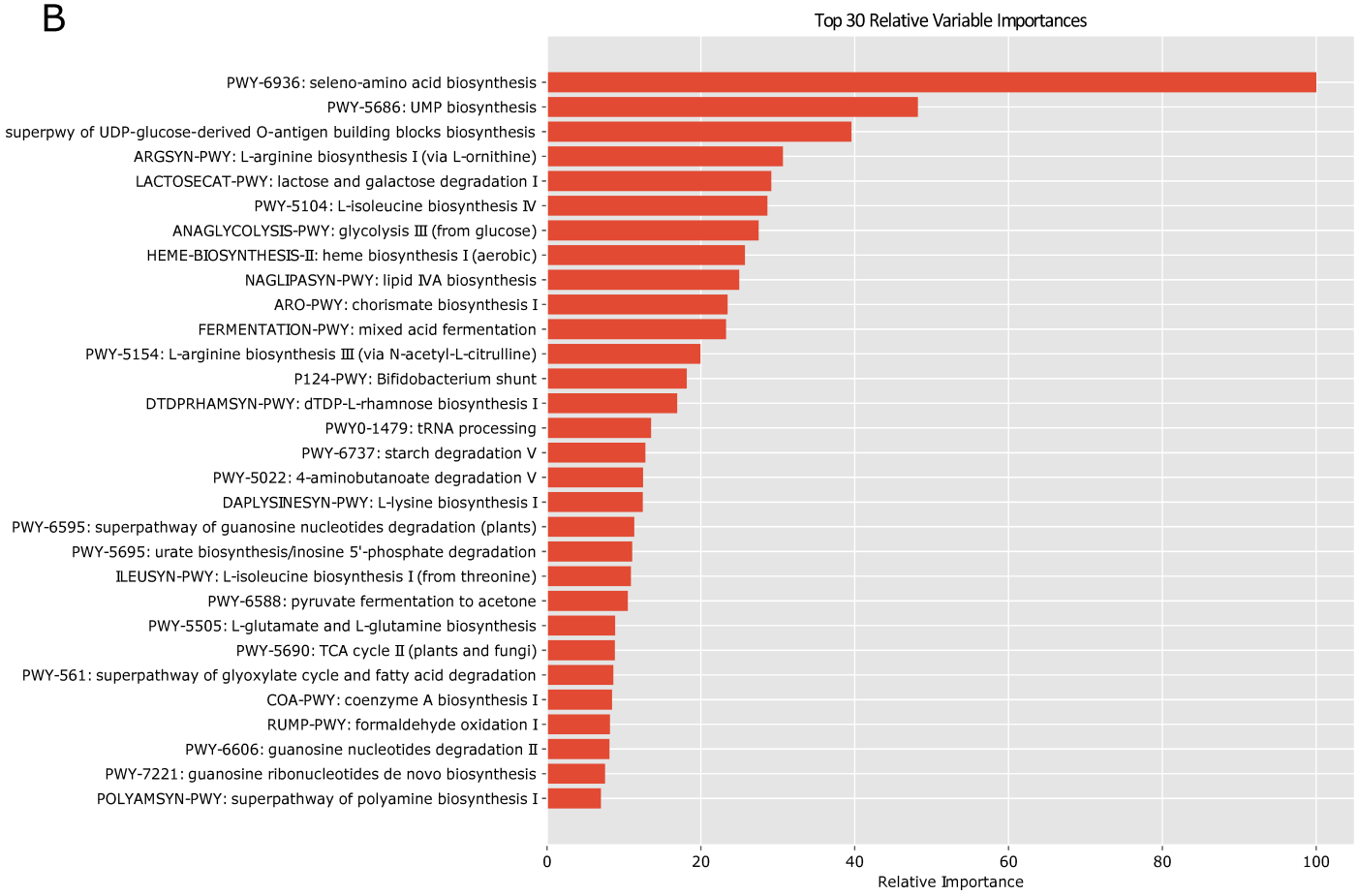
Top 30 Relative Variable Importances
PWY-6936: seleno-amino acid biosynthesis
PWY-5686: UMP biosynthesis
superpwy of UDP-glucose-derived O-antigen building blocks biosynthesis
ARGSYN-PWY: L-arginine biosynthesis I (via L-ornithine)
LACTOSECAT-PWY: lactose and galactose degradation I
PWY-5104: L-isoleucine biosynthesis IV
ANAGLYCOLYSIS-PWY: glycolysis III (from glucose)
HEME-BIOSYNTHESIS-II: heme biosynthesis I (aerobic)
NAGLIPASYN-PWY: lipid IVA biosynthesis
ARO-PWY: chorismate biosynthesis I
FERMENTATION-PWY: mixed acid fermentation
PWY-5154: L-arginine biosynthesis III (via N-acetyl-L-citrulline)
P124-PWY: Bifidobacterium shunt
DTDPRHAMSYN-PWY: dTDP-L-rhamnose biosynthesis I
PWY0-1479: tRNA processing
PWY-6737: starch degradation V
PWY-5022: 4-aminobutanoate degradation V
DAPLYSINESYN-PWY: L-lysine biosynthesis I
PWY-6595: superpathway of guanosine nucleotides degradation (plants)
PWY-5695: urate biosynthesis/inosine 5'-phosphate degradation
ILEUSYN-PWY: L-isoleucine biosynthesis I (from threonine)
PWY-6588: pyruvate fermentation to acetone
PWY-5505: L-glutamate and L-glutamine biosynthesis
PWY-5690: TCA cycle II (plants and fungi)
PWY-561: superpathway of glyoxylate cycle and fatty acid degradation
COA-PWY: coenzyme A biosynthesis I
RUMP-PWY: formaldehyde oxidation I
PWY-6606: guanosine nucleotides degradation II
PWY-7221: guanosine ribonucleotides de novo biosynthesis
POLYAMSYN-PWY: superpathway of polyamine biosynthesis I
0
20
40
60
80
100
Relative Importance

S7

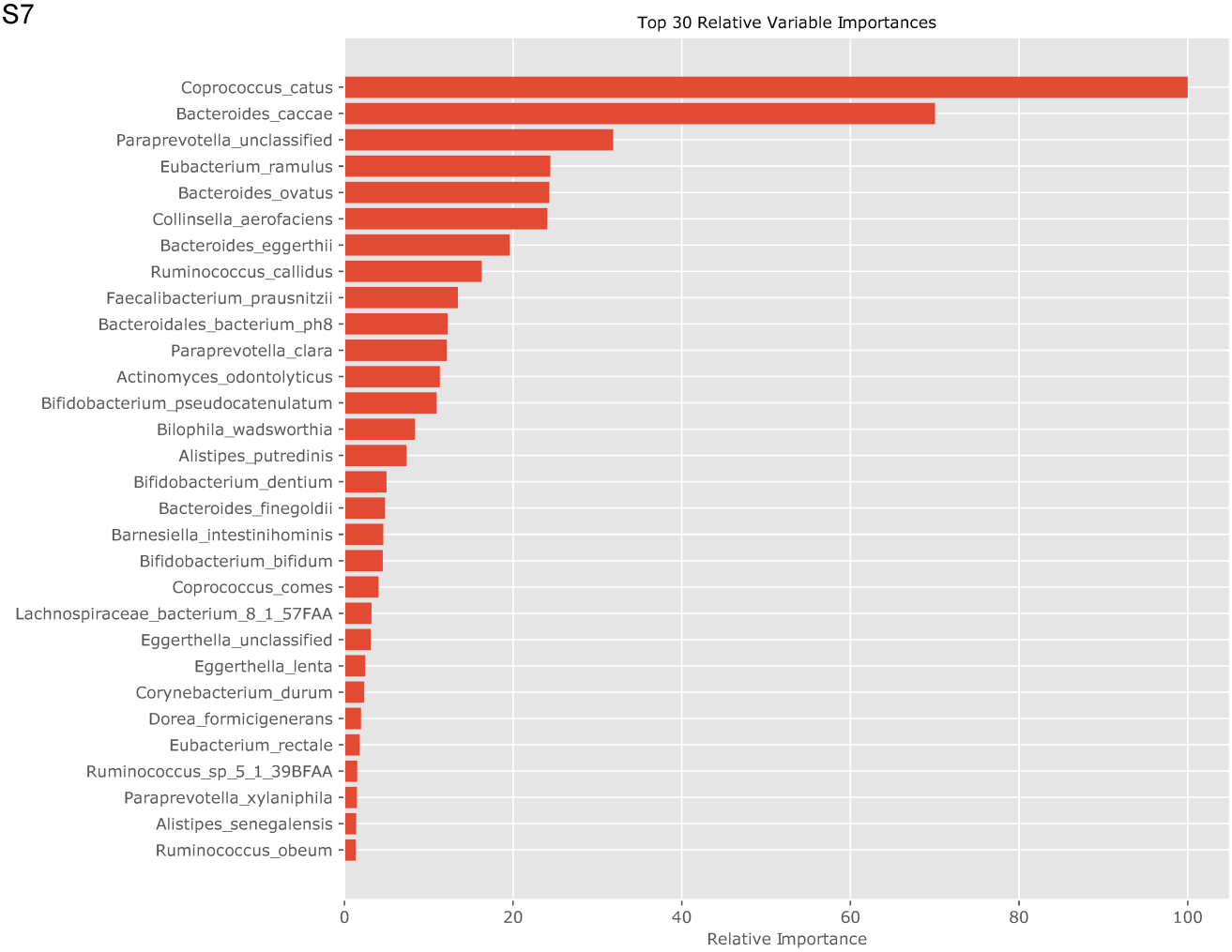
Top 30 Relative Variable Importances
Coprococcus_catus
Bacteroides_caccae
Paraprevotella_unclassified
Eubacterium_ramulus
Bacteroides_ovatus
Collinsella_aerofaciens
Bacteroides_eggerthii
Ruminococcus_callidus
Faecalibacterium_prausnitzii
Bacteroidales_bacterium_ph8
Paraprevotella_clara
Actinomyces_odontolyticus
Bifidobacterium_pseudocatenulatum
Bilophila_wadsworthia
Alistipes_putredinis
Bifidobacterium_dentium
Bacteroides_finegoldii
Barnesiella_intestinihominis
Bifidobacterium_bifidum
Coprococcus_comes
Lachnospiraceae_bacterium_8_1_57FAA
Eggerthella_unclassified
Eggerthella_lenta
Corynebacterium_durum
Dorea_formicigenerans
Eubacterium_rectale
Ruminococcus_sp_5_1_39BFAA
Paraprevotella_xylaniphila
Alistipes_senegalensis
Ruminococcus_obeum
0
20
40
60
80
100
Relative Importance

S8

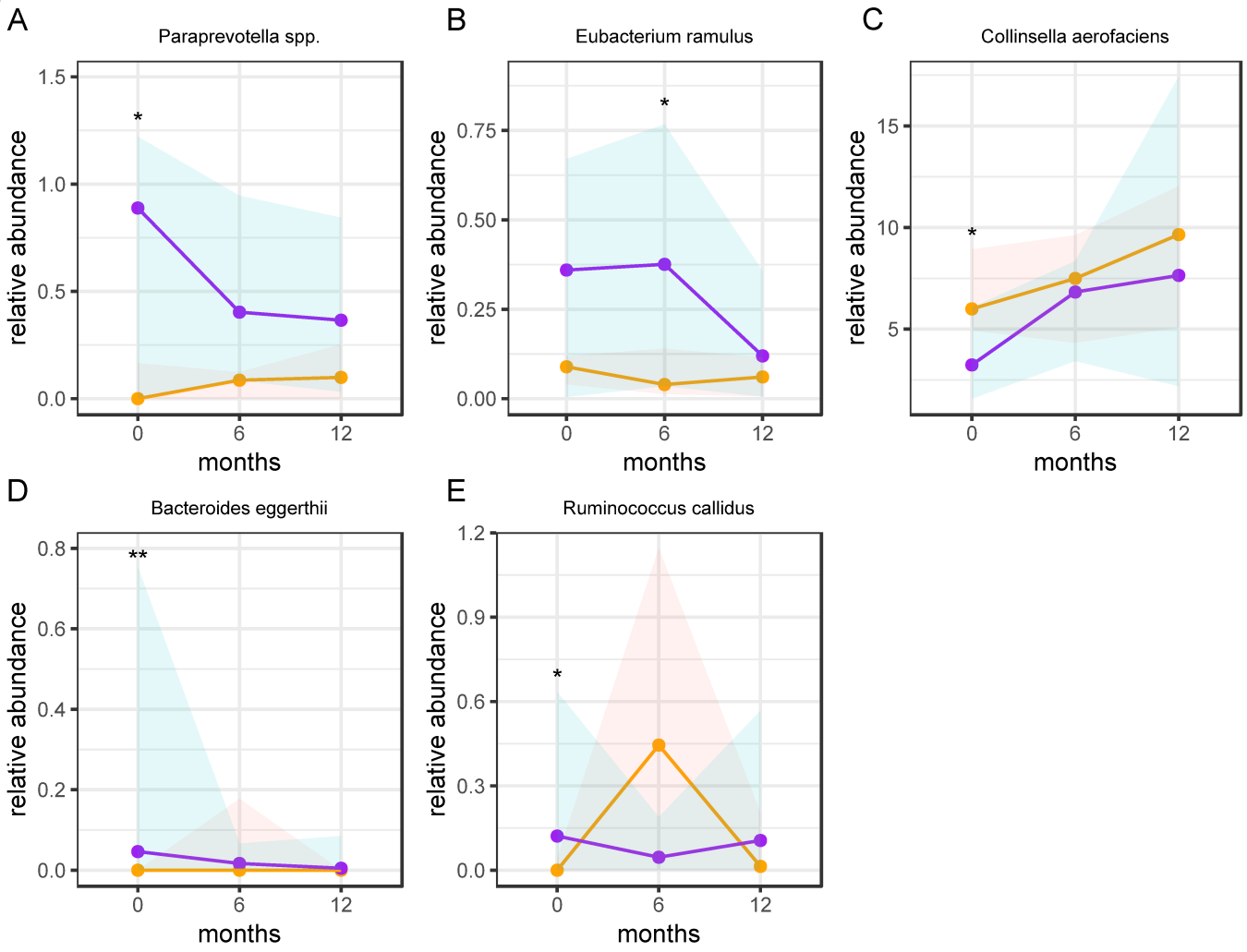
A
Paraprevotella spp.
relative abundance
1.5
1.0
0.5
0.0
*
0
6
12
months
B
Eubacterium ramulus
relative abundance
0.75
0.50
0.25
0.00
*
0
6
12
months
C
Collinsella aerofaciens
relative abundance
15
10
5
*
0
6
12
months
D
Bacteroides eggerthii
relative abundance
0.8
0.6
0.4
0.2
0.0
**
0
6
12
months
E
Ruminococcus callidus
relative abundance
1.2
0.9
0.6
0.3
0.0
*
0
6
12
months

S9

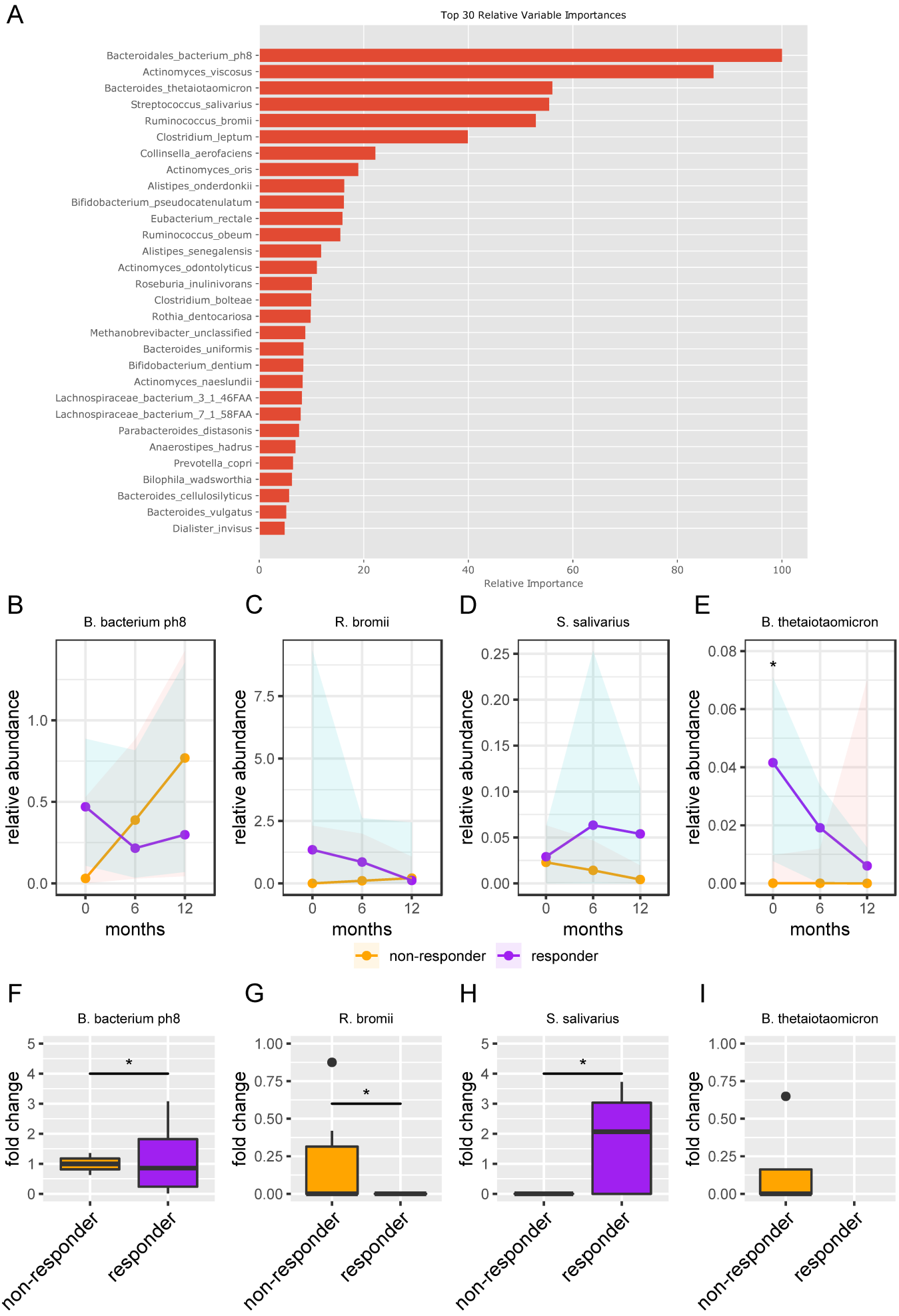
A
Top 30 Relative Variable Importances
Bacteroidales_bacterium_ph8
Actinomyces_viscosus
Bacteroides_thetaiotaomicron
Streptococcus_salivarius
Ruminococcus_bromii
Clostridium_leptum
Collinsella_aerofaciens
Actinomyces_oris
Alistipes_onderdonkii
Bifidobacterium_pseudocatenulatum
Eubacterium_rectale
Ruminococcus_obeum
Alistipes_senegalensis
Actinomyces_odontolyticus
Roseburia_inulinivorans
Clostridium_bolteae
Rothia_dentocariosa
Methanobrevibacter_unclassified
Bacteroides_uniformis
Bifidobacterium_dentium
Actinomyces_naeslundii
Lachnospiraceae_bacterium_3_1_46FAA
Lachnospiraceae_bacterium_7_1_58FAA
Parabacteroides_distasonis
Anaerostipes_hadrus
Prevotella_copri
Bilophila_wadsworthia
Bacteroides_cellulosilyticus
Bacteroides_vulgatus
Dialister_invisus
0
20
40
60
80
100
Relative Importance
B
B. bacterium ph8
C
R. bromii
D
S. salivarius
E
B. thetaiotaomicron
relative abundance
months
non-responder
responder
F
G
H
I
fold change
*

S10

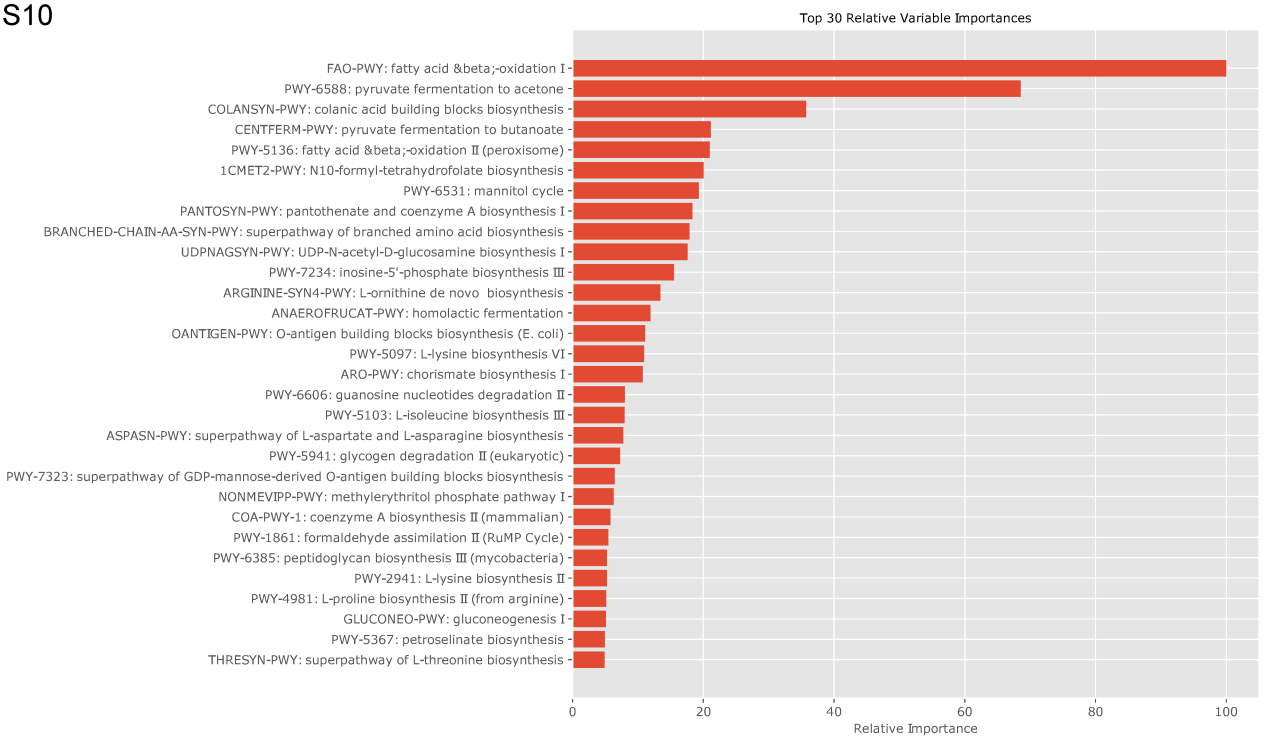
Top 30 Relative Variable Importances
FAO-PWY: fatty acid β-oxidation I
PWY-6588: pyruvate fermentation to acetone
COLANSYN-PWY: colanic acid building blocks biosynthesis
CENTFERM-PWY: pyruvate fermentation to butanoate
PWY-5136: fatty acid β-oxidation II (peroxisome)
1CMET2-PWY: N10-formyl-tetrahydrofolate biosynthesis
PWY-6531: mannitol cycle
PANTOSYN-PWY: pantothenate and coenzyme A biosynthesis I
BRANCHED-CHAIN-AA-SYN-PWY: superpathway of branched amino acid biosynthesis
UDPNAGSYN-PWY: UDP-N-acetyl-D-glucosamine biosynthesis I
PWY-7234: inosine-5'-phosphate biosynthesis III
ARGININE-SYN4-PWY: L-ornithine de novo biosynthesis
ANAEROFRUCAT-PWY: homolactic fermentation
OANTIGEN-PWY: O-antigen building blocks biosynthesis (E. coli)
PWY-5097: L-lysine biosynthesis VI
ARO-PWY: chorismate biosynthesis I
PWY-6606: guanosine nucleotides degradation II
PWY-5103: L-isoleucine biosynthesis III
ASPASN-PWY: superpathway of L-aspartate and L-asparagine biosynthesis
PWY-5941: glycogen degradation II (eukaryotic)
PWY-7323: superpathway of GDP-mannose-derived O-antigen building blocks biosynthesis
NONMEVIPP-PWY: methylerythritol phosphate pathway I
COA-PWY-1: coenzyme A biosynthesis II (mammalian)
PWY-1861: formaldehyde assimilation II (RuMP Cycle)
PWY-6385: peptidoglycan biosynthesis III (mycobacteria)
PWY-2941: L-lysine biosynthesis II
PWY-4981: L-proline biosynthesis II (from arginine)
GLUCONEO-PWY: gluconeogenesis I
PWY-5367: petroselinate biosynthesis
THRESYN-PWY: superpathway of L-threonine biosynthesis
0
20
40
60
80
100
Relative Importance

S11

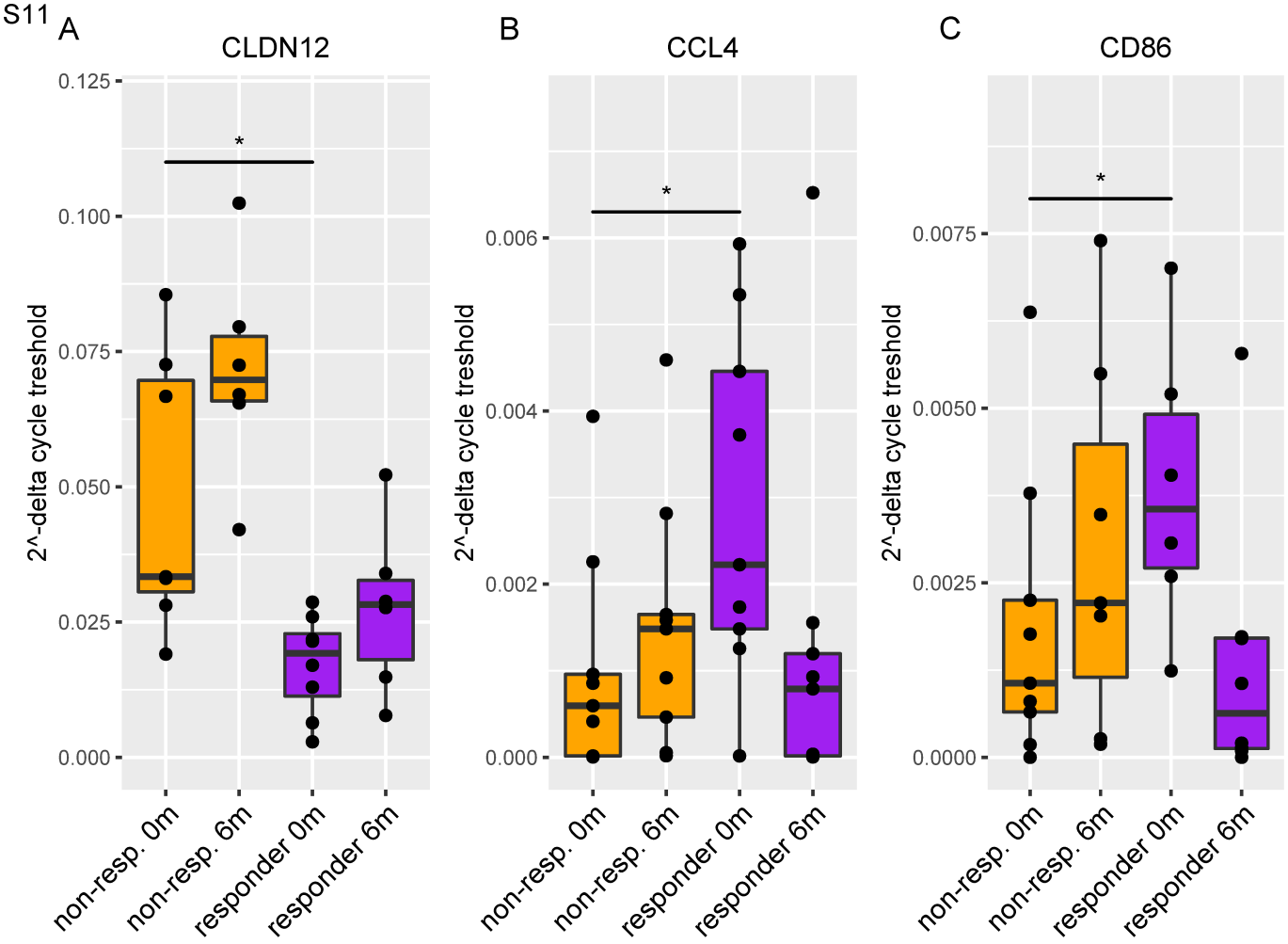
A
CLDN12
B
CCL4
C
CD86
2^-delta cycle treshold
0.125
0.100
0.075
0.050
0.025
0.000
0.006
0.004
0.002
0.0075
0.0050
0.0025
0.0000
*
non-resp. 0m
non-resp. 6m
responder 0m
responder 6m

S12

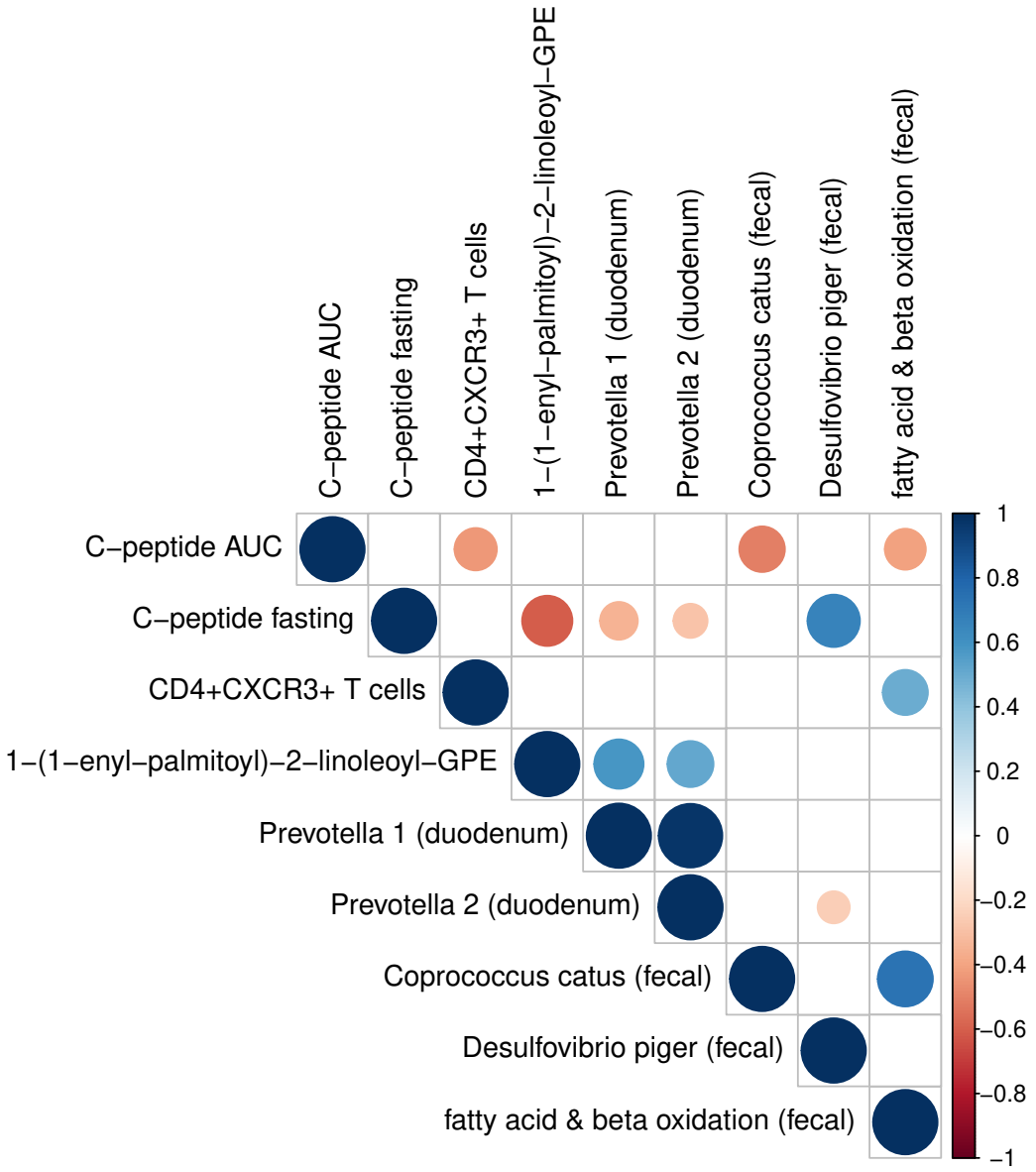
C–peptide AUC
C–peptide fasting
CD4+CXCR3+ T cells
1–(1–enyl–palmitoyl)–2–linoleoyl–GPE
Prevotella 1 (duodenum)
Prevotella 2 (duodenum)
Coprococcus catus (fecal)
Desulfovibrio piger (fecal)
fatty acid & beta oxidation (fecal)
1
0.8
0.6
0.4
0.2
0
–0.2
–0.4
–0.6
–0.8
–1

Cell type	Autologous (n=10)	Allogenic (N=10)	P value
Dendritic cells	17123	14529	0.07
Total monocytes	119555	73615	0.39
CD16 pos monocytes	7395	5539	0.07
CD14 pos monocytes	93804	72016	0.44
B cells	105975	172553	0.22
Naive B	61851	105175	0.22
non CS memory B	21187	20716	0.39
Transitional B	4463	3089	0.07
CS memory B	16577	21048	0.30
plasmablasts and plasmacells	3548	2826	0.07
NK cells	112375	123638	0.75
CD16 pos NK	95077	94477	0.82
CD56 NK	12090	18402	0.62
NKT cells	11571	11847	0.69
T cells	629591	588006	0.44
CD4 T pos cells	251710	228152	0.39
CD4 pos Naive T cells	120264	63899	1.00
CD4 pos CM	73353	46334	0.62
CD4 pos EM	36782	59531	0.75
CD4 TEMRA	7228	4172	0.50
CD4 pos B7 pos	5262	3544	0.34
CD4 pos CCR5 pos	11380	10425	0.15
CD4 CXCR3	39267	24162	0.06
CD8 pos	85578	67805	0.96
CD8 pos Naive	49335	28281	0.13
CD8 pos CM	7266	6906	0.34
CD8 pos EM	14732	6080	0.16
CD8 TEMRA	7688	5519	0.39
CD8 pos B7 pos	2413	1091	0.09
CD8 pos CCR5 pos	5141	3240	0.77
CD8 CXCR3	9237	3039	0.89
nTreg	8005	6190	0.30
Treg B7 pos	1070	339	0.96
Treg CCR5 pos	969	319	0.75
Treg CXCR3	847	303	0.62

Supplementary table 3: Number of Whole blood immune cells per group at baseline. p-values were calculated using Mann-Whitney U test.